Introduction to Membrane Proteins

- History
- Membranes and membrane proteins
- Structure determination of membrane proteins
- 2D crystallization
- Methods for high-throughput screening
- Types of 2D crystals
- Software for 2D crystallography

NRAMM Workshop – Nov 12, 2009

David Stokes

Revival of electron crystallography

Richard K Hite, Stefan Raunser and Thomas Walz

Since the structure determination of bacteriorhodopsin in 1990, much progress has been made in the further development and use of electron crystallography. In this review, we provide a concise overview of the new developments in electron crystallography concerning 2D crystallization, data collection and data processing. Based on electron crystallographic work on bacteriorhodopsin, the acetylcholine receptor and aquaporins, we highlight the unique advantages and future perspectives of electron crystallography for the structural study of membrane proteins. These advantages include the visualization of membrane proteins in their native environment without detergent-induced artifacts, the trapping of different states in a reaction pathway by time-resolved experiments, the study of non-specific protein–lipid interactions and the

receptor [8,9], sheep aquaporin-0 [10,11••], rat aquaporin-4 (solved using recombinant protein expressed in insect cells) [12••] and rat microsomal glutathione transferase 1 [13•].

A game of numbers

The number of solved structures

Seven structures may appear a modest accomplishment compared to the many more membrane protein structures that have been determined by X-ray crystallography over the past few years. Considering, however, that less than two dozen groups are currently pursuing electron crystallography, compared to the hundreds of X-ray groups, the seven membrane protein structures determined by elec-

Current Opinion in Structural Biology, 2007 17:389

Table 1. 3D structures of membrane proteins determined by electron crystallography. Atomic-resolution structures are highlighted in bold.

Integral Membrane Protein	Resol. (Å)	Year	Reference
Eye lens Aquaporin 0	1.9	2005	(Gonen, Cheng et al.)
Aquaporin-4	2.8	2009	(Tani, Mitsuma et al.)
Bacteriorhodopsin	3.0	1997	(Kimura, Vassylyev et al.)
Glutathione transferase	3.2	2006	(Holm, Bhakat et al.)
Plant LHC-II	3.4	1991	(Kühlbrandt and Wang)
Bacteriorhodopsin	3.5	1990	(Henderson, Baldwin et al.)
Aquaporin-1	3.8	2000	(Murata, Mitsuoka et al.)
Acetylcholine receptor	4.0	2005	(Unwin)
Human aquaporin 2	4.5	2005	(Schenk, Werten et al.)
Plant Aquaporin SoPIP2	5.0	2005	(Kukulski, Schenk et al.)
Halorhodopsin	5.0	2000	(Kunji, von Gronau et al.)
Bovine Rhodopsin	5.5	2003	(Krebs, Edwards et al.)
Porin PhoE	6.0	1991	(Jap, Walian et al.)
Glutathione transferase	6.0	2002	(Holm, Morgenstern et al.)
Bacteriorhodopsin	6.5	1983	(Leifer and Henderson)
Oxalate transporter OxlT	6.5	2002	(Hirai, Heymann et al.)
Frog Rhodopsin frog	6.5	1997	(Unger, Hargrave et al.)
Ca^{2+}-ATPase	6.5	2002	(Xu, Rice et al.)
Glycerol channel GlpF	6.9	2000	(Stahlberg, Braun et al.
Bacteriorhodopsin	7.0	1975	(Henderson and Unwin)
Gap junction channel	7.0	2007	(Oshima, Tani et al.)
NhaA Na/ H^+ antiporter	7.0	2000	(Williams)
EmrE multidrug transporter	7.0	2003	(Ubarretxena-Belandia et al.)
hCTR1 Cu transporter	7.0	2009	(De Feo, Aller et al.)
Gap junction channel	7.5	1999	(Unger, Kumar et al.)
Sec YEG complex	8.0	2005	(Bostina, Mohsin et al.)
Plant photosystem II RC	8.0	1998	(Rhee, Morris et al.)
Neurospora H^+-ATPase	8.0	1998	(Auer, Scarborough et al.)
Acetylcholine receptor	9.0	1993	(Unwin)

Table 1. 3D structures of membrane proteins determined by electron crystallography. Atomic-resolution structures are highlighted in bold.

Integral Membrane Protein	Resol. (Å)	Year	Reference
Bacteriorhodopsin	7.0	1975	(Henderson and Unwin)
Bacteriorhodopsin	6.5	1983	(Leifer and Henderson)
Bacteriorhodopsin	3.5	1990	(Henderson, Baldwin et al.)
Plant LHC-II	3.4	1991	(Kühlbrandt and Wang)
Porin PhoE	6.0	1991	(Jap, Walian et al.)
Acetylcholine receptor	9.0	1993	(Unwin)
Frog Rhodopsin frog	6.5	1997	(Unger, Hargrave et al.)
Bacteriorhodopsin	3.0	1997	(Kimura, Vassylyev et al.)
Plant photosystem II RC	8.0	1998	(Rhee, Morris et al.)
Neurospora H^+-ATPase	8.0	1998	(Auer, Scarborough et al.)
Gap junction channel	7.5	1999	(Unger, Kumar et al.)
NhaA Na/ H^+ antiporter	7.0	2000	(Williams)
Glycerol channel GlpF	6.9	2000	(Stahlberg, Braun et al.
Halorhodopsin	5.0	2000	(Kunji, von Gronau et al.)
Aquaporin-1	3.8	2000	(Murata, Mitsuoka et al.)
Glutathione transferase	6.0	2002	(Holm, Morgenstern et al.)
Oxalate transporter OxlT	6.5	2002	(Hirai, Heymann et al.)
Ca^{2+}-ATPase	6.5	2002	(Xu, Rice et al.)
Bovine Rhodopsin	5.5	2003	(Krebs, Edwards et al.)
EmrE multidrug transporter	7.0	2003	(Ubarretxena-Belandia et al.)
Eye lens Aquaporin 0	1.9	2005	(Gonen, Cheng et al.)
Acetylcholine receptor	4.0	2005	(Unwin)
Human aquaporin 2	4.5	2005	(Schenk, Werten et al.)
Plant Aquaporin SoPIP2	5.0	2005	(Kukulski, Schenk et al.)
Sec YEG complex	8.0	2005	(Bostina, Mohsin et al.)
Glutathione transferase	3.2	2006	(Holm, Bhakat et al.)
Gap junction channel	7.0	2007	(Oshima, Tani et al.)
Aquaporin-4	2.8	2009	(Tani, Mitsuma et al.)
hCTR1 Cu transporter	7.0	2009	(De Feo, Aller et al.)

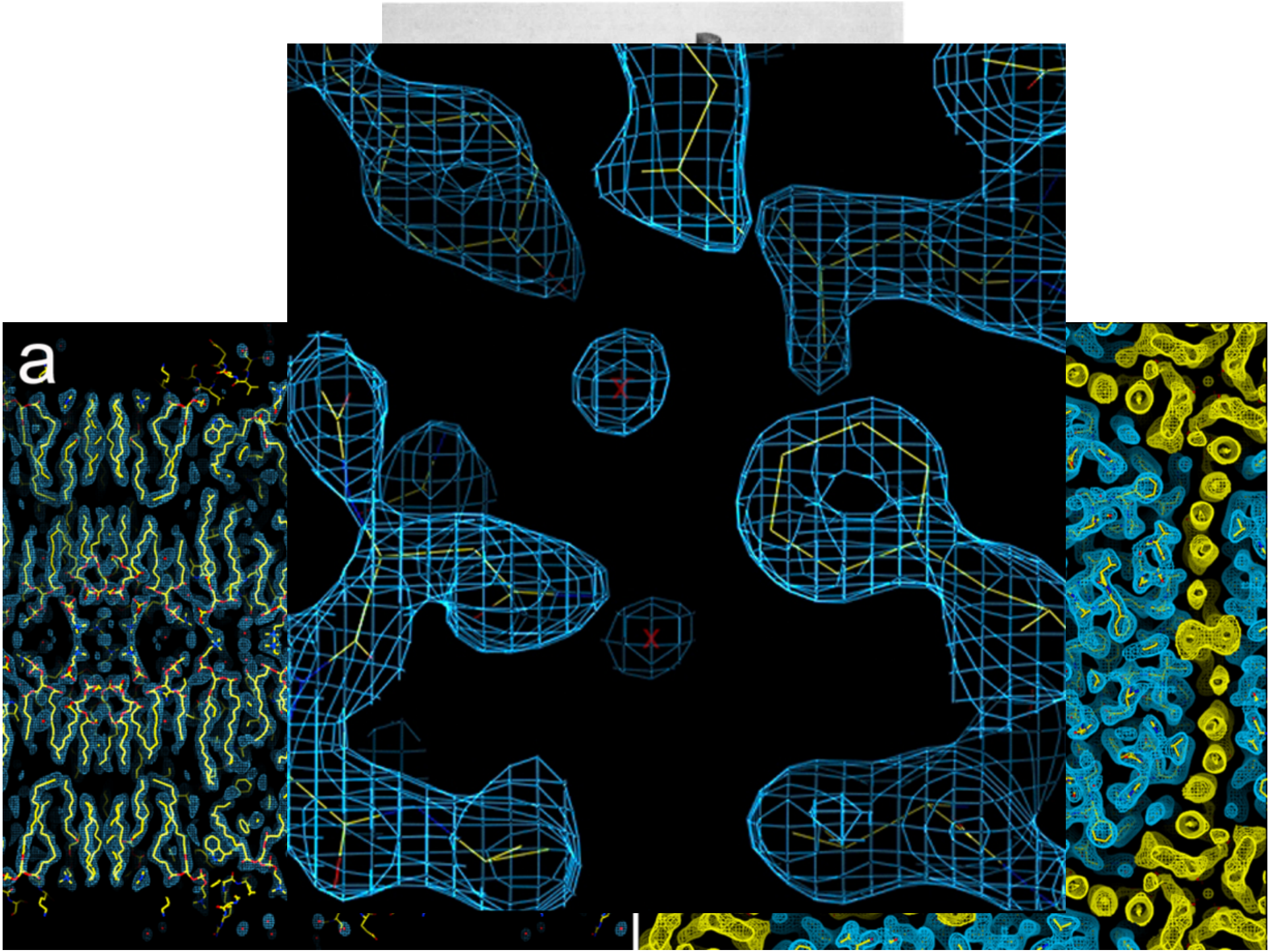
a

Singer & Nicholson
fluid-mosaic model of the membrane

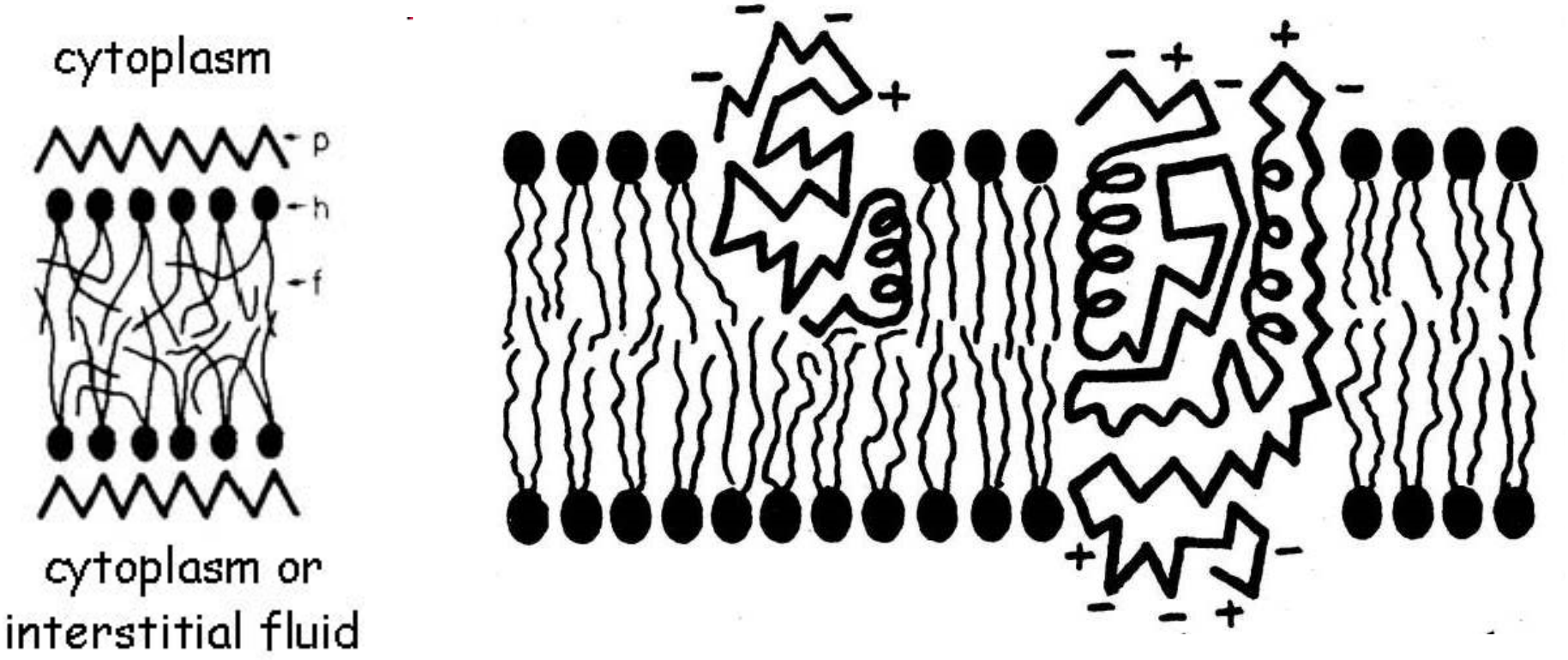

Singer & Nicholson
fluid-mosaic model of the membrane

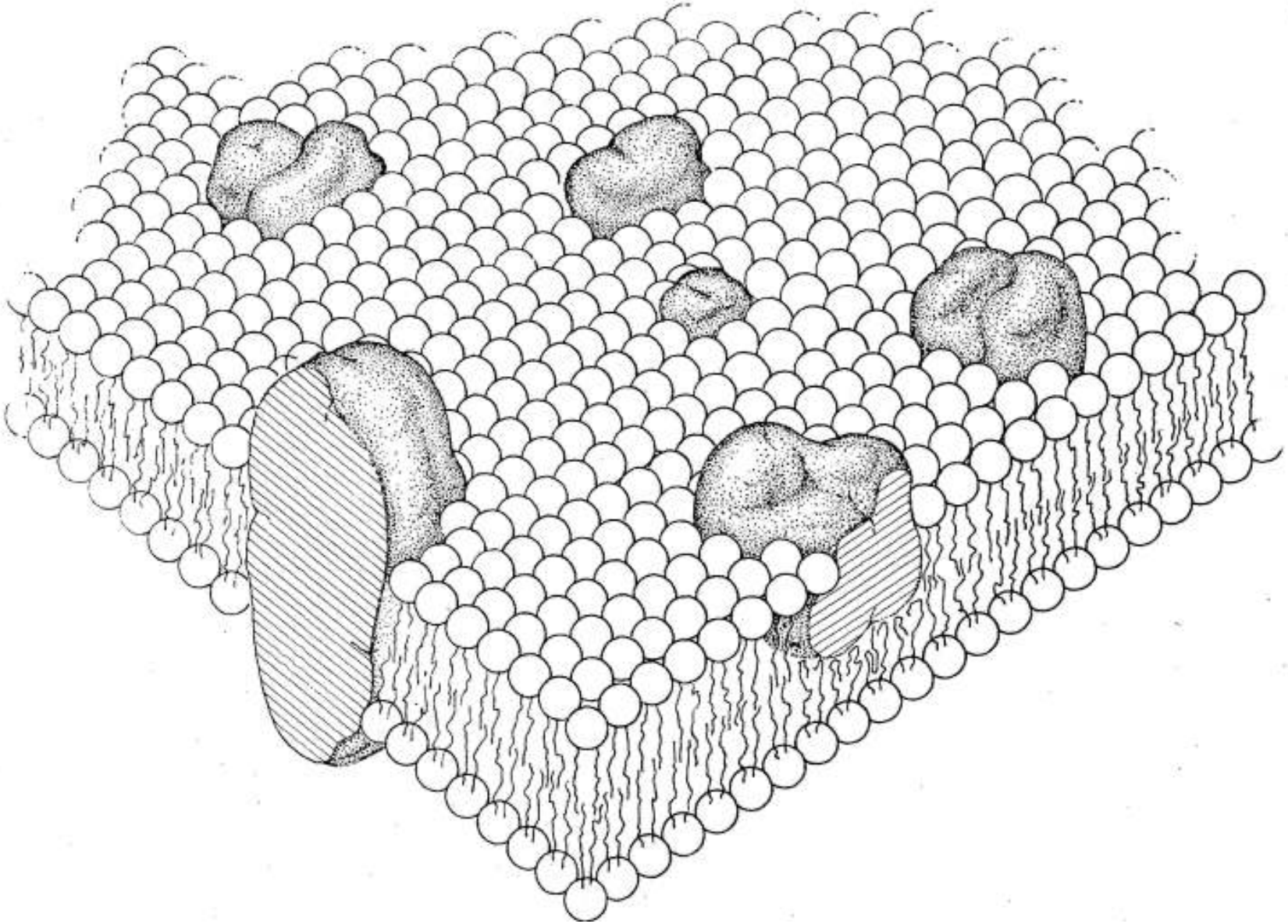

Synaptosome

(Takamori, Jahn et al, 2006, Cell)

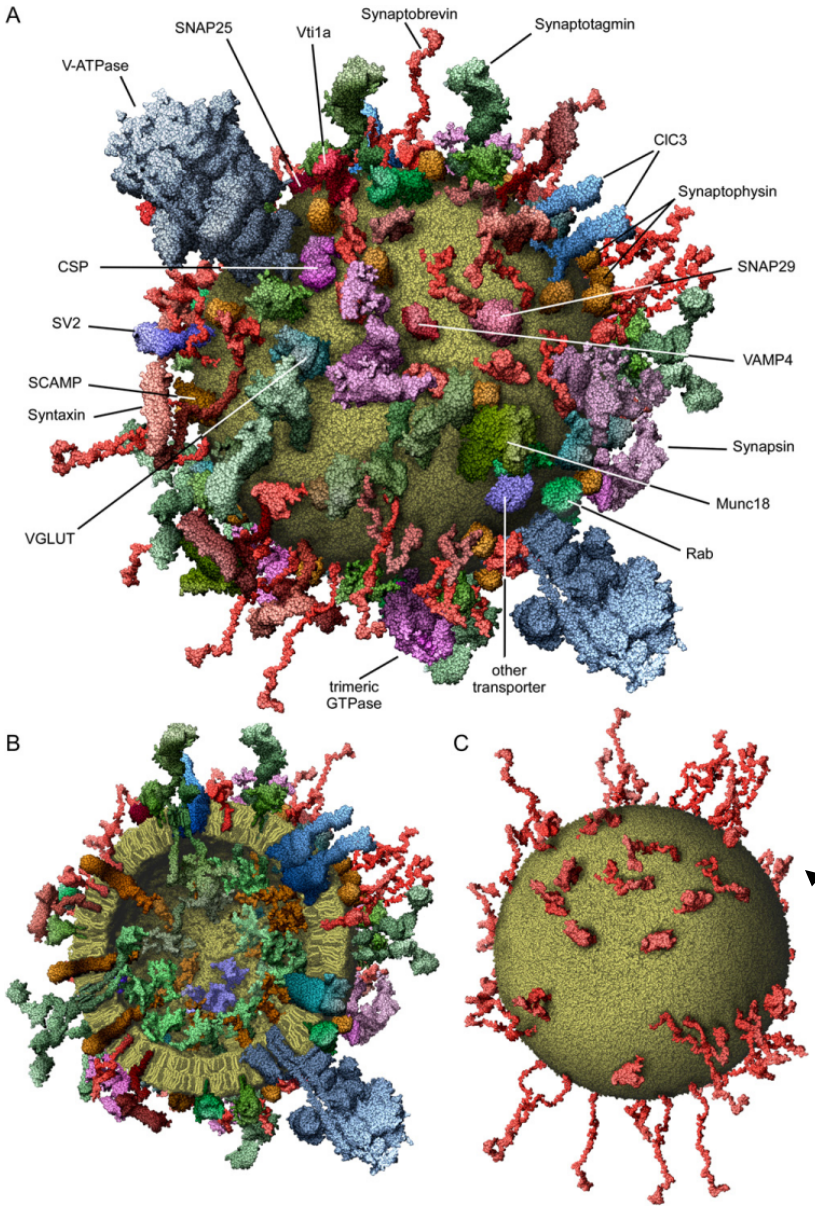

42 nm diameter
80 different IMPs
16 MDa total mass
65% protein by mass
600 TM-helices
(18% outer/25% inner surface area)

Synaptobrevin is most abundant

Why are membrane proteins important?

Membrane proteins:
mediate signaling, transport, adhesion at cell surface
40% of transcripts from all phyla
60% of all therapeutic drugs on the market

PDB:
60,000 total structures deposited
553 structures from 204 different membrane proteins
(25% β-barrel proteins from bacterial outer membrane)

Structure Determination of Membrane Proteins

Expression in cellular membrane

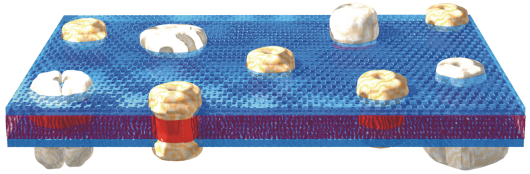

Solubilisation with detergent

Purification in detergent

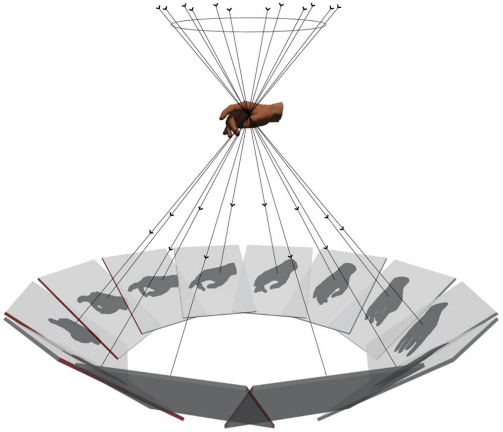

single particle analysis

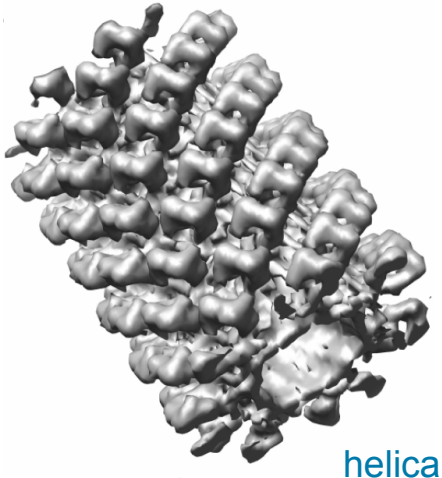

helical reconstruction

Detergent removal

Vapor diffusion

3D crystallisation – X-ray crystallography

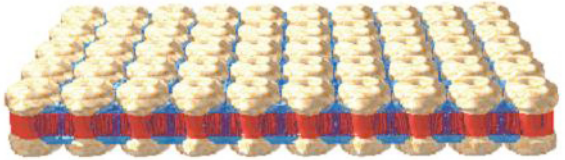

2D crystallisation – electron crystallography

X-ray crystallography

Electron crystallography

Single particle reconstructions

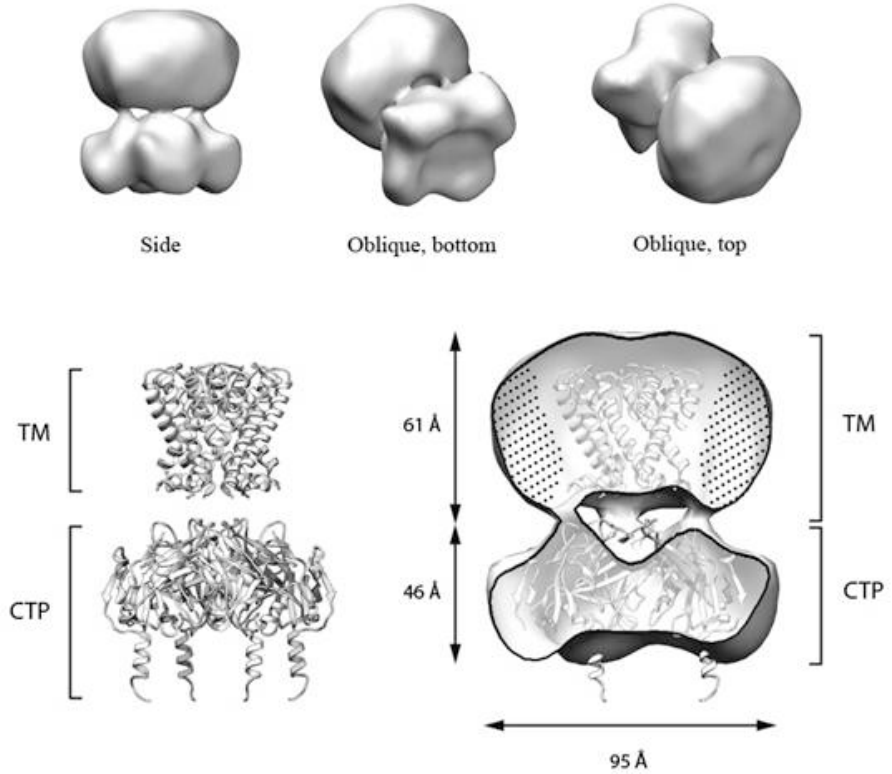

GIRK channel - Ubarretxena

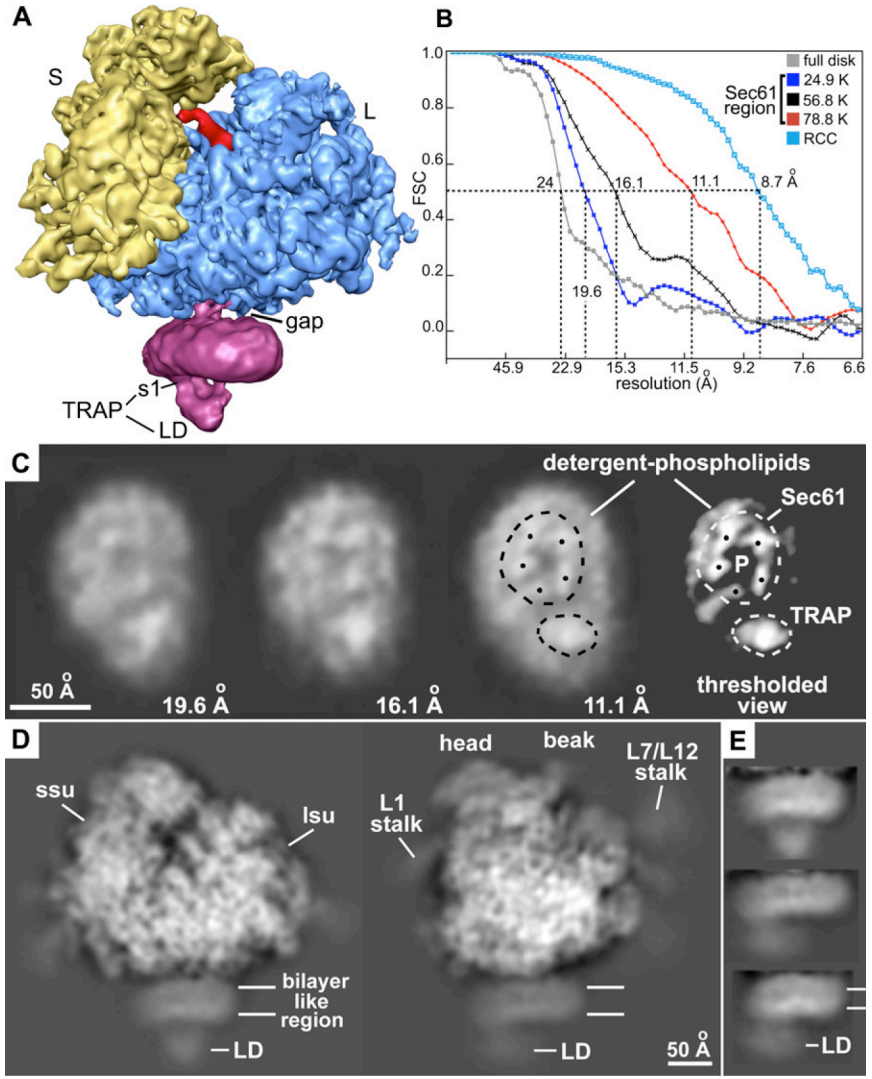

ribosome - Sec61 – TRAP complex, Menetret, Akey 2008

Spherical Reconstruction

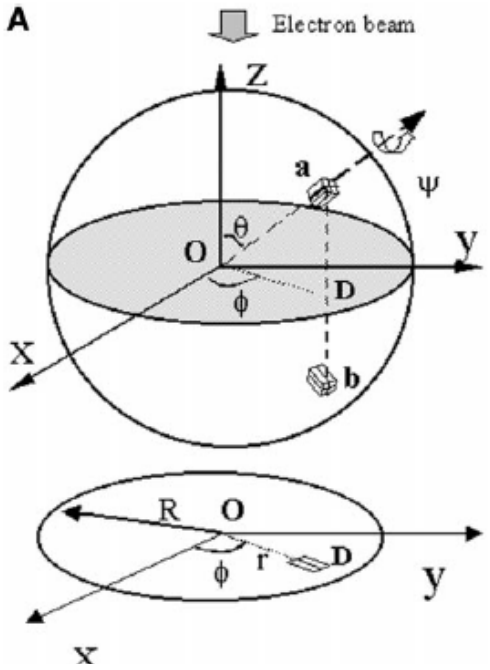

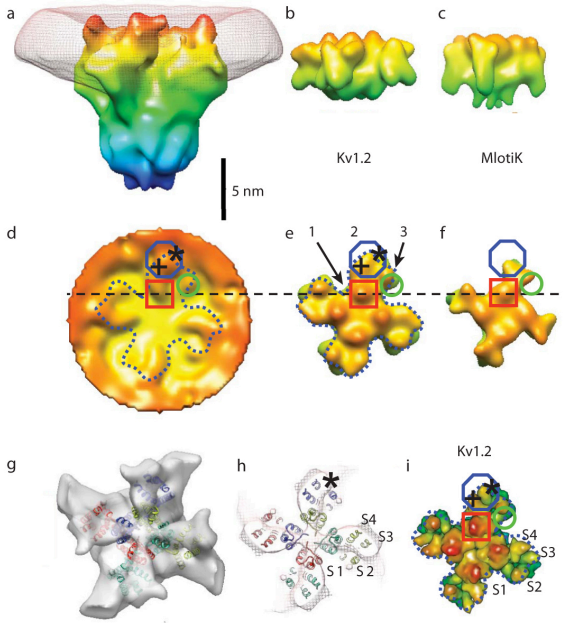

BK K^+ channel – 2nm resolution

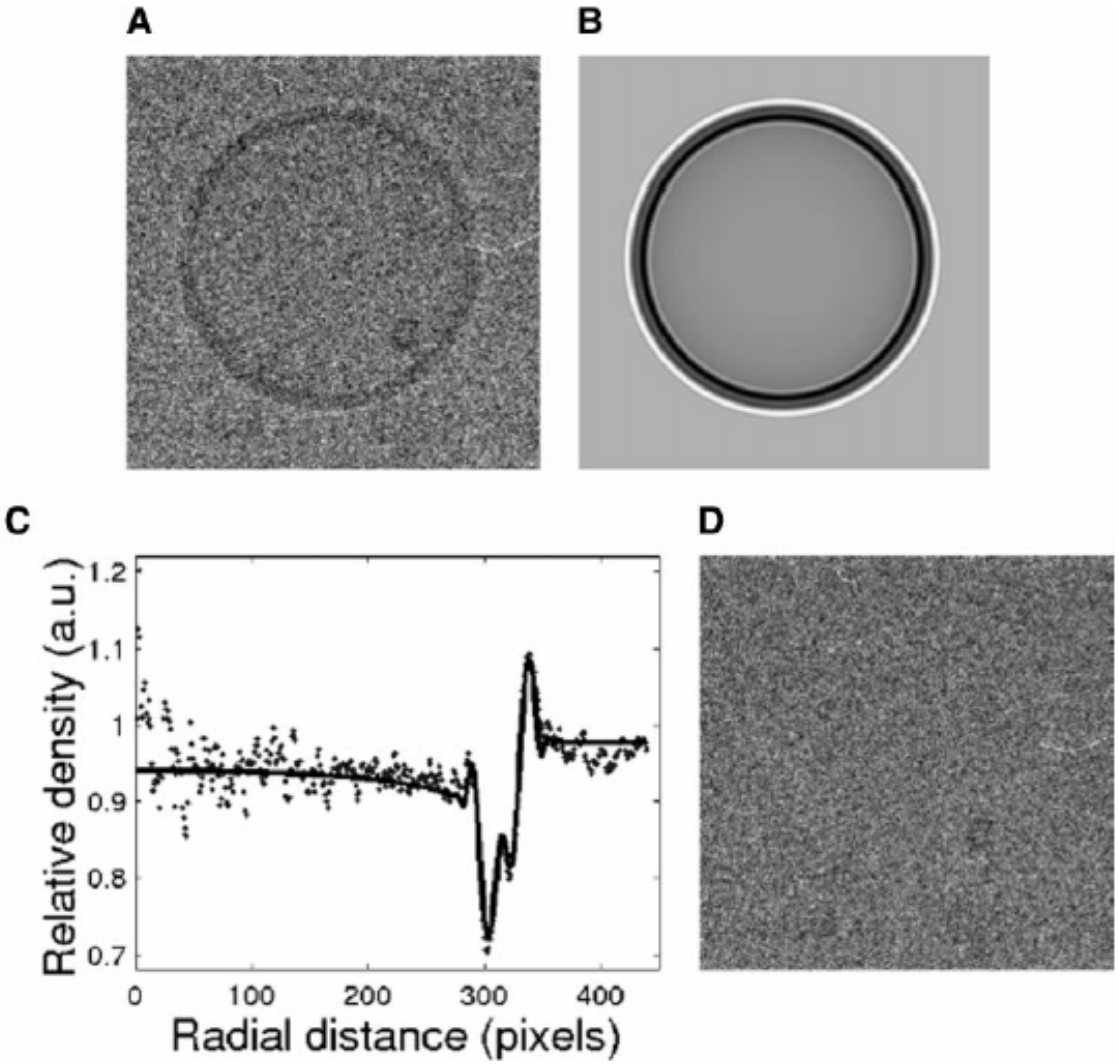

Sigworth & colleagues, J Struct Biol. 133:119, 2001, Nature 2009

Types of membrane protein crystals
(Iwata a la Michel 1985)

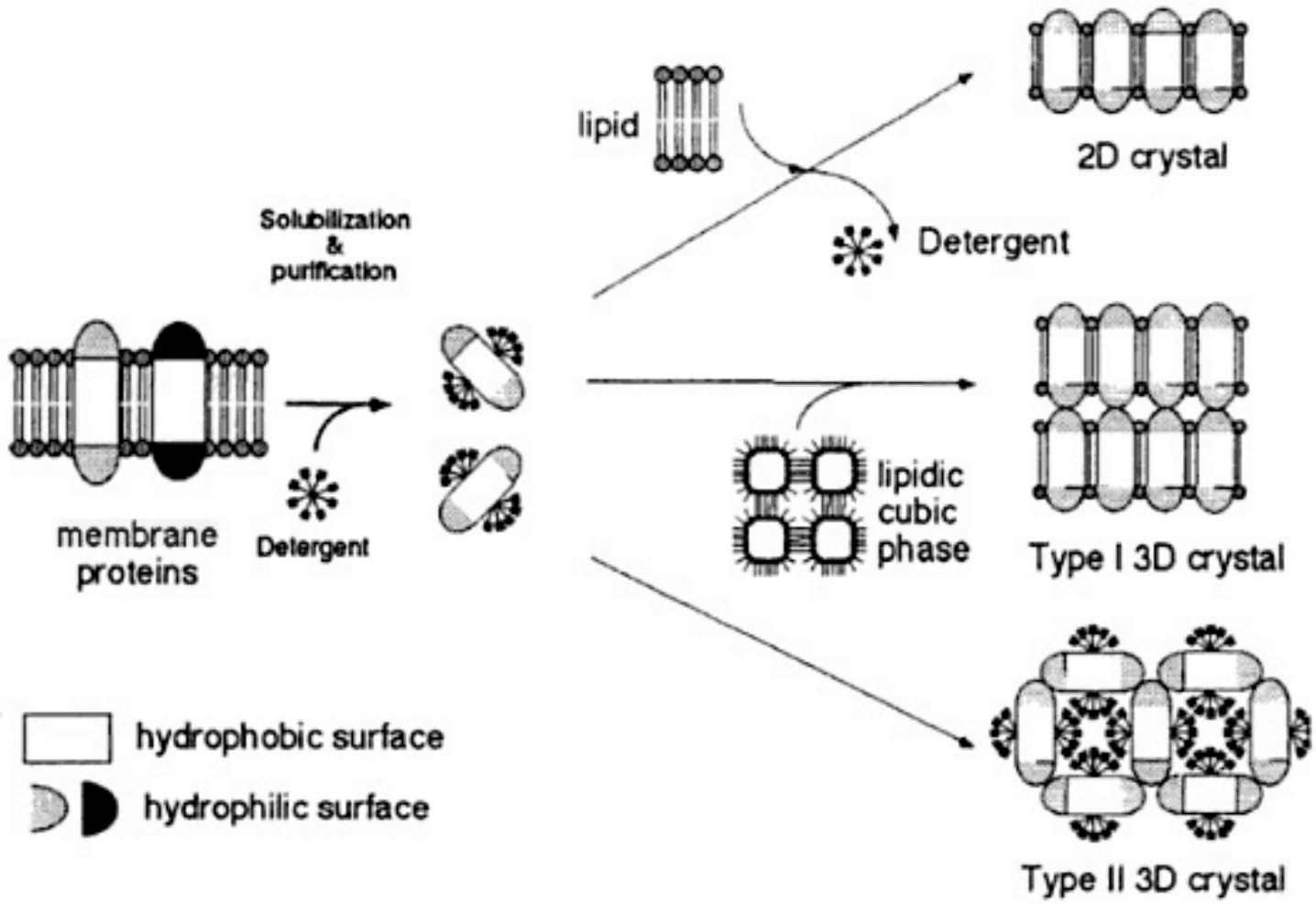

Figure 18.1. Types of membrane protein crystals

Fv antibody mediated crystallization
(Hunte and Michel)

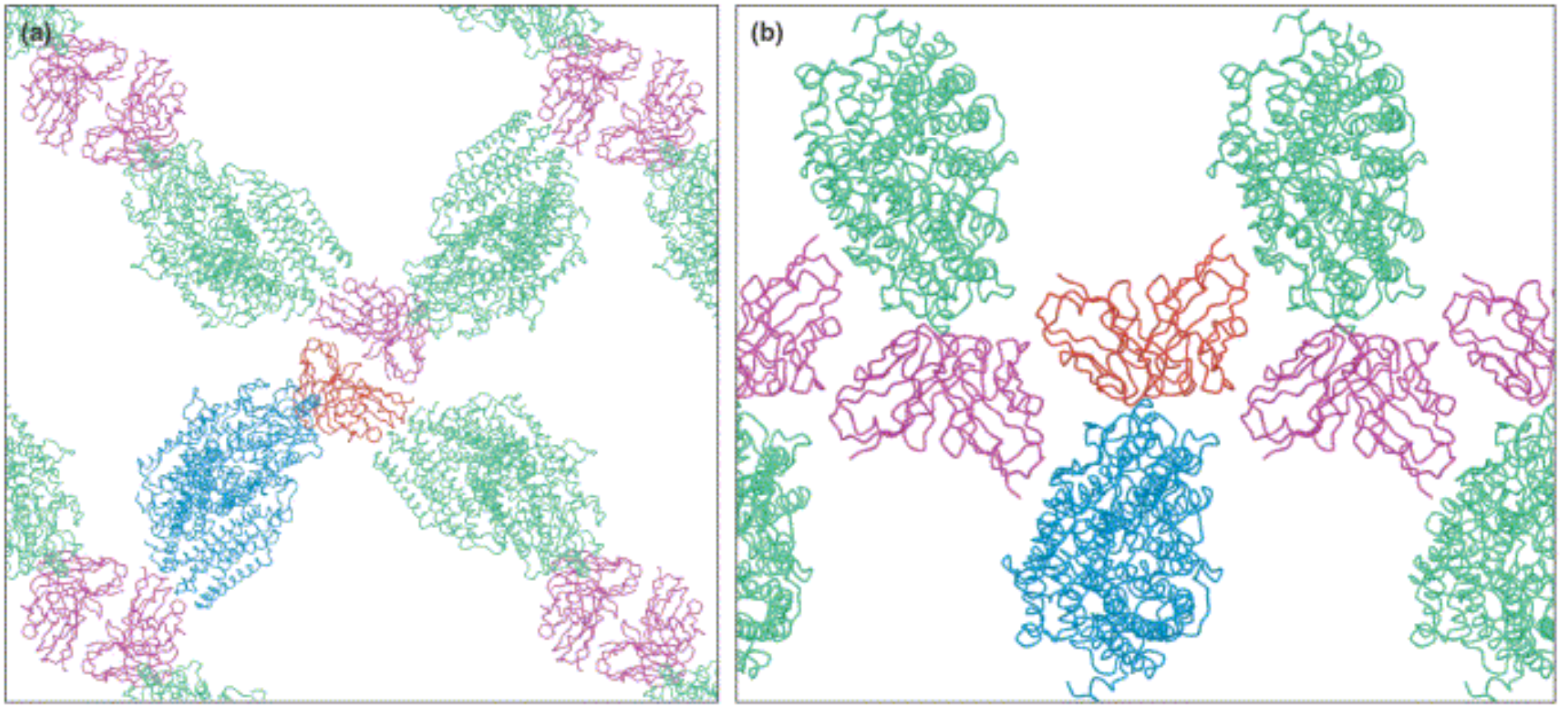

Crystallisation of COX from *P. denitrificans* in complex with an antibody Fv fragment. Crystal contacts are solely brought about by interactions involving the Fv fragment. The co-complex was crystallised and the structure determined at 2.8 Å resolution.

Meso lipidic phase – monoacyl lipids

(M. Caffrey)

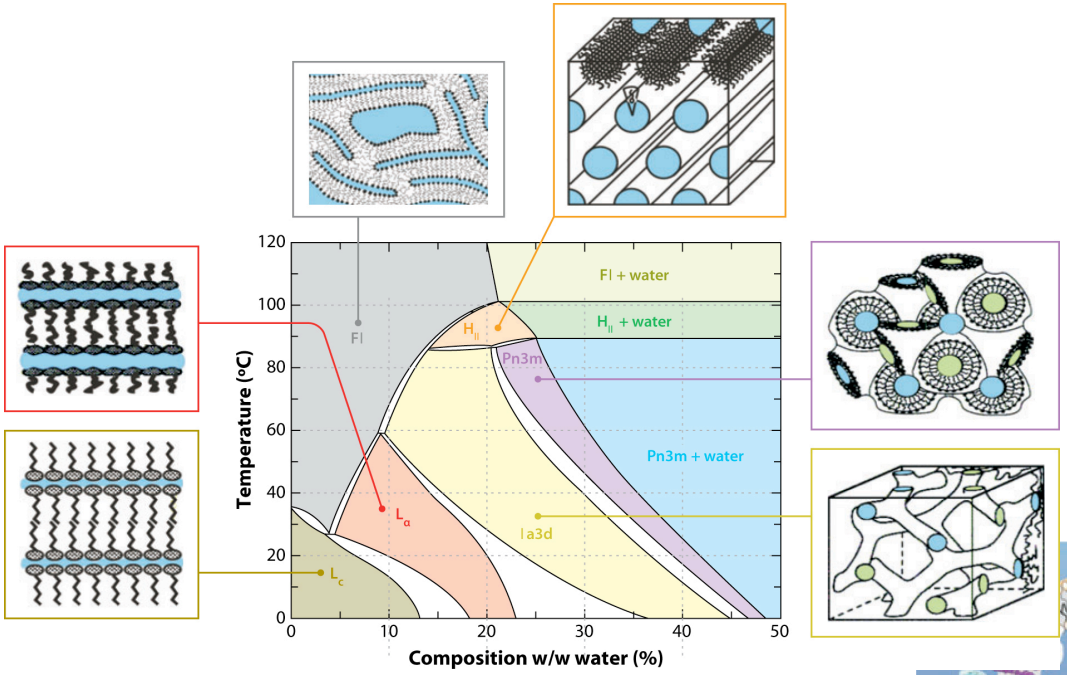

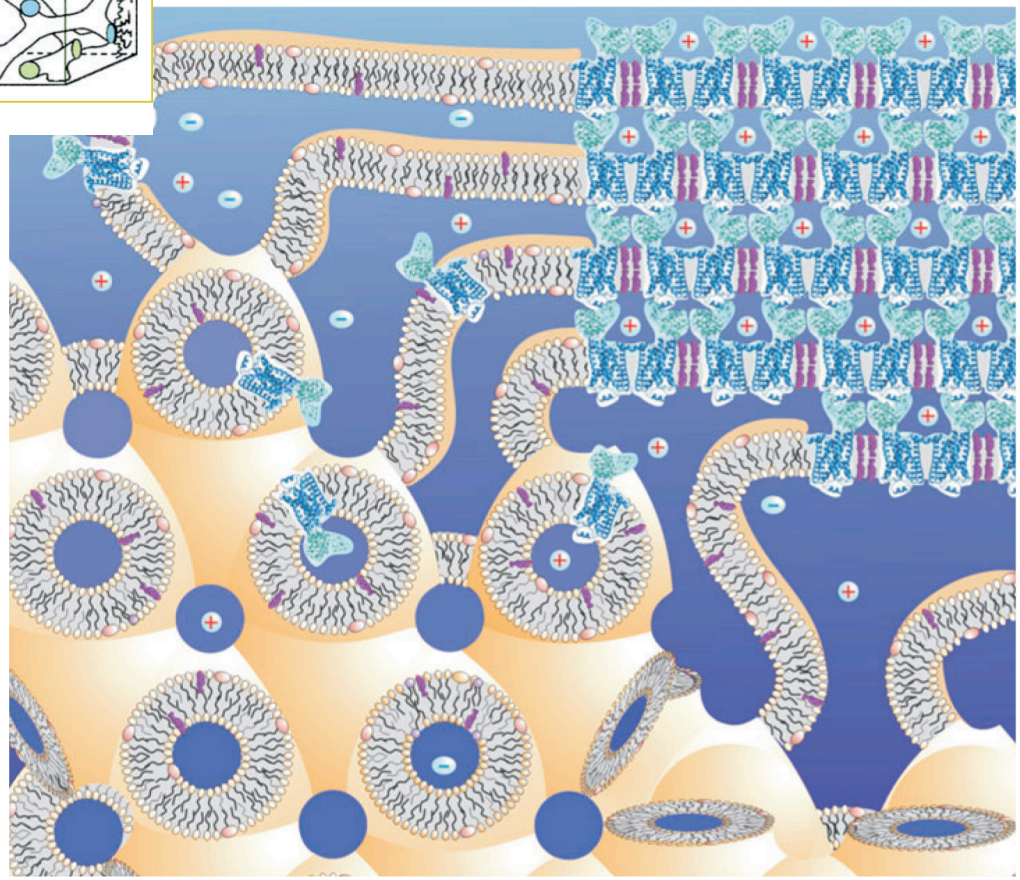

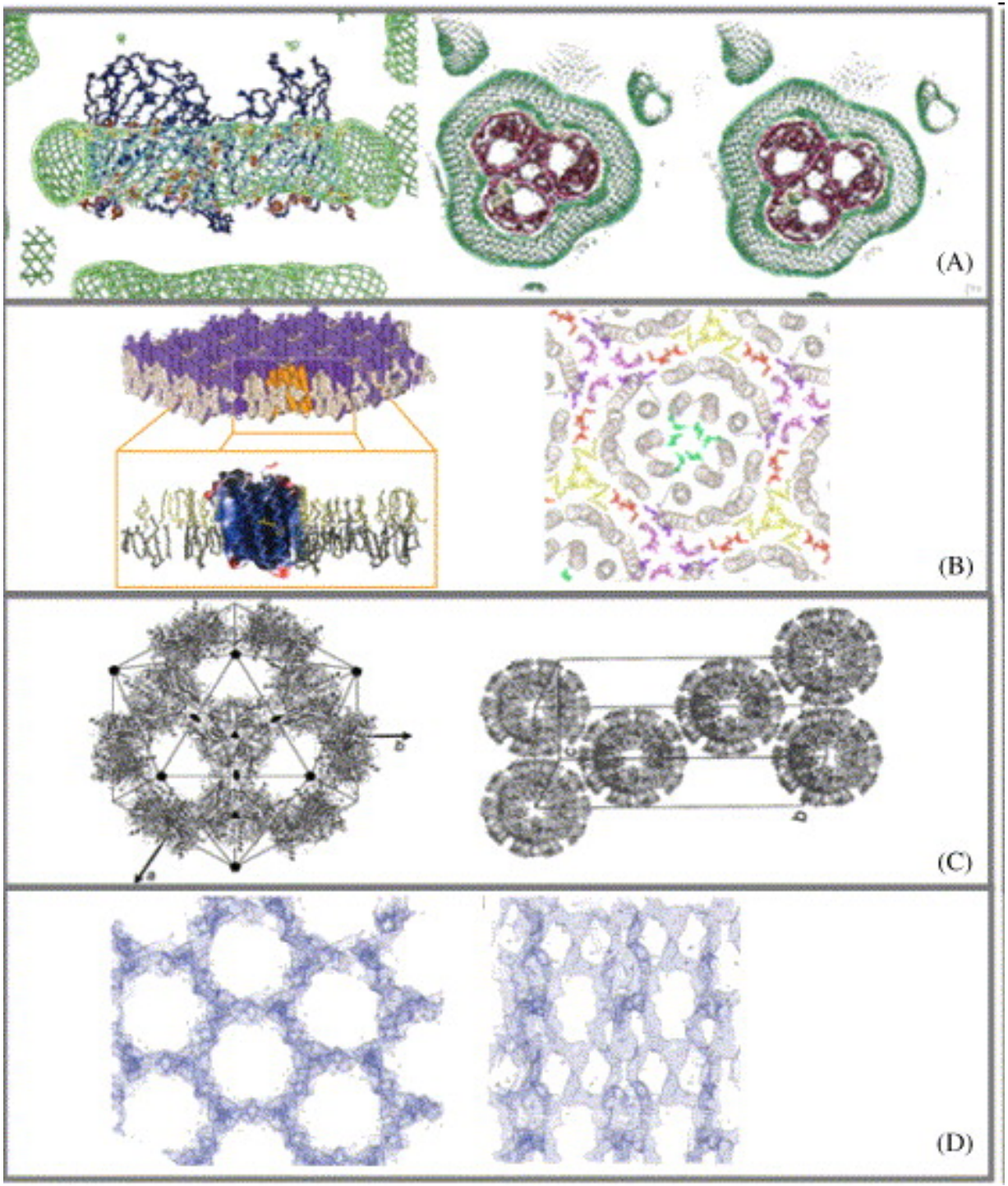

‘Type II’ discontinuous arrangement of micellar Octyl-POE around the hydrophobic perimeter of the detergent C8E4 and OmpF porin (*E. coli*) R3 crystal

‘Type I’ continuous arrangement of stacked layers consisting of extended two-dimensional sheets of purple membrane bR trimers are separated in plane by a belt of native lipids.

Hollow spherical shell assemblies of LHC-II were produced and packed into well-ordered three-dimensional crystals. The icosahedral spheres have a diameter of 250 Å and contain 20 protein trimers and several disordered lipid molecules.

Continuous network of *β*-Octylglucoside extending throughout the entire P3121 crystal of phospholipase A OmpIA

2D Crystallization

Expression

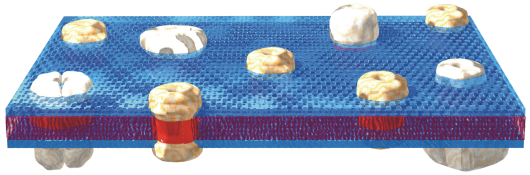

Solubilisation

Purification

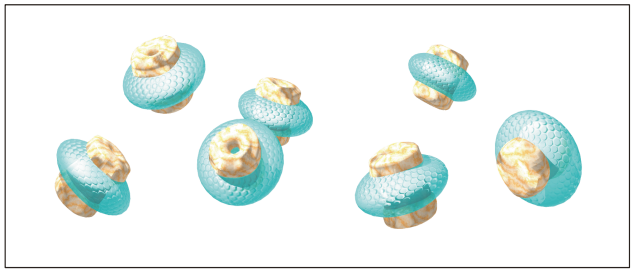

Vapor diffusion

Detergent removal

3D crystallisation

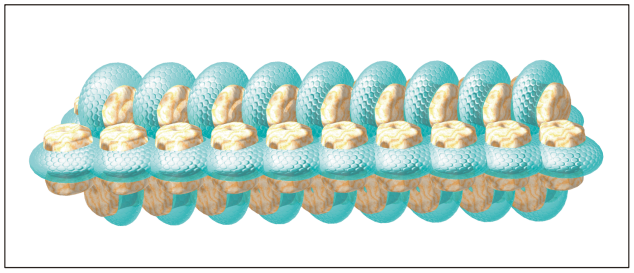

2D crystallisation

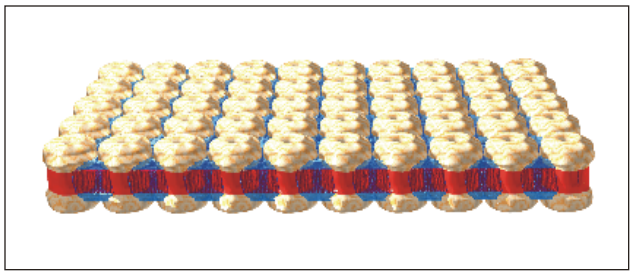

X-ray crystallography

Electron crystallography

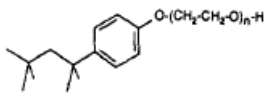

Triton X–100

Octylphenolpoly(ethyleneglycolether)$_n$

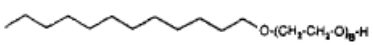

$C_{12}E_8$

Dodecylpoly(ethyleneglycolether)$_8$

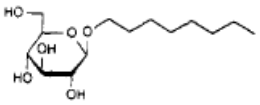

n_Octylglucoside

1-O-n-Octyl-β-D-glucopyranoside

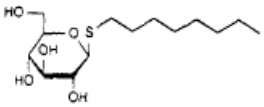

Octylthioglucoside

n-Octyl-1-thio-β-D-glucopyranoside

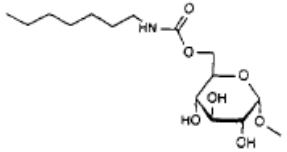

HECAMEG

6-O-(N-heptyl-carbamoyl)-methyl-α-D-glucopyranoside

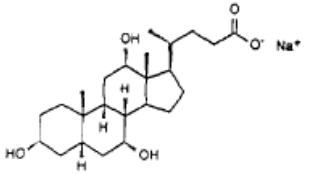

Cholic acid, sodium salt

Sodium cholate

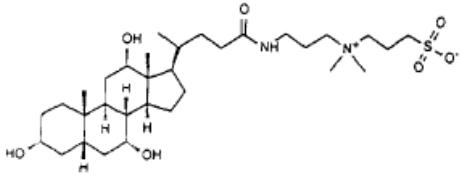

CHAPS

3-[(3-Cholamidopropyl)dimethylammonio]-1-propane-sulfonate

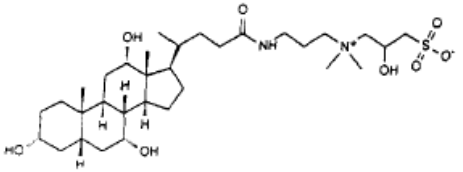

CHAPSO

3-[(3-Cholamidopropyl)dimethylammonio]-2-hydroxy-1-propane

-sulfonate

TABLE 1 PHYSICAL PROPERTIES OF COMMONLY USED DETERGENTS

Detergent	Monomer, Da mw	Micelle, Da mw	CMC % (w/v)	CMC Molarity
Anionic				
SDS	288	18,000	0.23	8.0×10^{-3}
Cholate	430	4,300	0.60	1.4×10^{-2}
Deoxycholate	432	4,200	0.21	5.0×10^{-3}
Cationic				
C_{16}TAB	365	62,000	0.04	1×10^{-3}
Amphoteric				
LysoPC	495	92,000	0.0004	7×10^{-6}
CHAPS	615	6,150	0.49	1.4×10^{-3}
Zwittergent 3-14	364	30,000	0.011	3.0×10^{-4}
Nonionic				
Octylglucoside	292	8,000	0.73	2.3×10^{-2}
Digitonin	1,229	70,000	-----	----
$C_{12}E_8$	542	65,000	0.005	8.7×10^{-5}
Lubrol	582	64,000	0.006	1.0×10^{-4}
Triton X-100	650	90,000	0.021	3.0×10^{-4}
Nonidet P-40	650	90,000	0.017	3.0×10^{-4}
Tween 80	1,310	76,000	0.002	1.2×10^{15}

critical micelle concentration

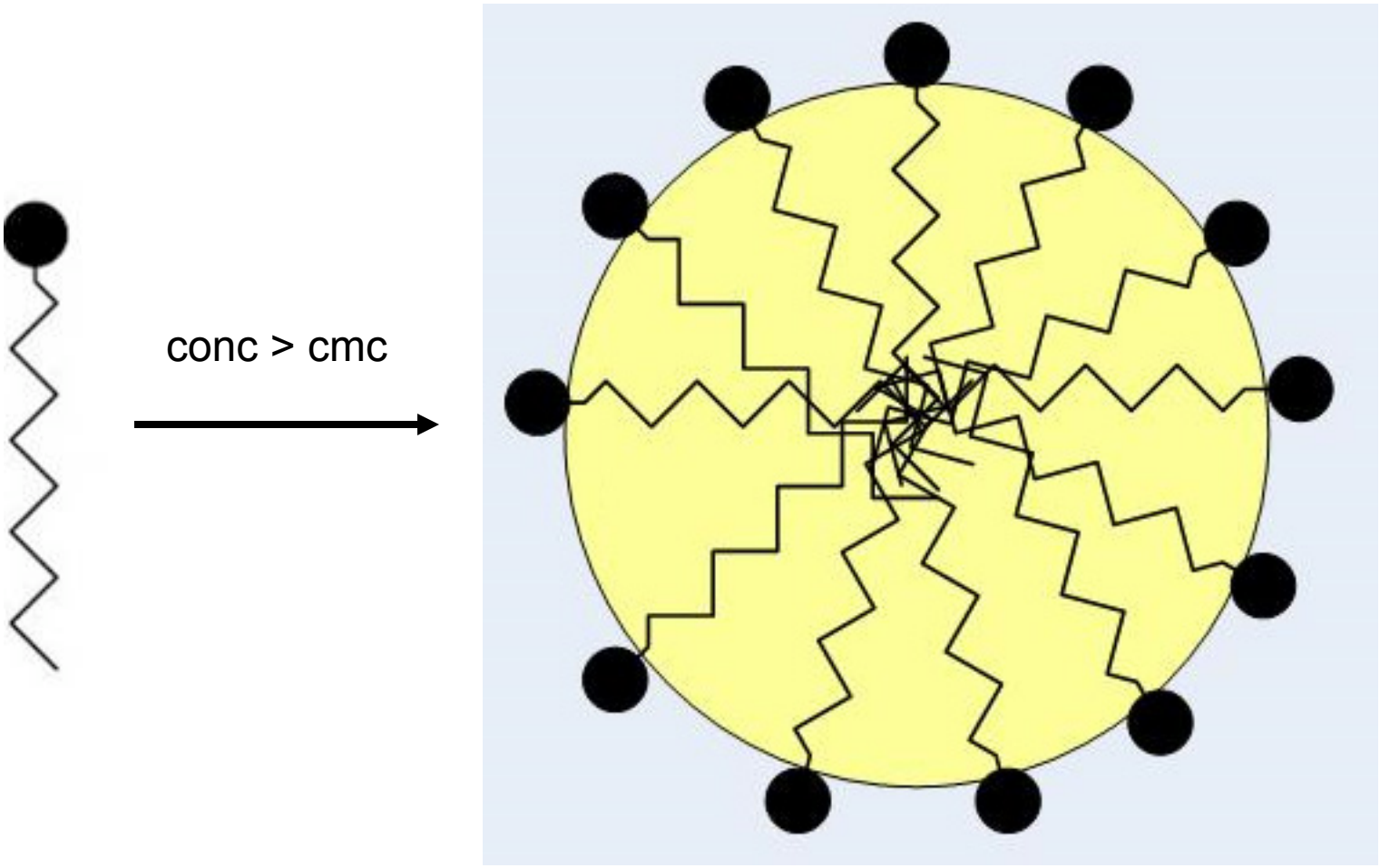

lipid solubilization by $C_{12}E_8$

(Levy, Rigaud et al. 1990)

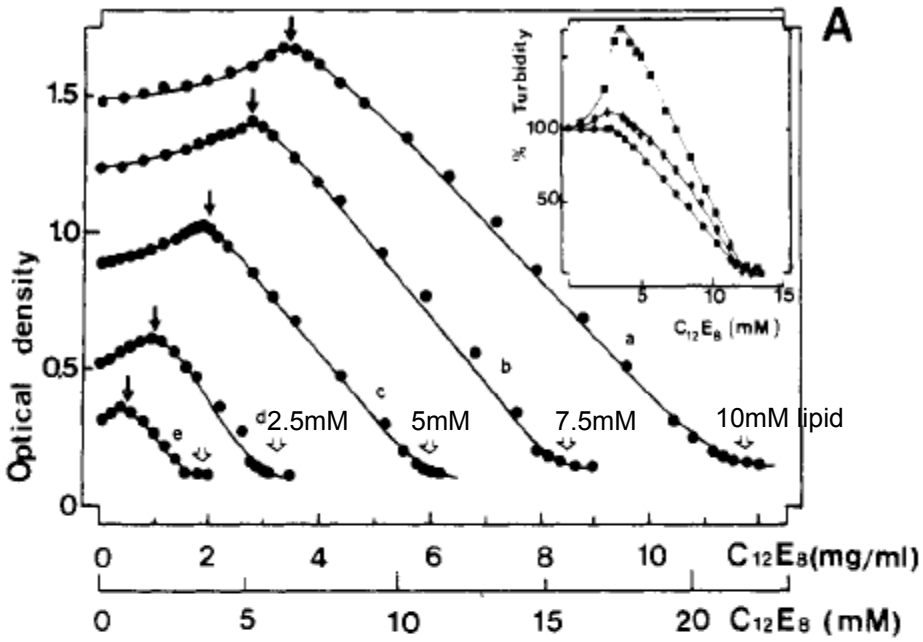

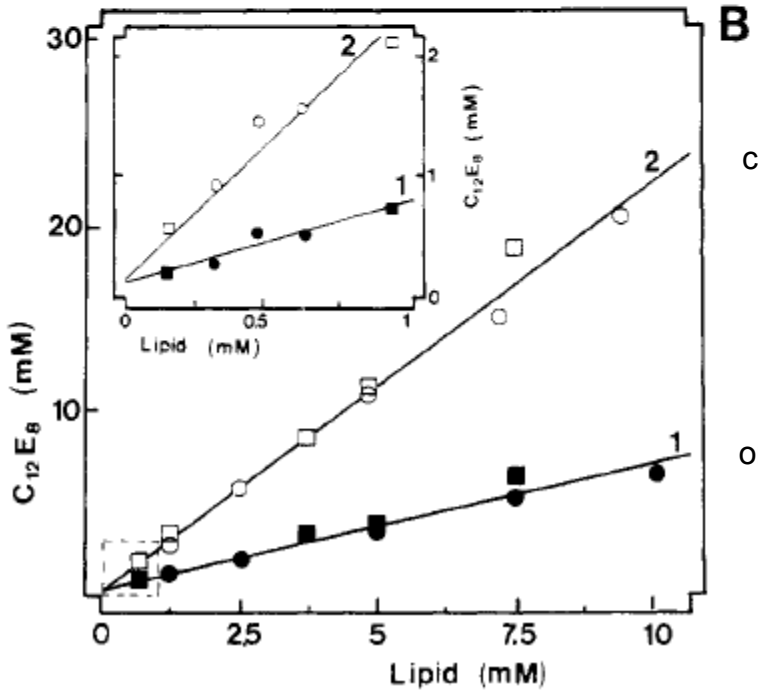

complete solubilization

onset of solubilization

Crystallization of OmpF by dilution

Hasler et al, 1998, Remigy 2003

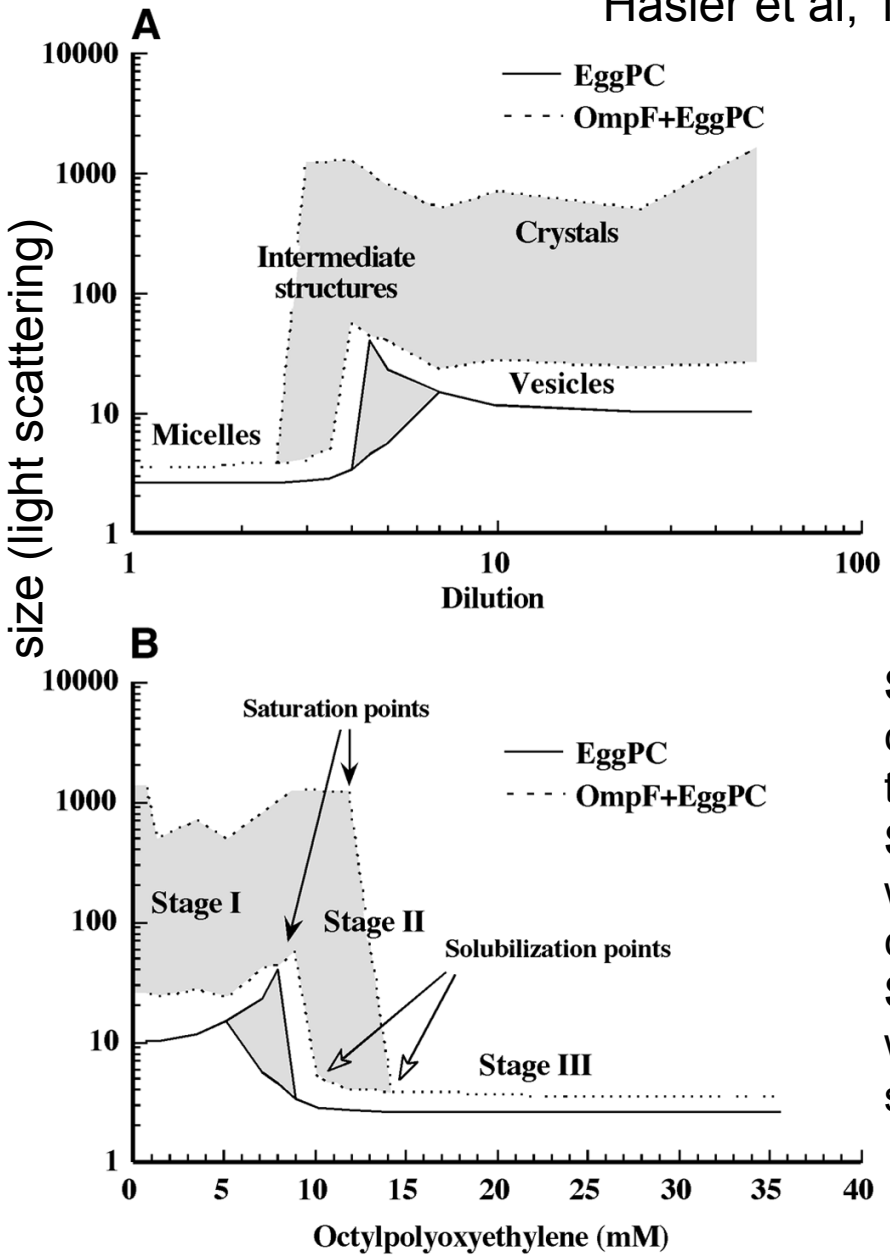

Stage I is characterized by a detergent concentration that is low enough not to disrupt the lipid bilayer.

Stage II is the region of detergent concentration where lipid bilayer and mixed micellar structures coexist.

Stage III covers the high detergent concentration where only small micellar structures occur. These specific regions are delineated by the ‘‘saturation

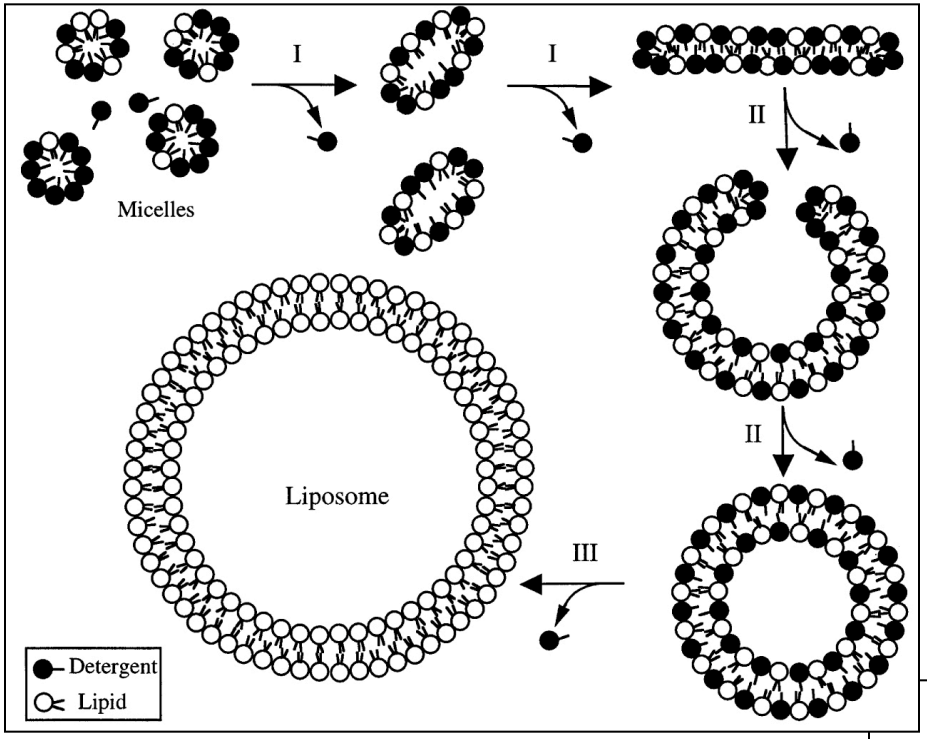

Lipid-detergent reconst

Protein-lipid-detergent reconst

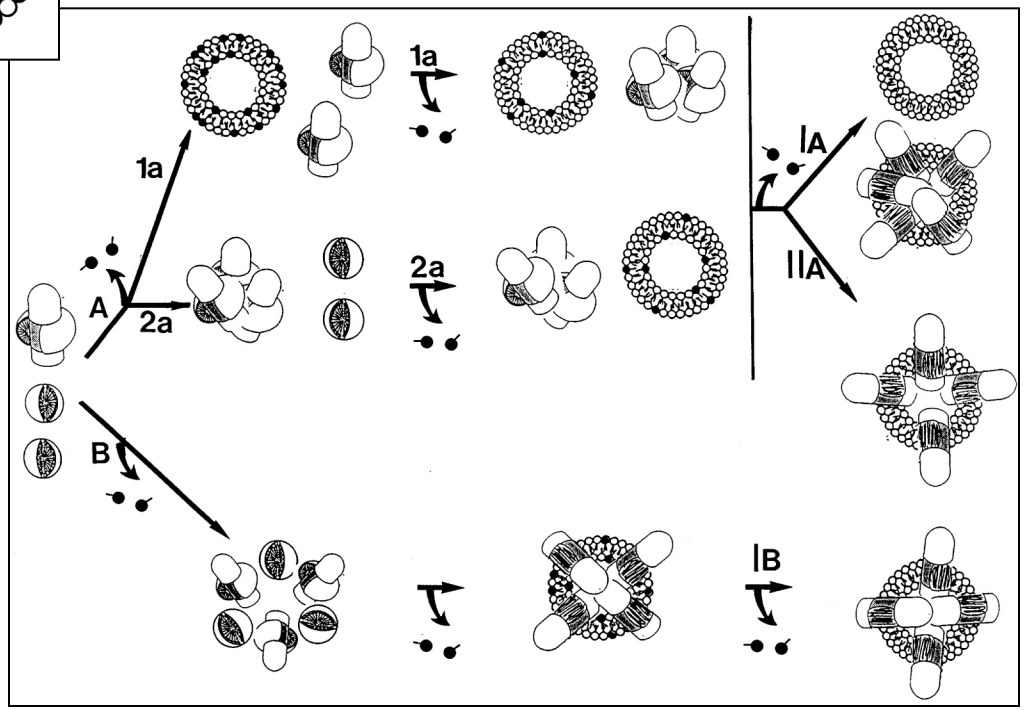

Detergent adsorption by Biobeads

(Rigaud et colleagues)

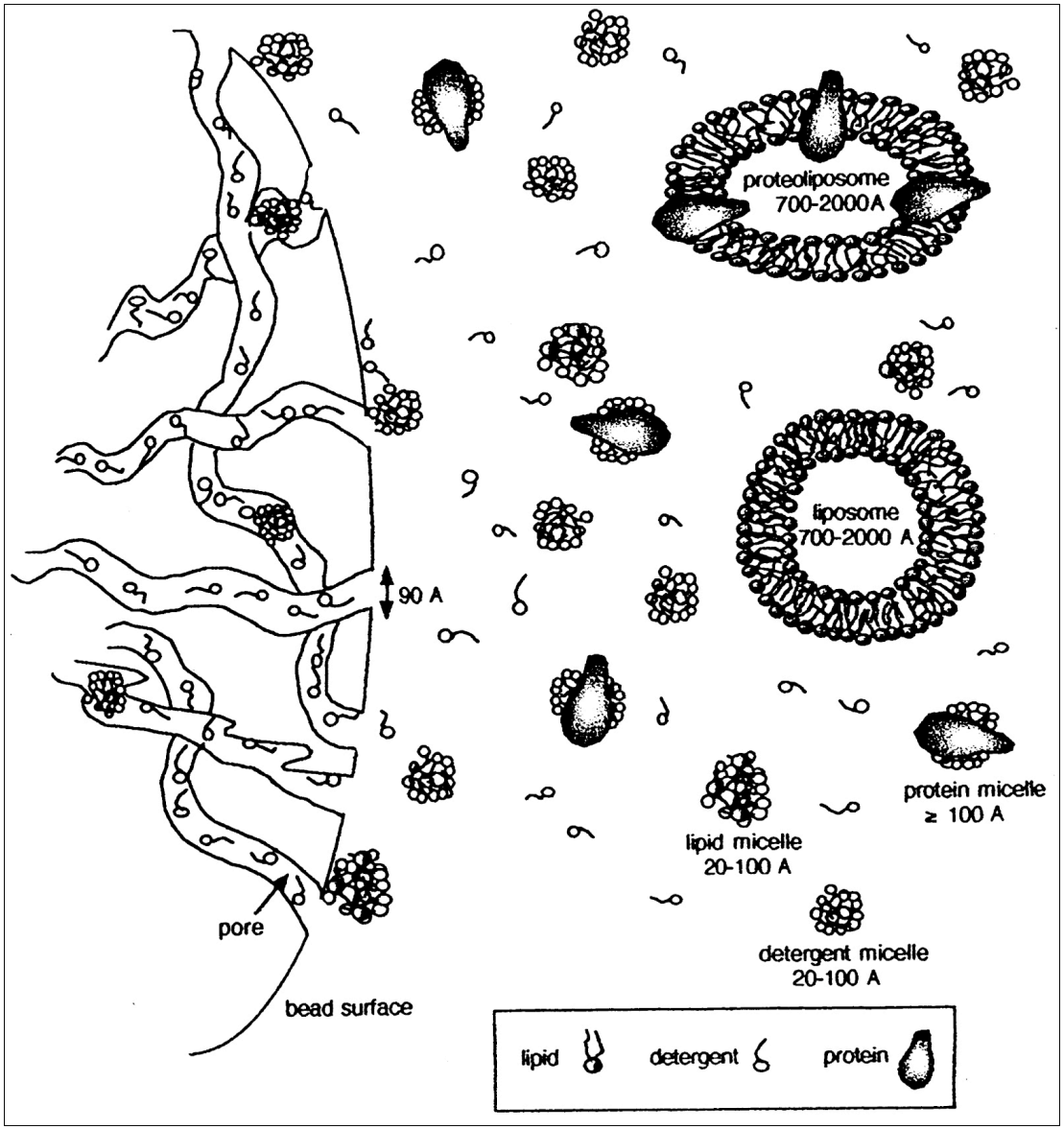

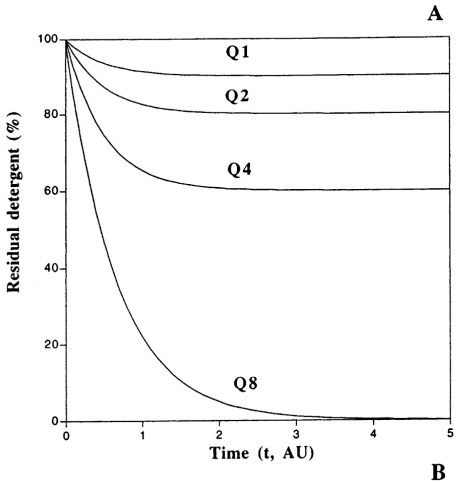

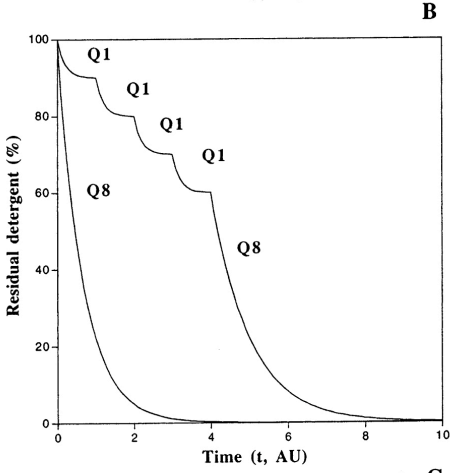

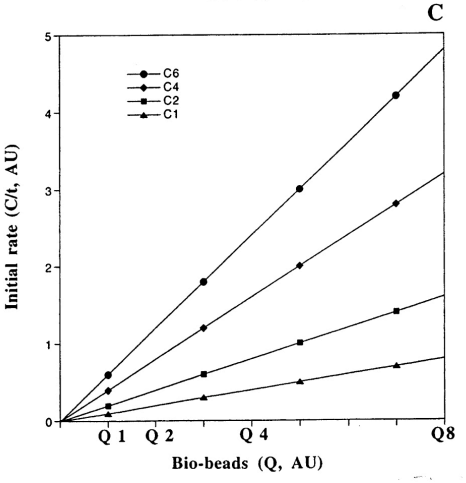

Crystallization by methyl-β-cyclodexrin adsorption

(Signorell, Engel, Remigy 2006)

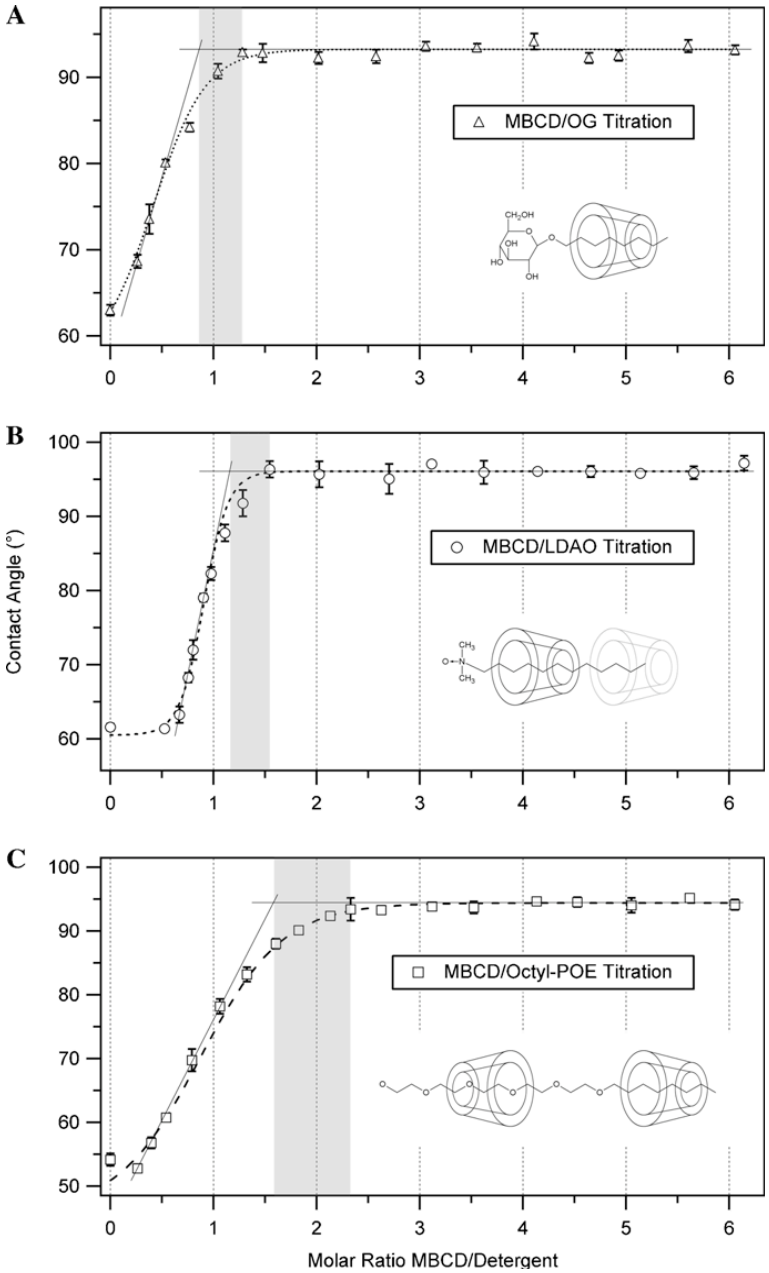

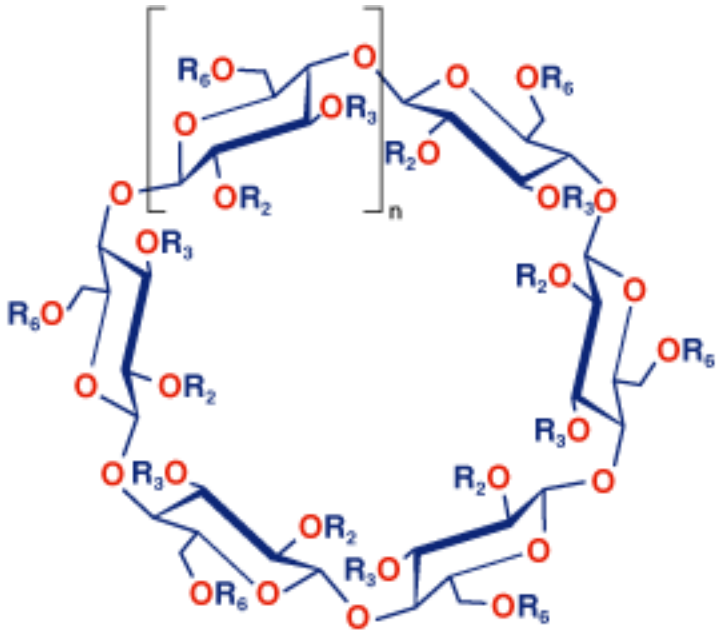

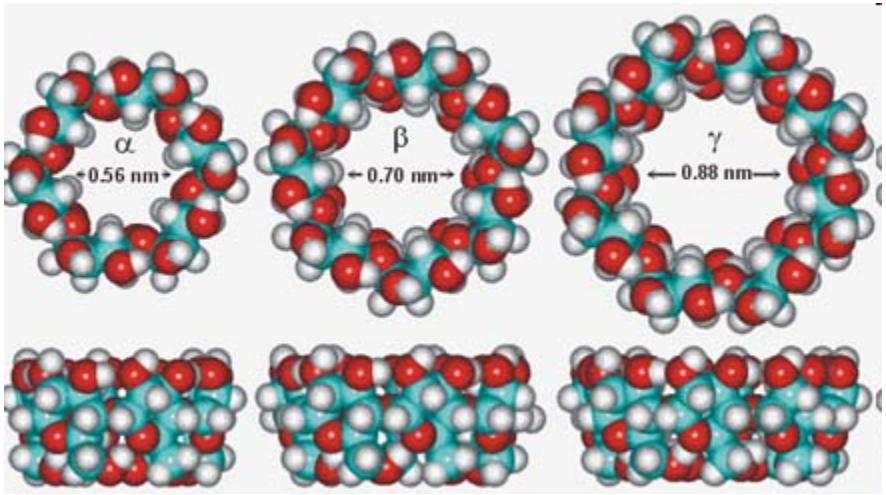

2D surface crystallization

(Levy, Mosser, Rigaud, 1999)

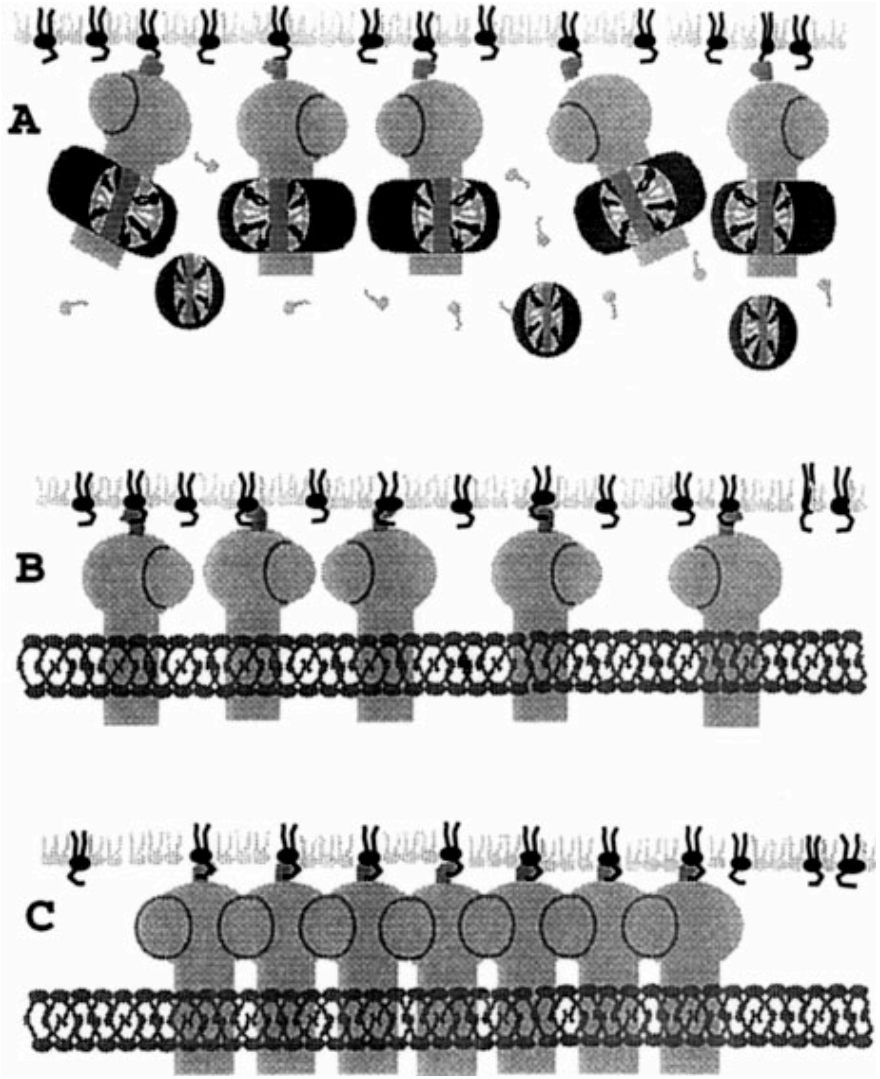

successful for FhuA & FoF1 ATPase

Use of Fluorinated lipids for 2D surface crystallization

(Lebeau et al. 2001)

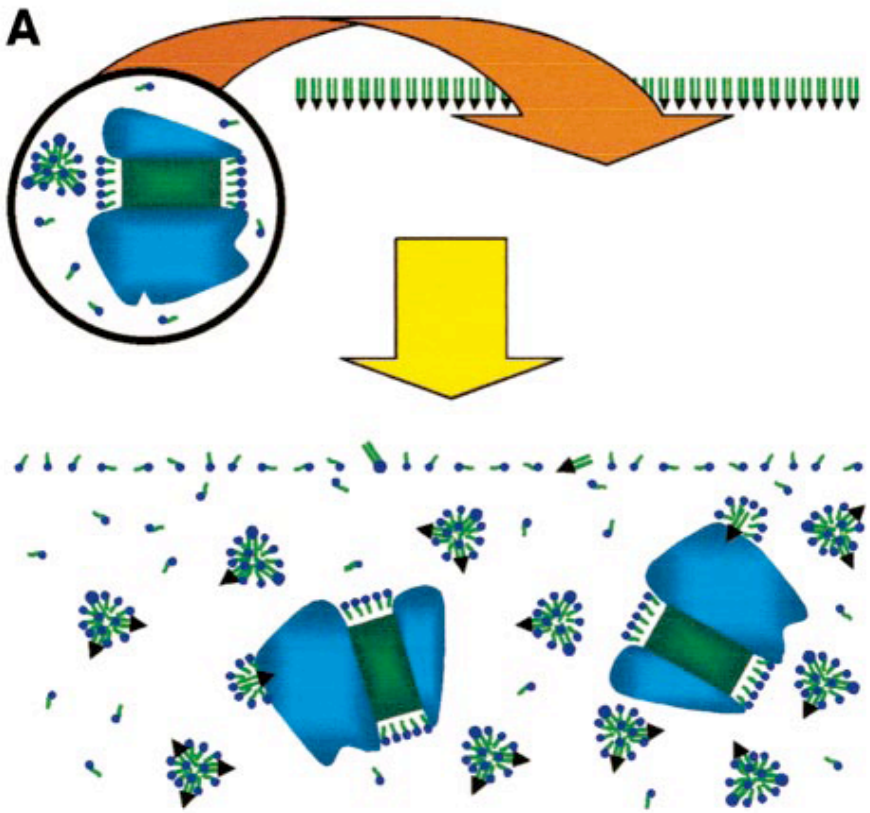

successful for H-ATPase

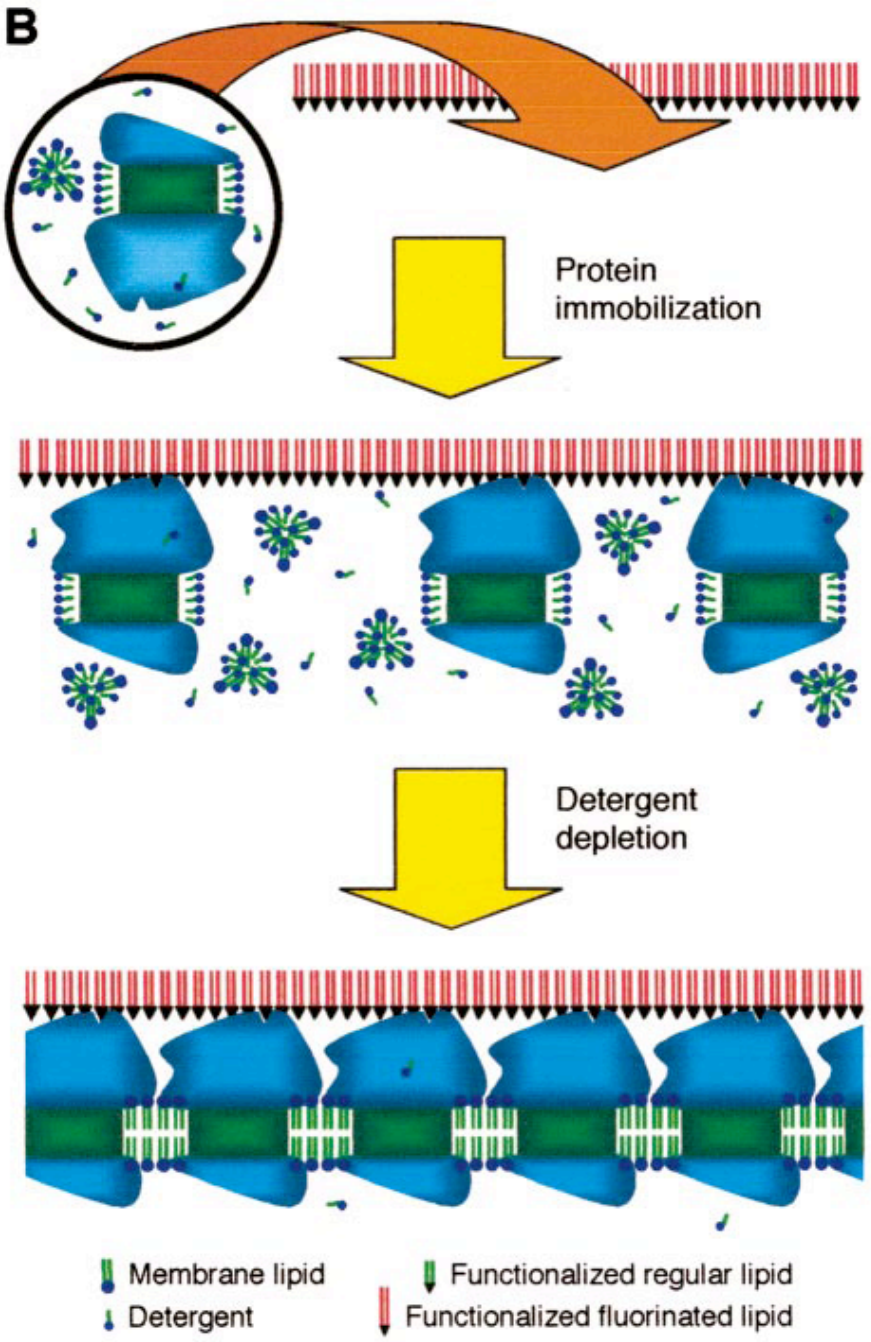

Crystallization by dialysis

Purify detergent-solubilized protein

Add lipids

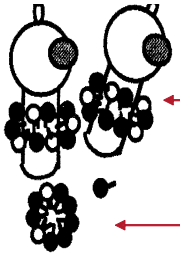

Protein micelle

Micelle

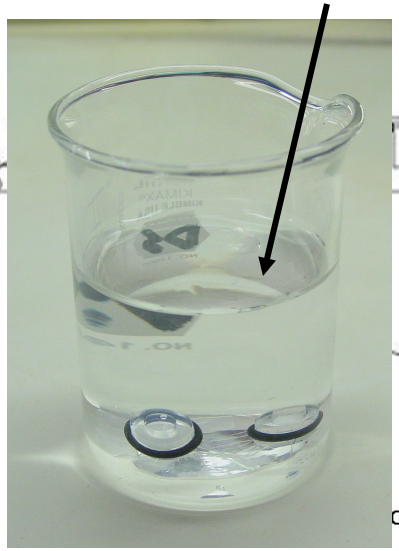

Dialysis buffer

remove detergent

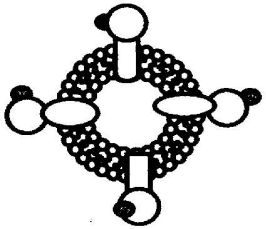

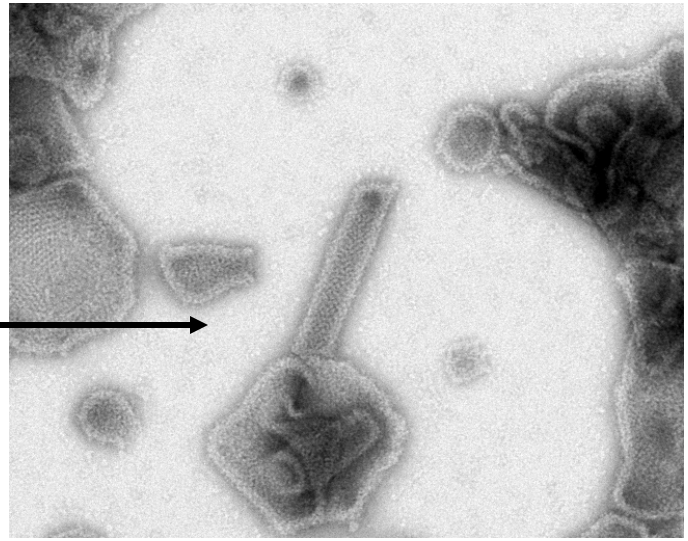

dialysis of detergent monomers

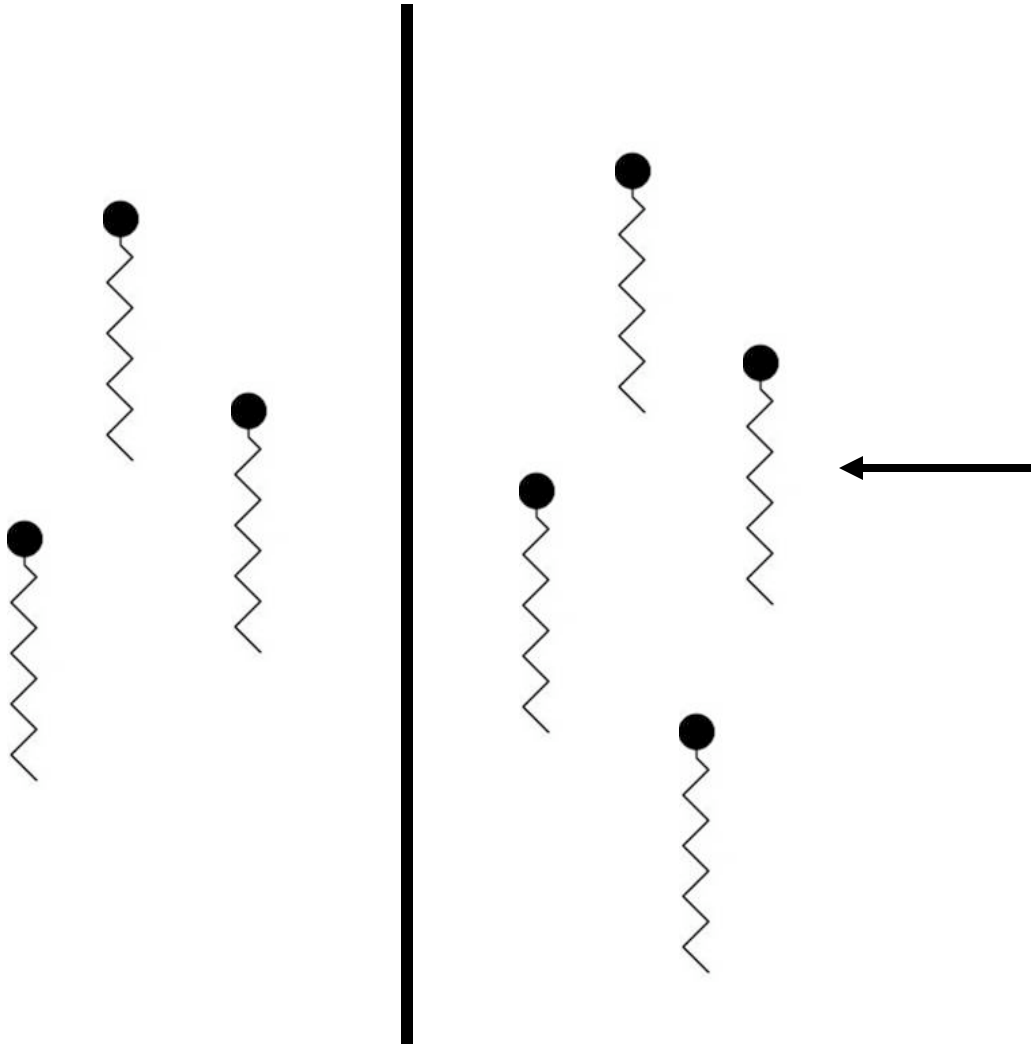

dialysis membrane

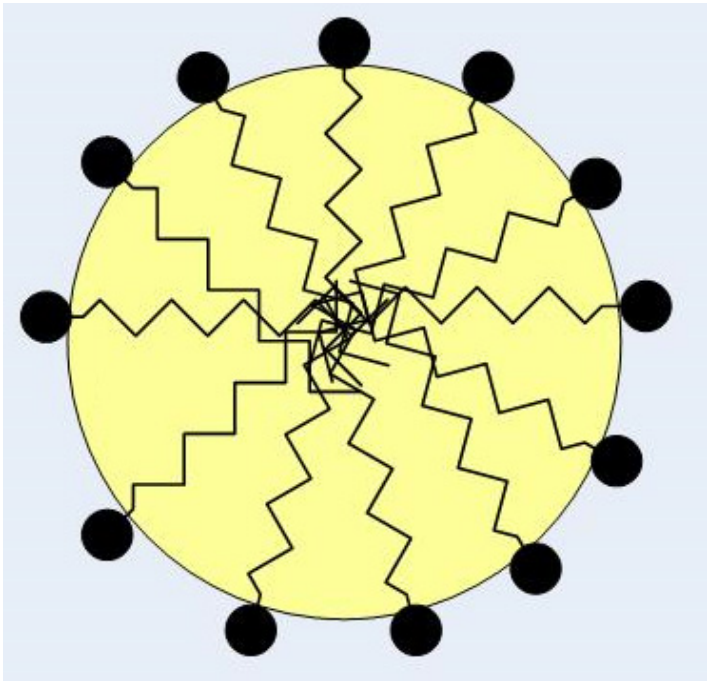

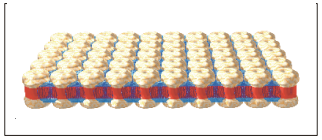

2D crystallization conditions:

Protein concentration: 0.4-1 mg/ml

Lipid type: DMPC, DOPC, POPC, DOPG, E. coli lipids

Lipid-to-protein-ratio (LPR, mg-mg): 0.2-1.5

Detergent type and concentration: DDM or OG

No precipitants used

Buffer: pH 6-8, monovalent/divalent cations, catalytically/conformationally active compounds

Multichannel (30) dialysis device

(H. Stahlberg)

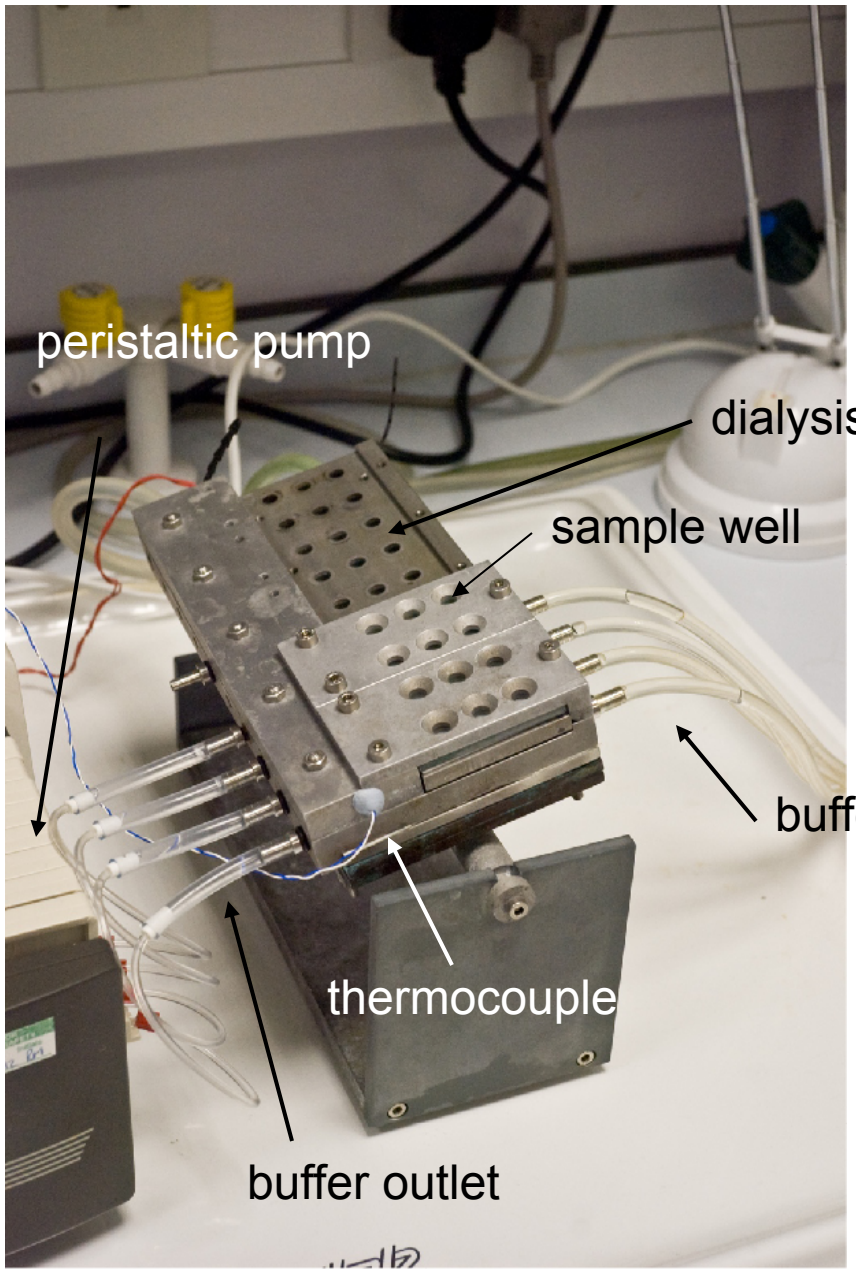

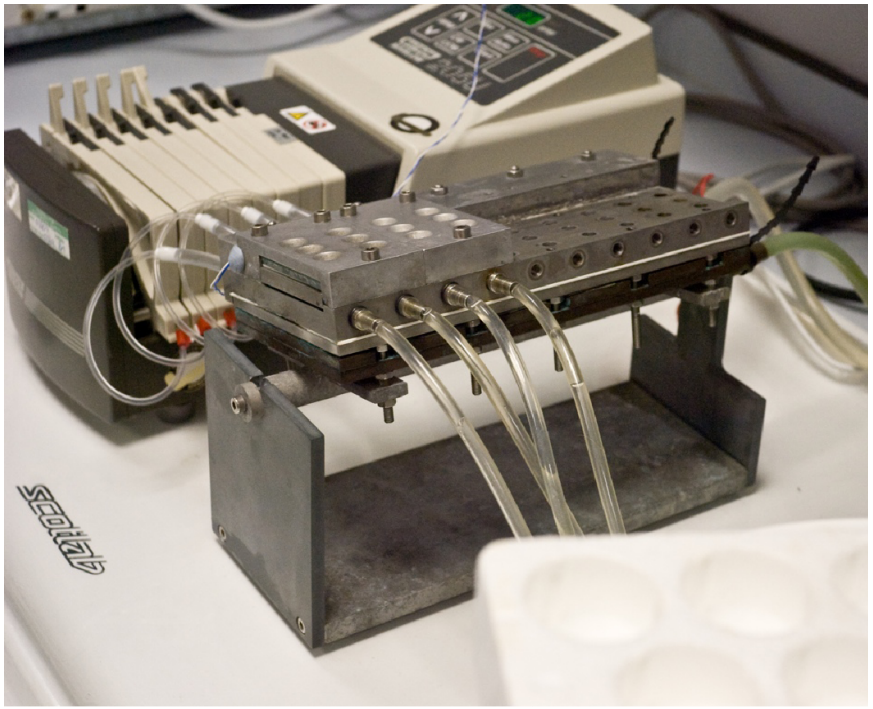

96-well dialysis block

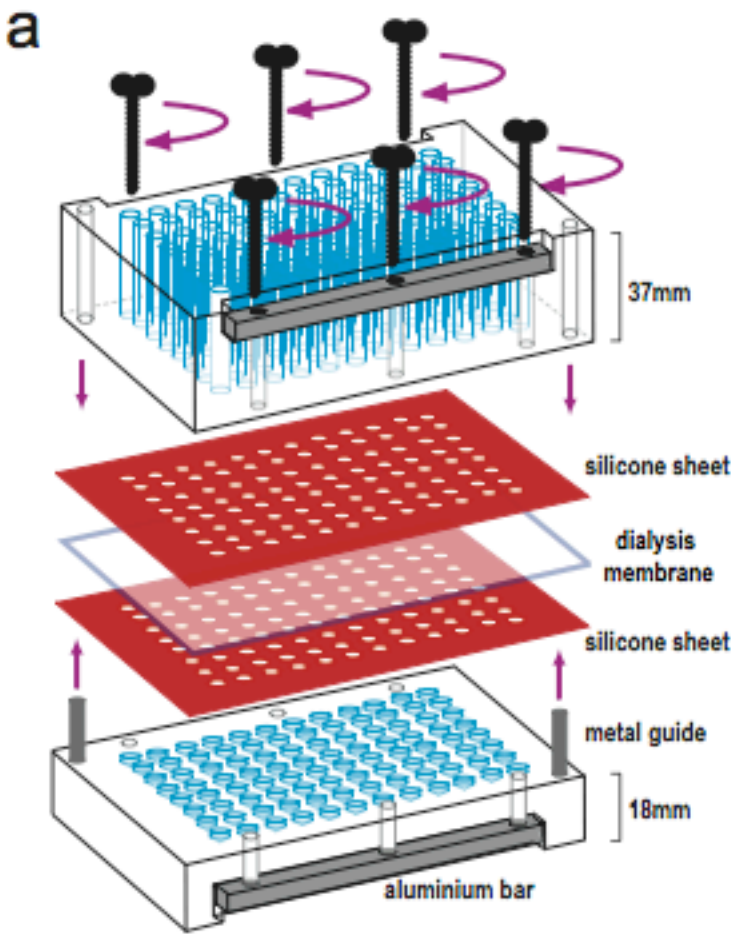

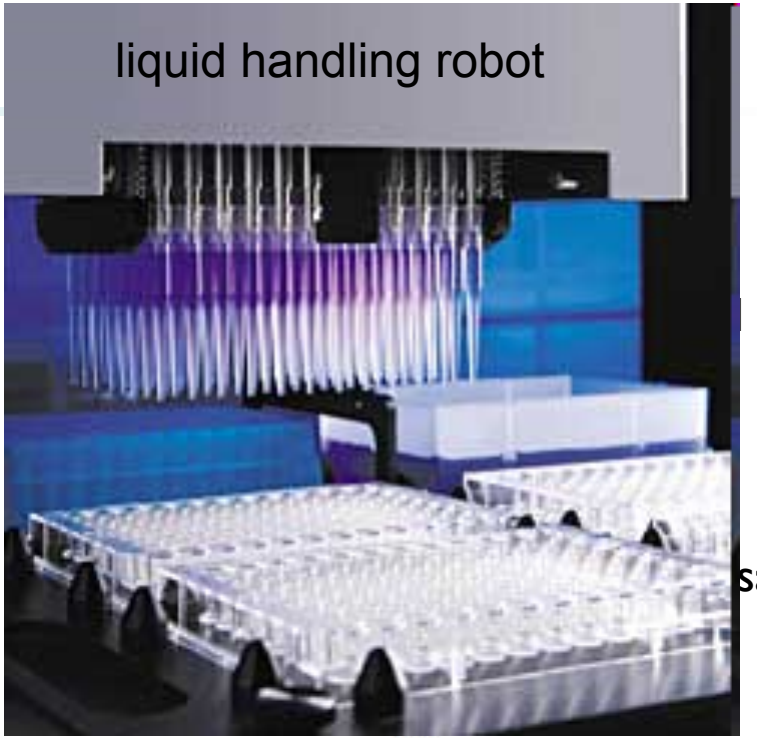

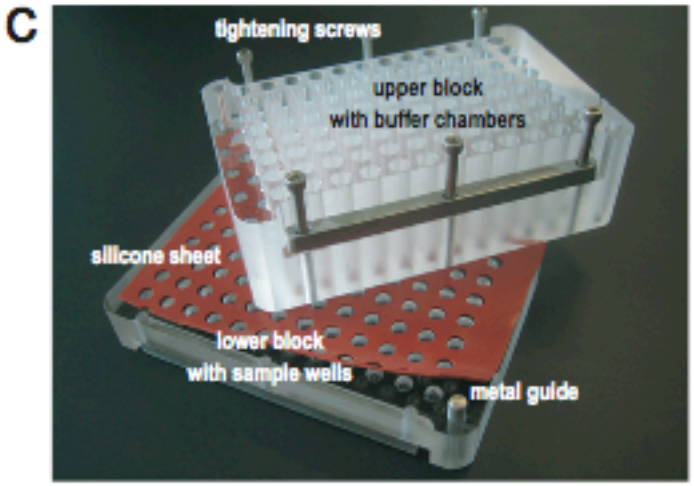

Time course for removal of low and high CMC detergents

octylglucoside (cmc=7.3mg/ml)

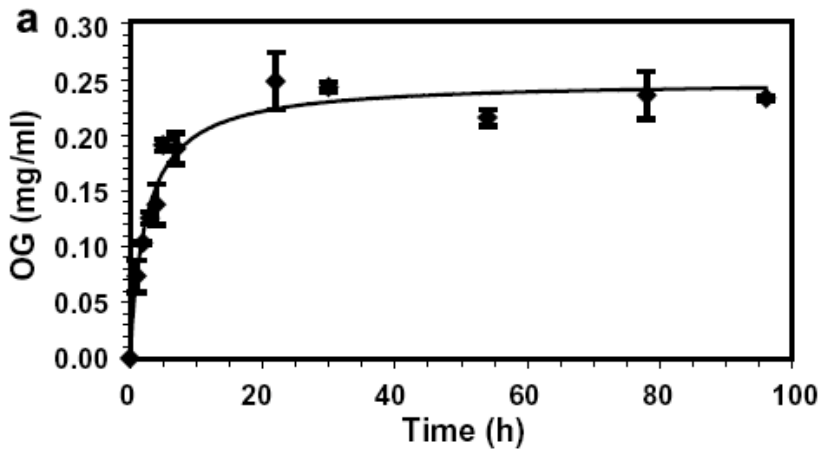

docecylmaltoside (cmc=0.05mg/ml)

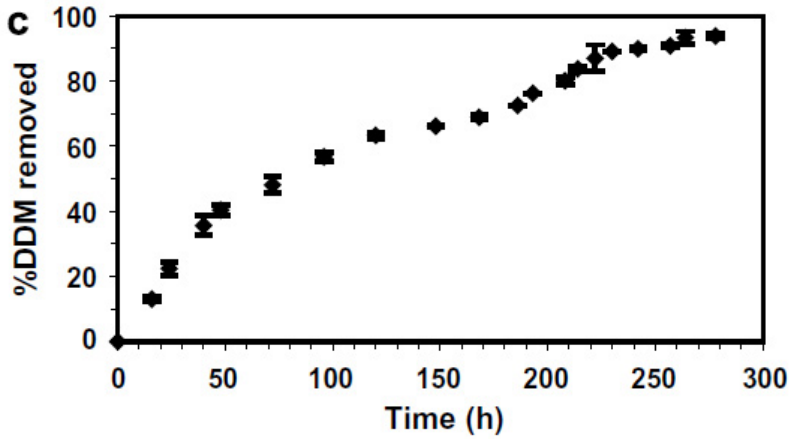

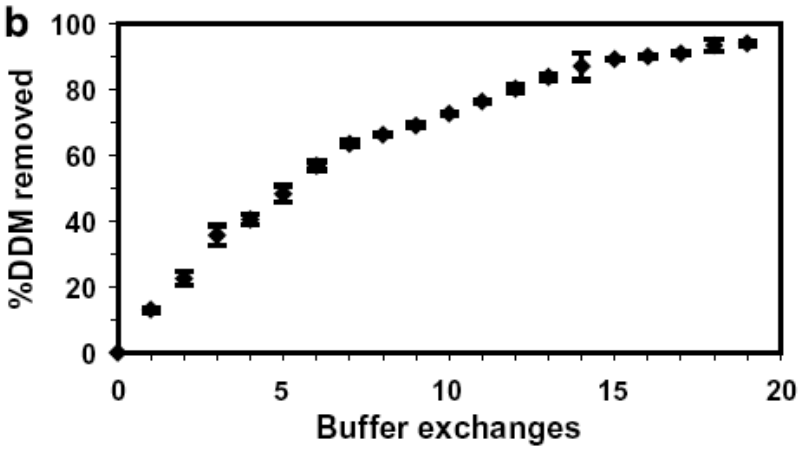

Microfluidic dialysis block
(GN Biosystems)

microfluidic dialysis tray (4-10 μl)

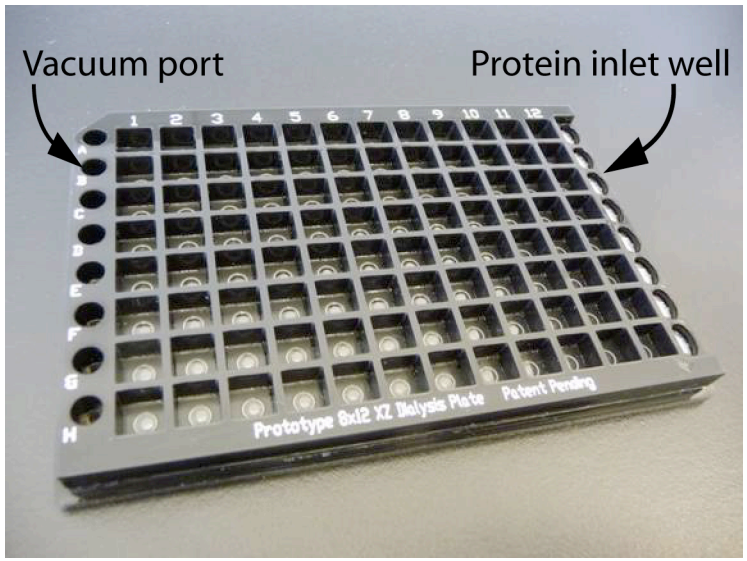

Programmable temperature (cycling)

Variomag thermoshake

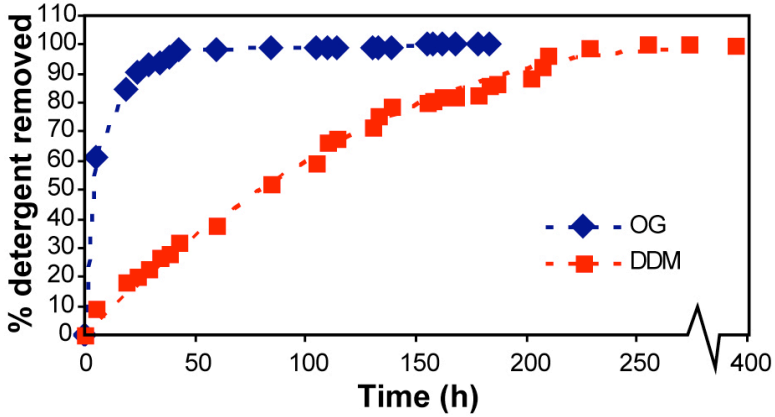

cyclodextrin dispensing robot

(Engel & colleagues)

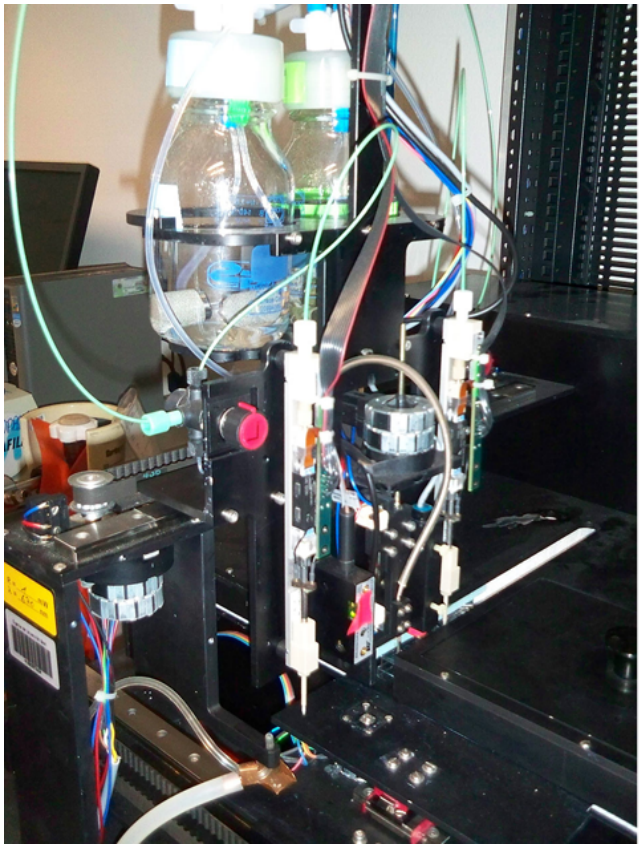

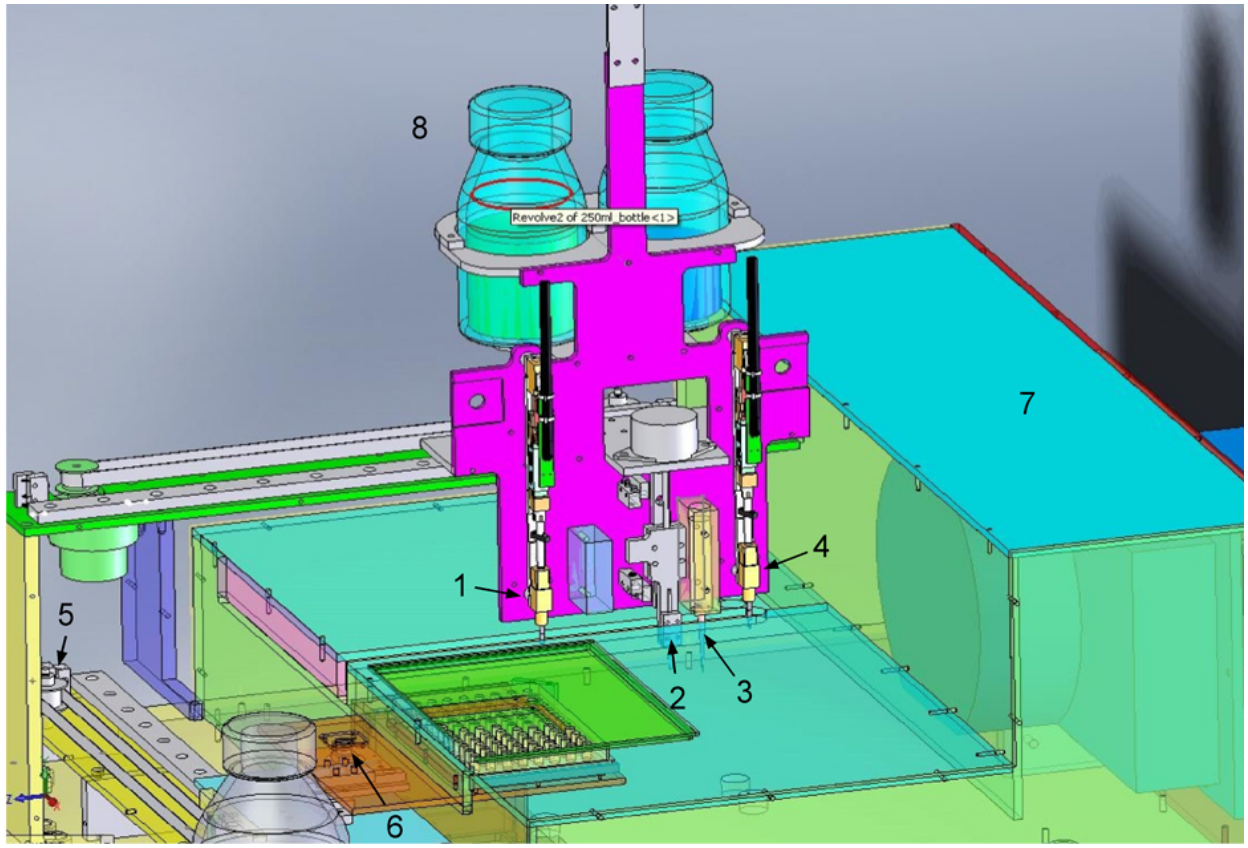

2-10 ul well volumes

(1) pipettor for cyclodextrin addition, (2) capacitive sensor for liquid level.
(3) laser system for light scattering. (4) second pipettor for maintaining the liquid level.
(5) Stepper motors control the X-Y. (6) shaker
(7) A cooling/heating element. (8) Solutions are stored in bottles under pressure.

Negatively staining of 96 specimens for evaluation by EM

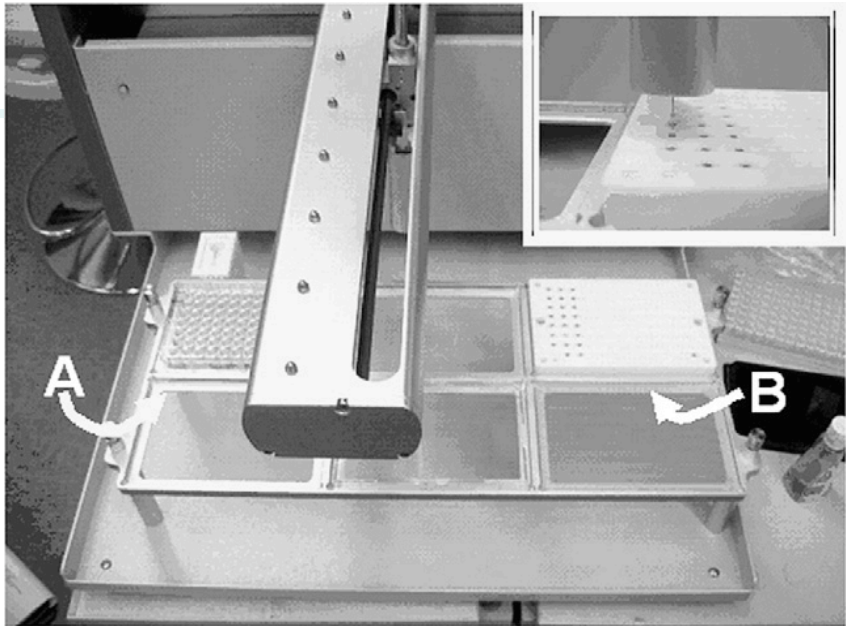

Cheng . . . Potter, 2007, JSB

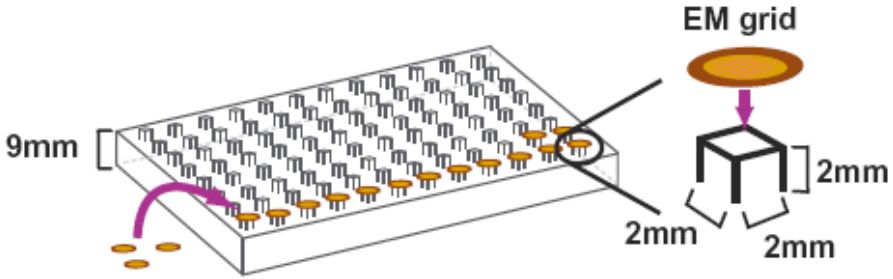

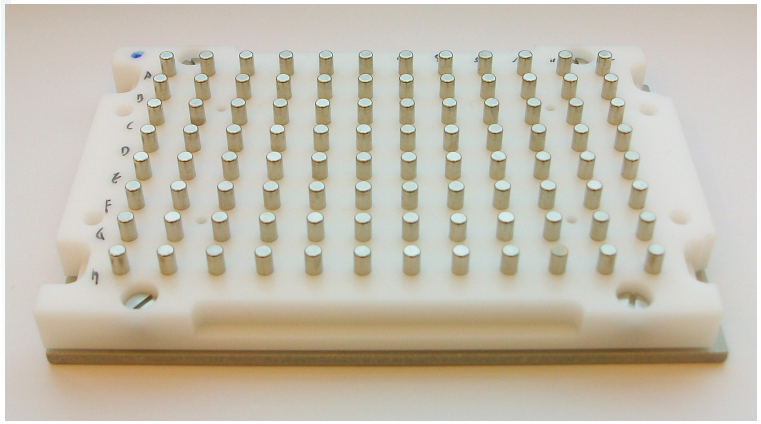

Magnetic 96-format platform
Nickel EM grids
Final blot with filter paper 8 at-a-time

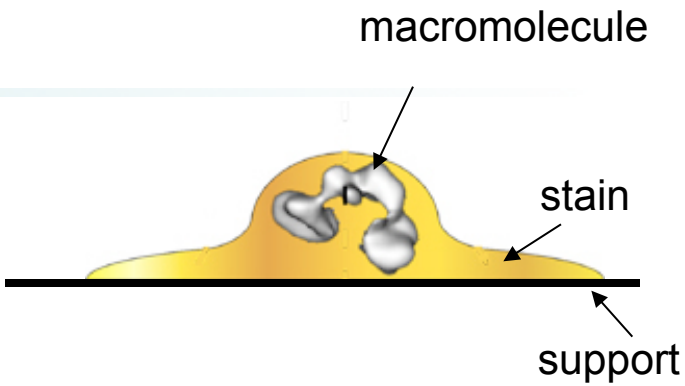

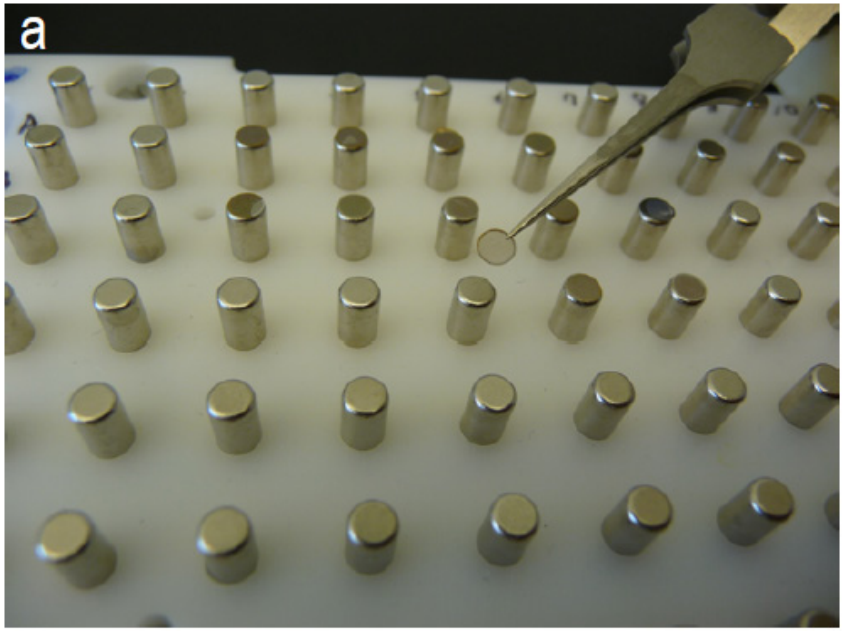

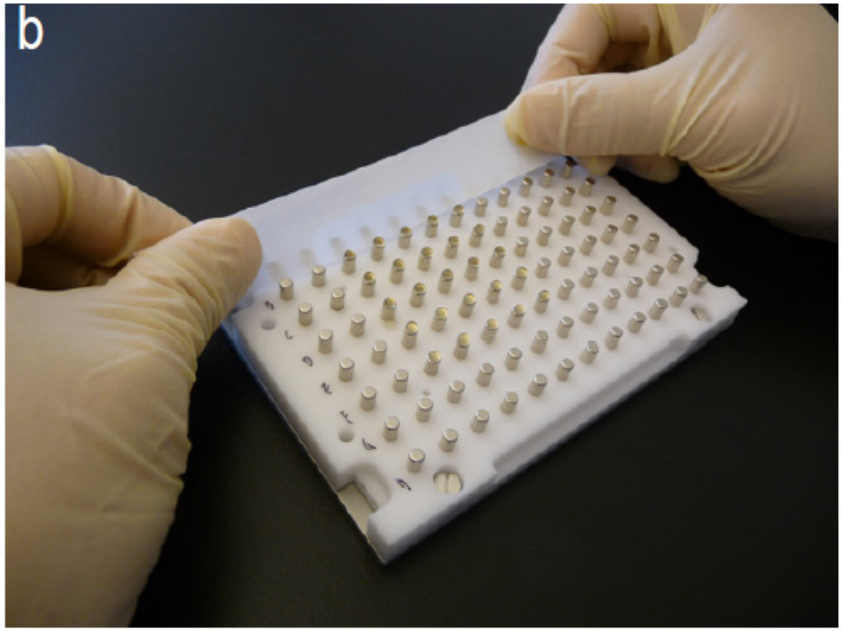

Imaging

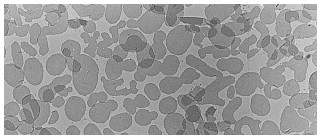

Need to image 96 grids in the electron microscope

Scara = John

Cartesian = Henry

John Koss
Kevin D'Amico
Argonne Lab

John loads the grid into the holder

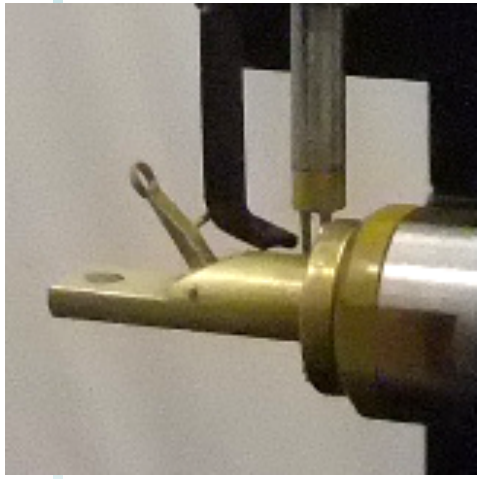

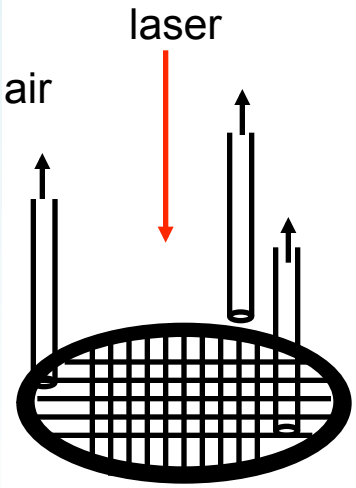

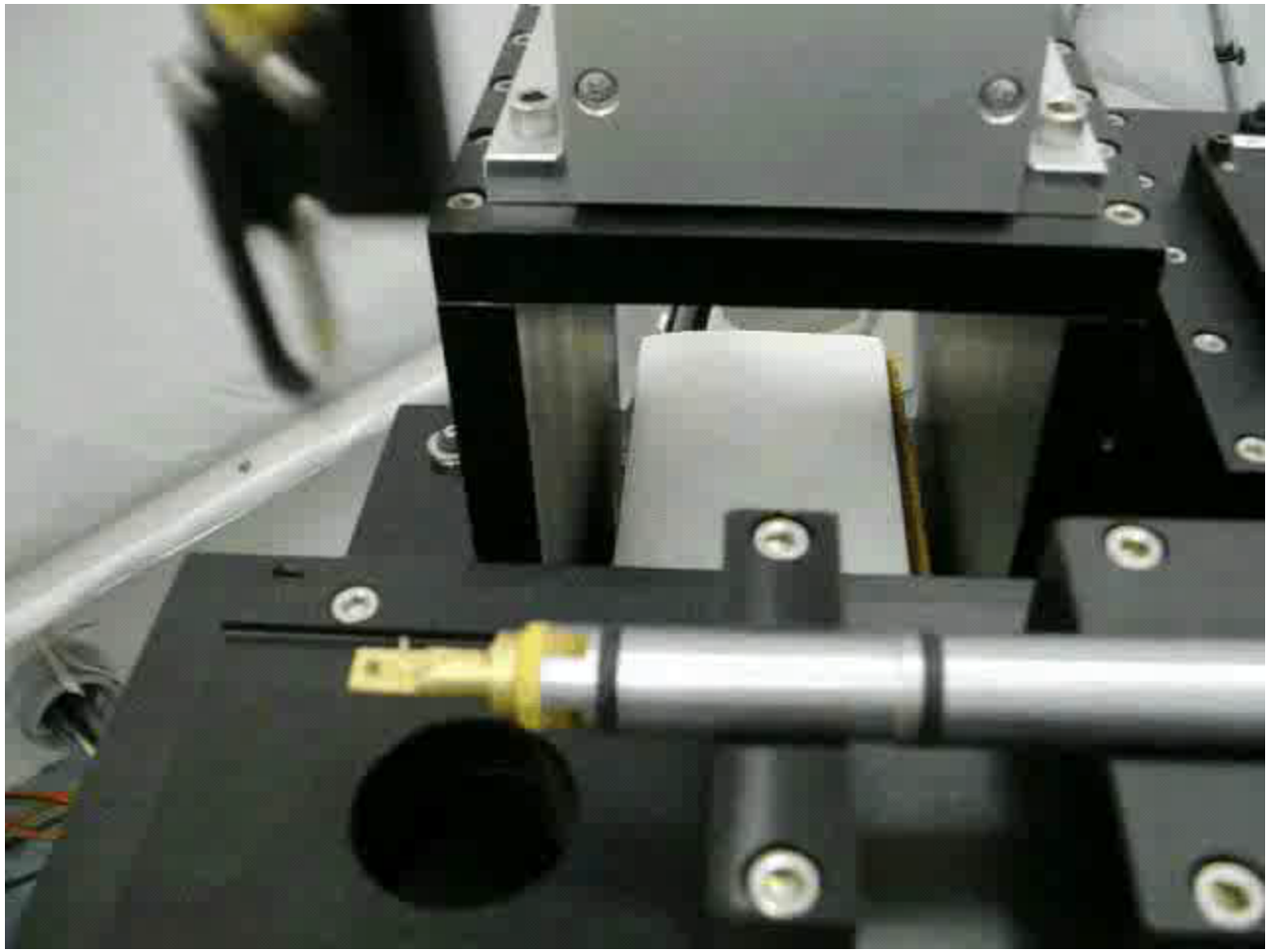

LEGINON SOFTWARE CONTROLS ROBOT AND 2DX IMAGING

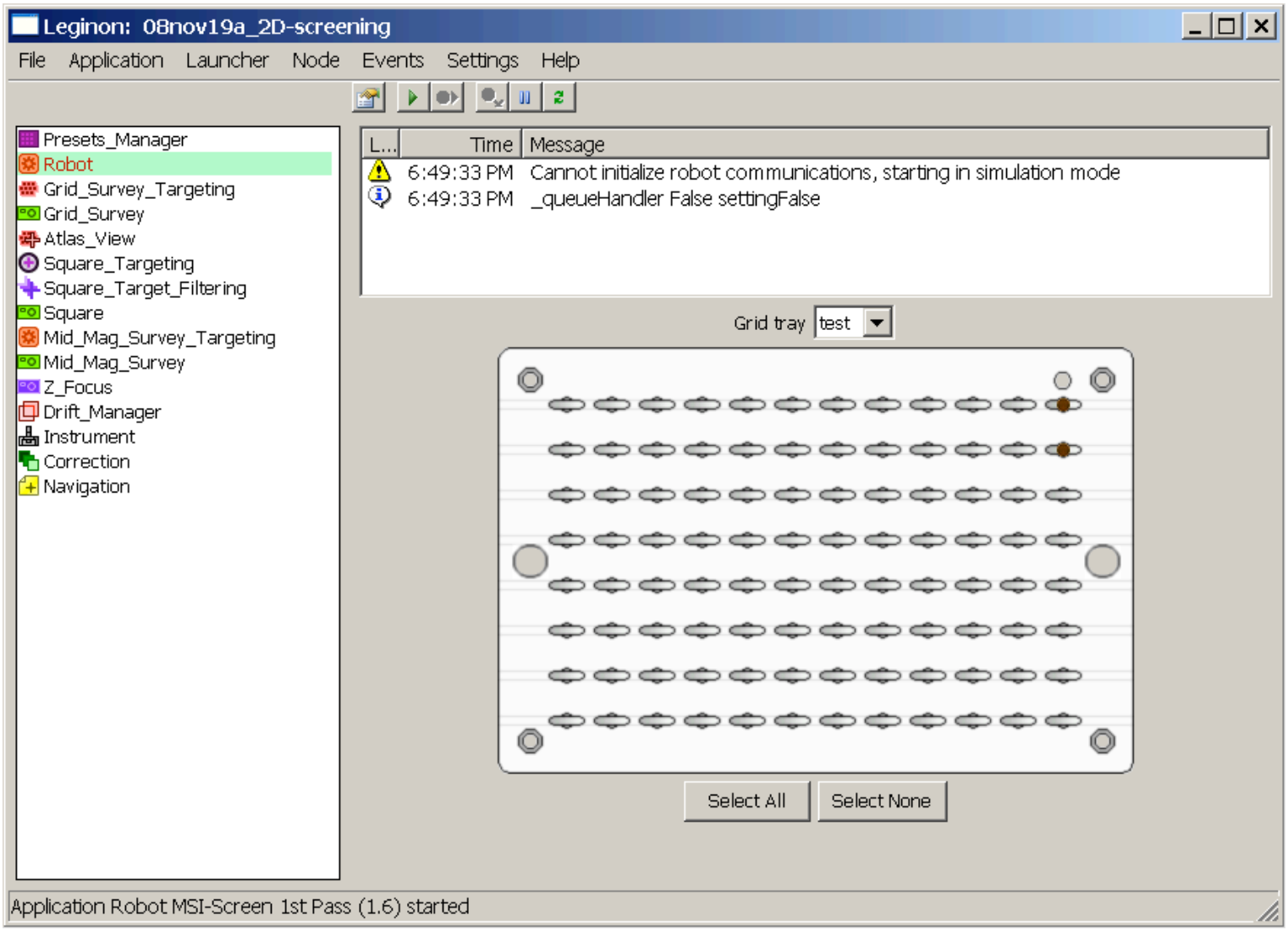

LEGINON is a system designed for automated collection of images by TEM (NRAMM at Scripps)

NRAMM
National Resource for Automated Molecular Microscopy
Supported by National Center for Research Resources

Define montage image area (e.g. 3x3)

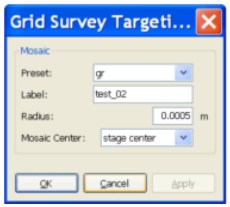

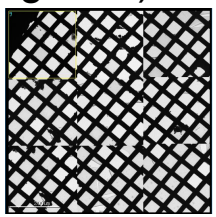

Take a images at low mag

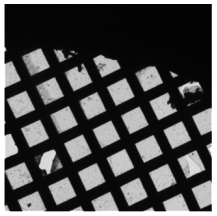

Pick target squares using square finder (histogram criteria)

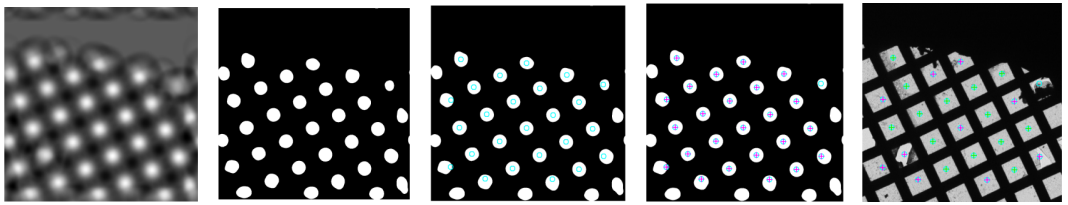

Take images of selected squares

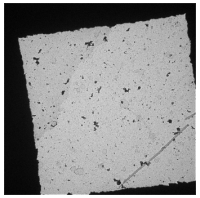

Pick targets from square images (histogram criteria)

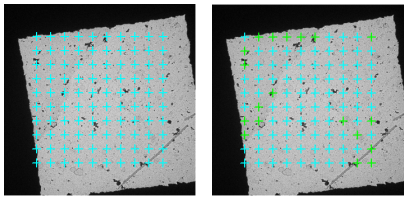

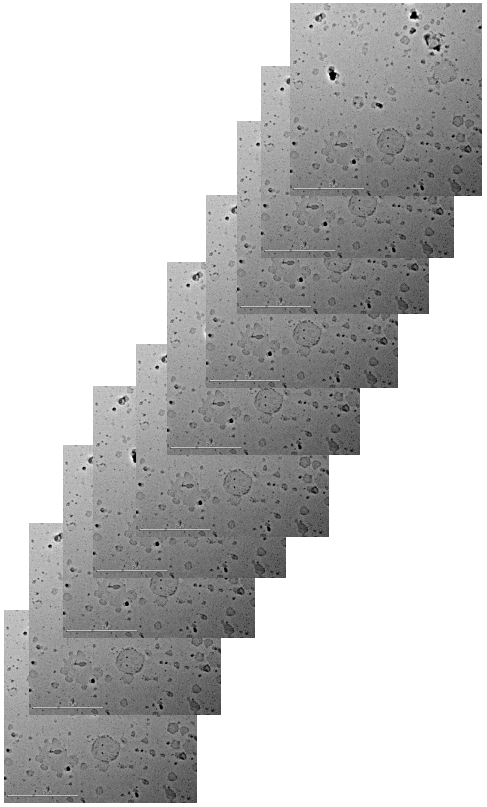

Take images at intermediate mag for evaluation

Density histogram evaluated to select suitable areas for ima

Metal grid square

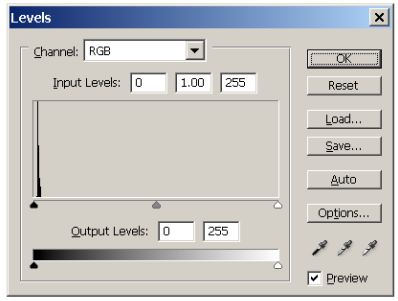

Edge of grid square

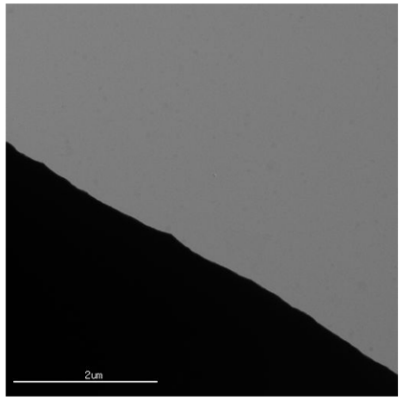

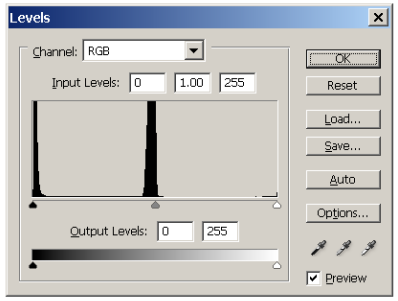

Sample present

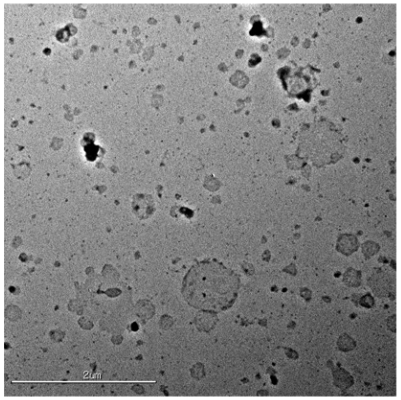

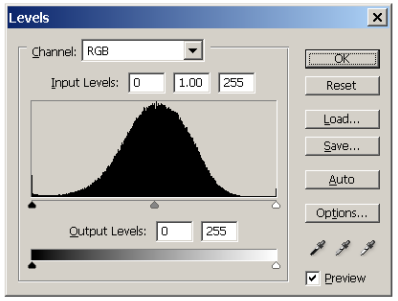

Broken support film

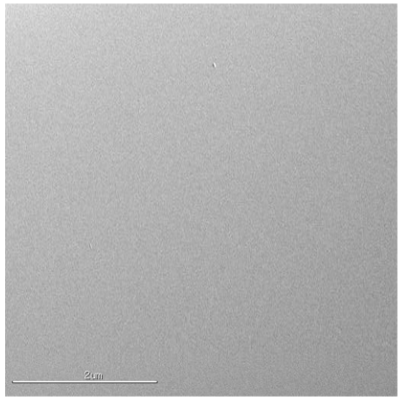

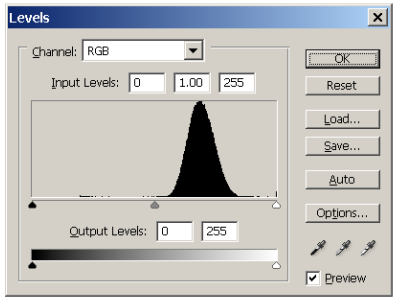

Shape recognition algorithms (neural net) represents a (near

autoloader on FEI T12

(Engel)

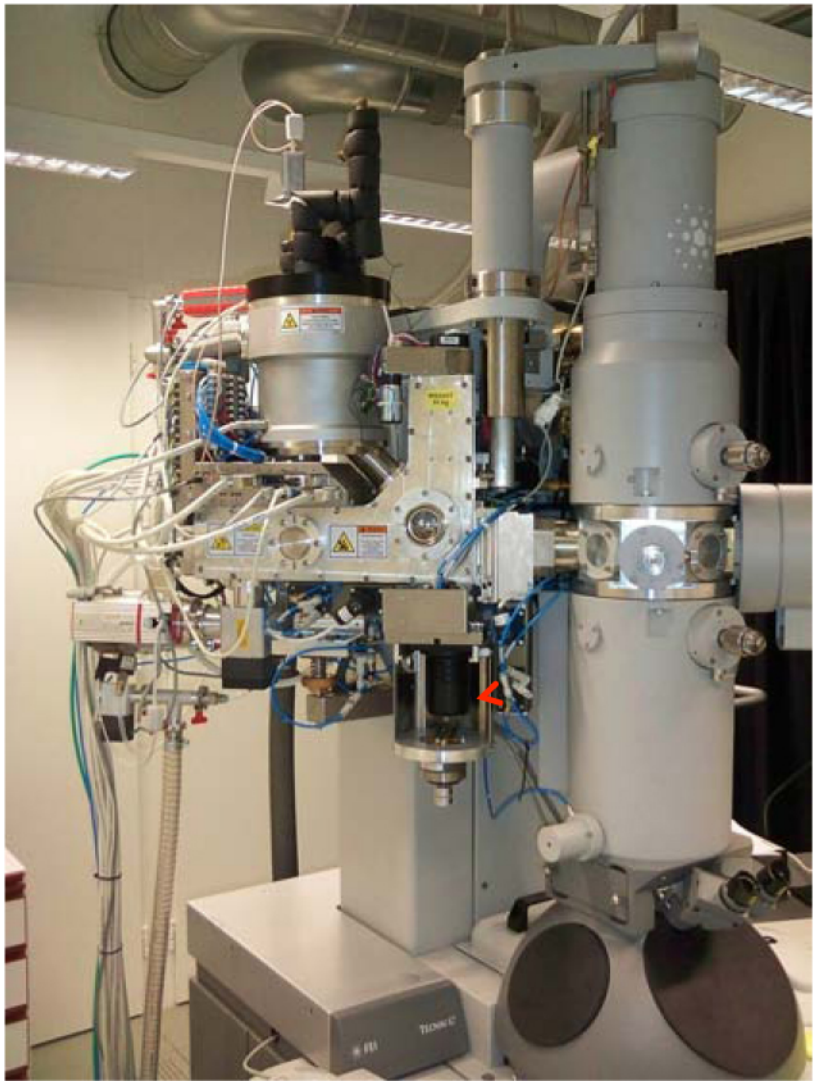

A

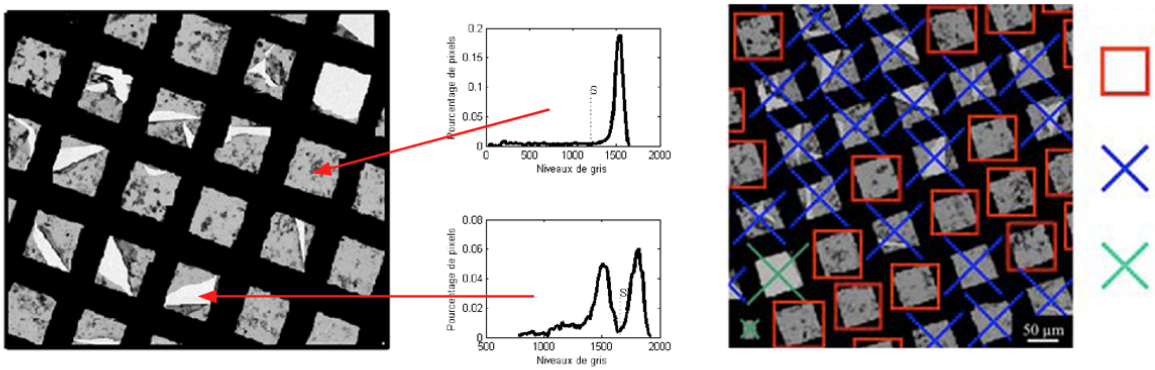

2dx_hunter
(Engel)

B

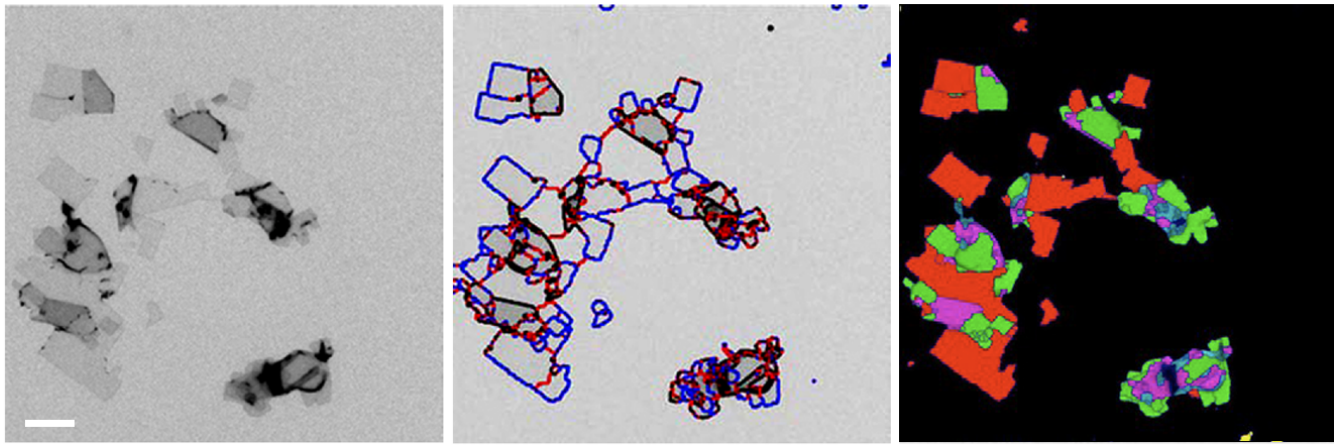

C

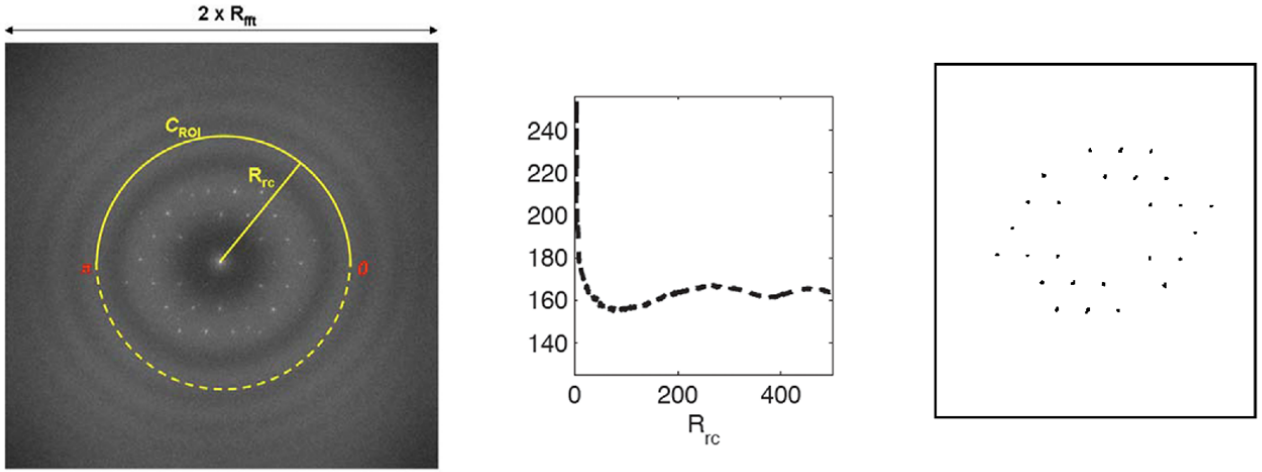

Gatling Gun

(Lefman & Subramaniam, 2007, JSB)

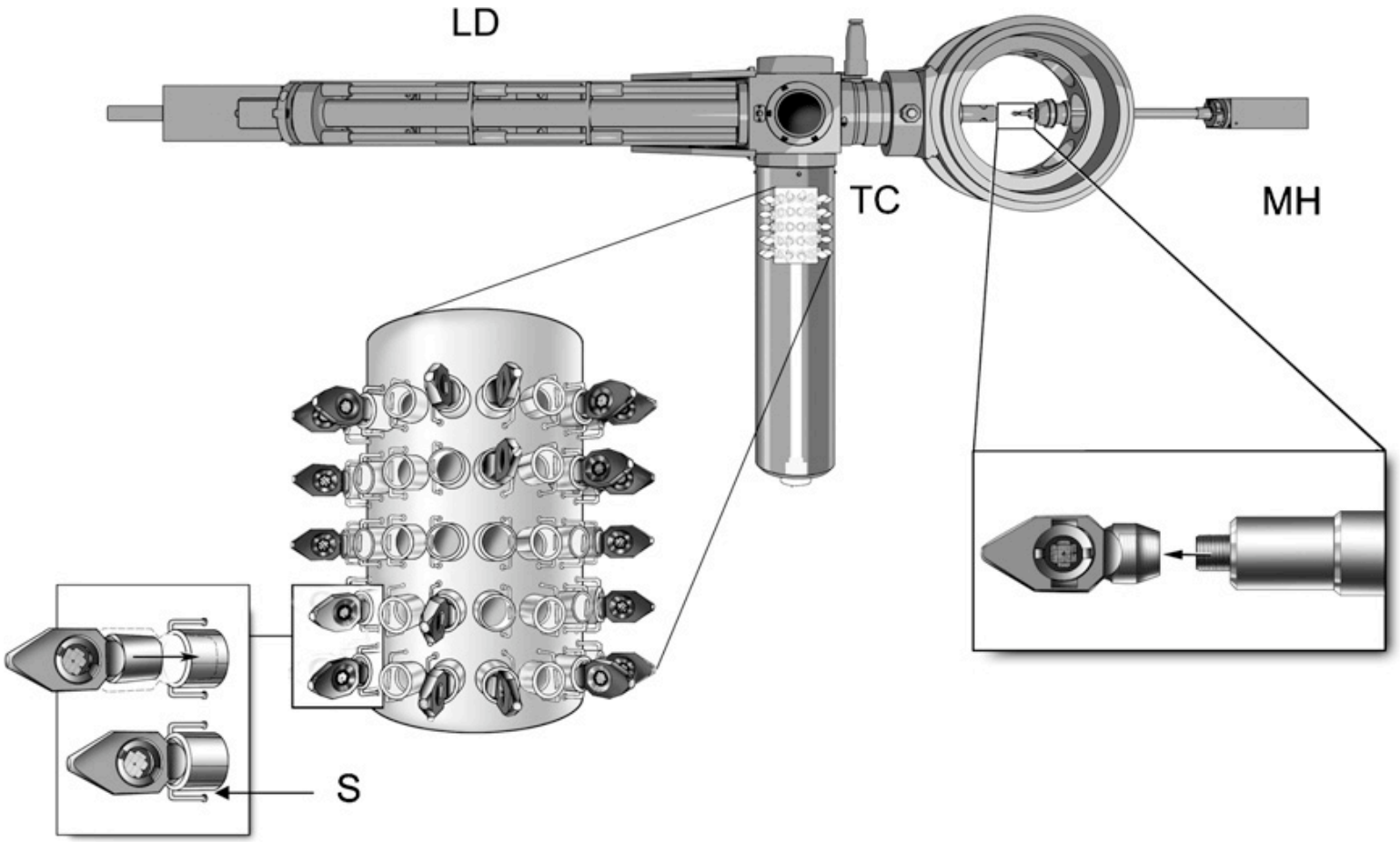

Classification of imaged objects

Class
A: Crystal with Lattice Pattern
B: Tubular Vesicle, Vesicle Sheet and Physical Growth
C: Vesicle, Vesicle Cluster, TV with irregular tubular vesicle
D: Protein aggregate and lipid aggregate
E: String of Lipid and Multi Lamella Lipid
F: Aggregate or Precipitate in solution

Class B

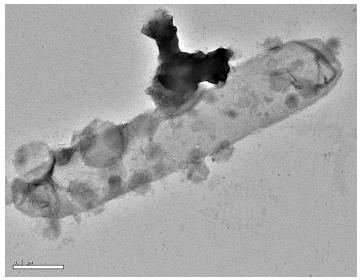

- Tubular Vesicle

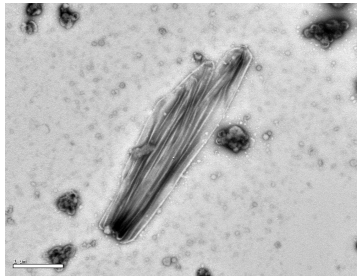

- Physical growth

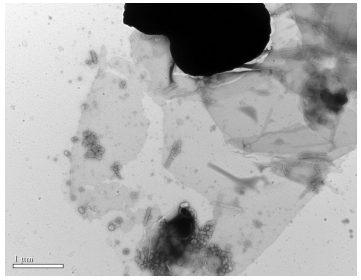

- Sheet

Class C

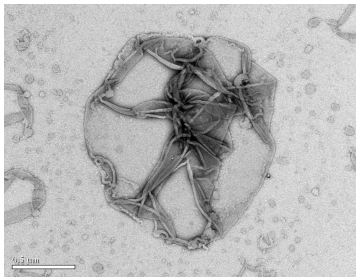

- Vesicle

Class D

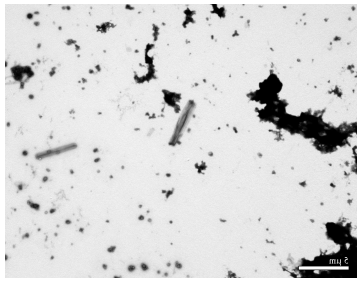

Protein aggregate

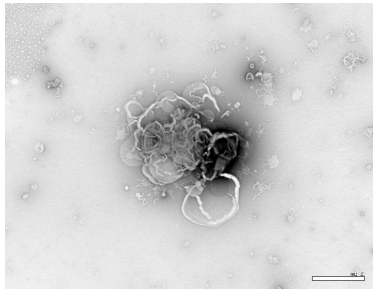

- Lipid aggregate
- with lipid thread

Class E

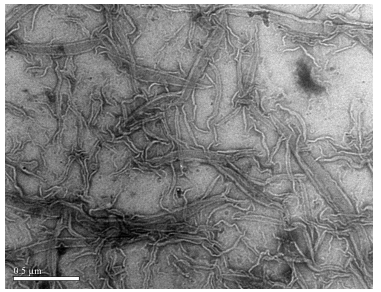

Strings of Lipid

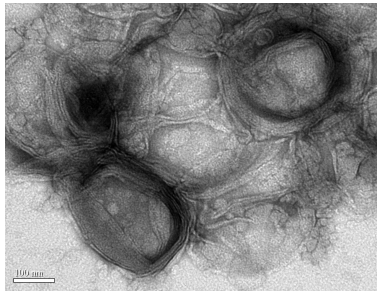

Multi-lamella Lipid

Classification of imaged objects

Class
A: Crystal with Lattice Pattern
B: Tubular Vesicle, Vesicle Sheet and Physical Growth
C: Vesicle, Vesicle Cluster, TV with irregular tubular vesicle
D: Protein aggregate and lipid aggregate
E: String of Lipid and Multi Lamella Lipid
F: Aggregate or Precipitate in solution

Class A

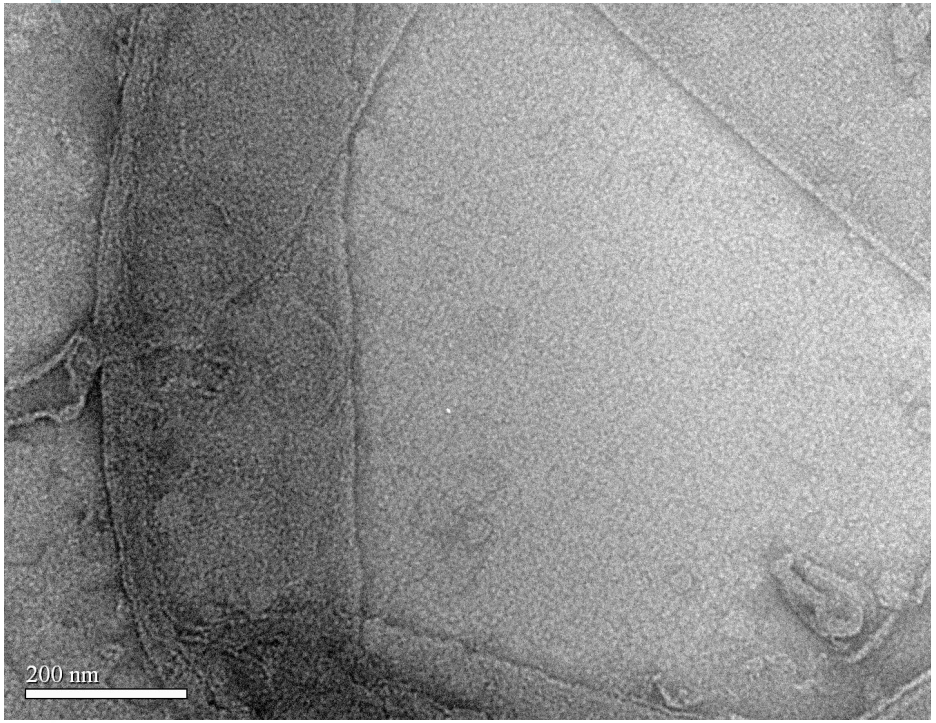

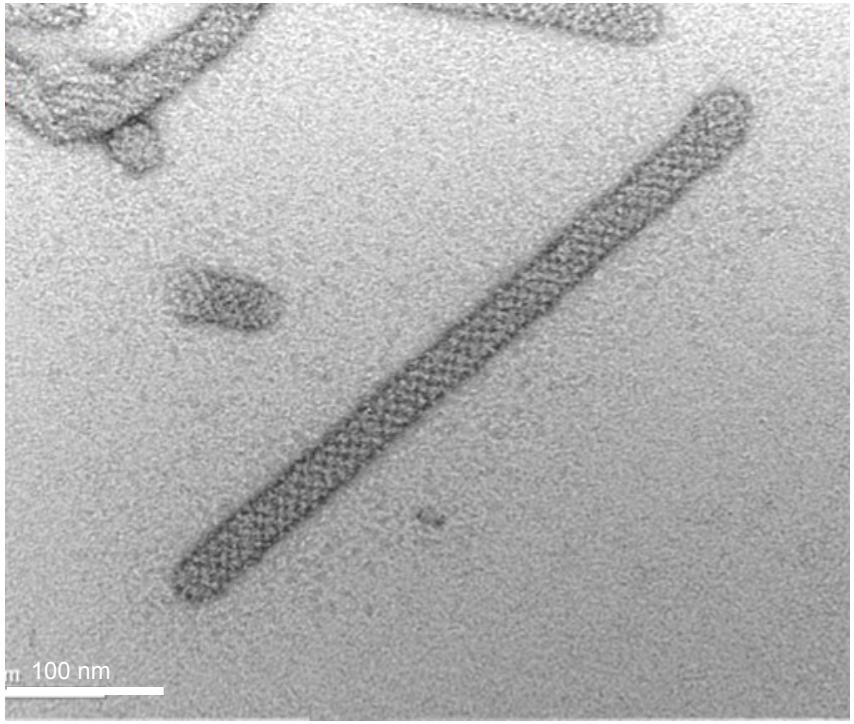

A 2DX SCREENING EXAMPLE

Sample: P2A3
33 kDa
Detergent: DDM
LPR 1.0

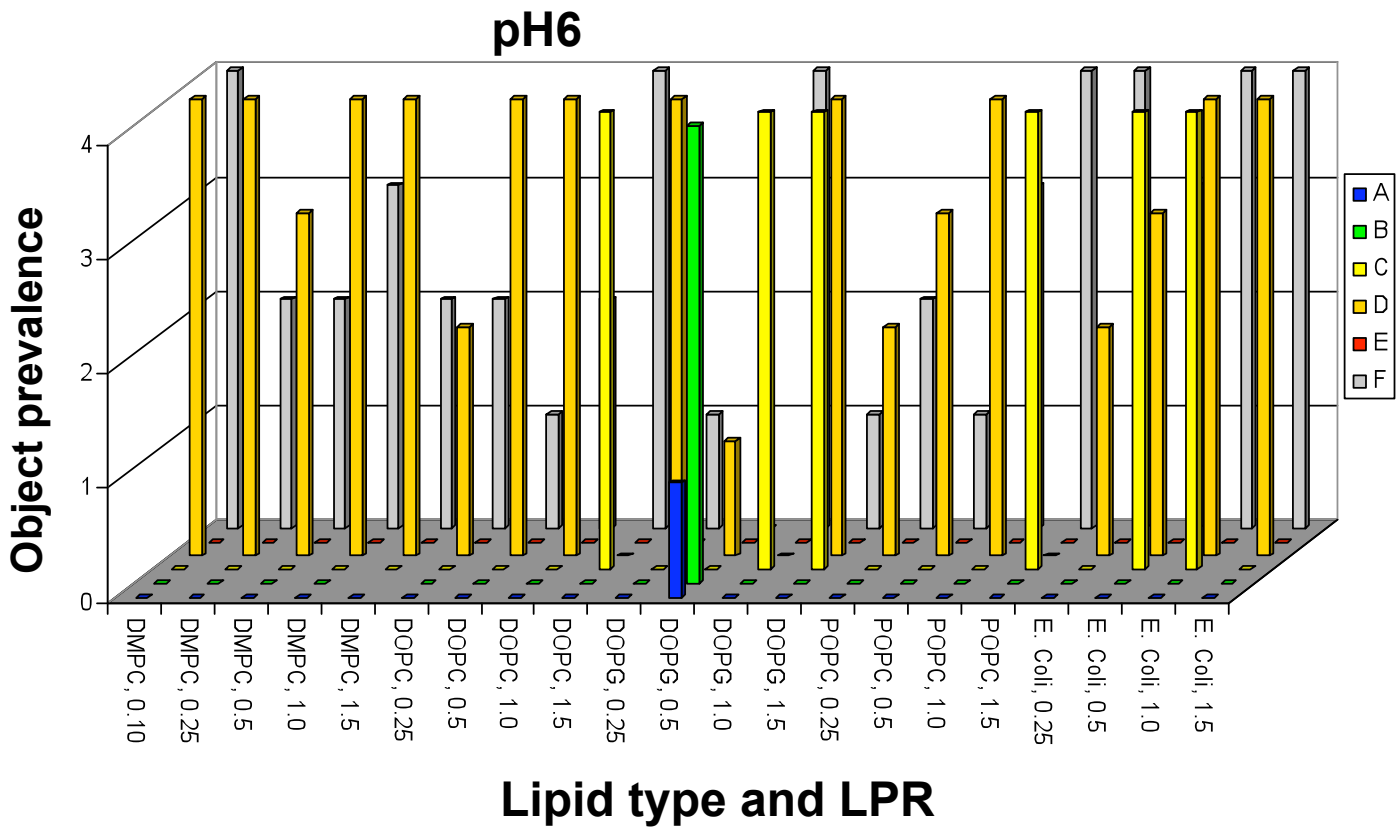

A: Crystal lattice
B: Tubular vesicle, sheets and physical growth
C: Vesicle and vesicle cluster
D: Protein aggregate and lipid aggregate
E: Lipid string
F: Failure, large precipitate (checked by light microcopy), bad staining, broken carbon, etc

A HT screening for 2DX: An example

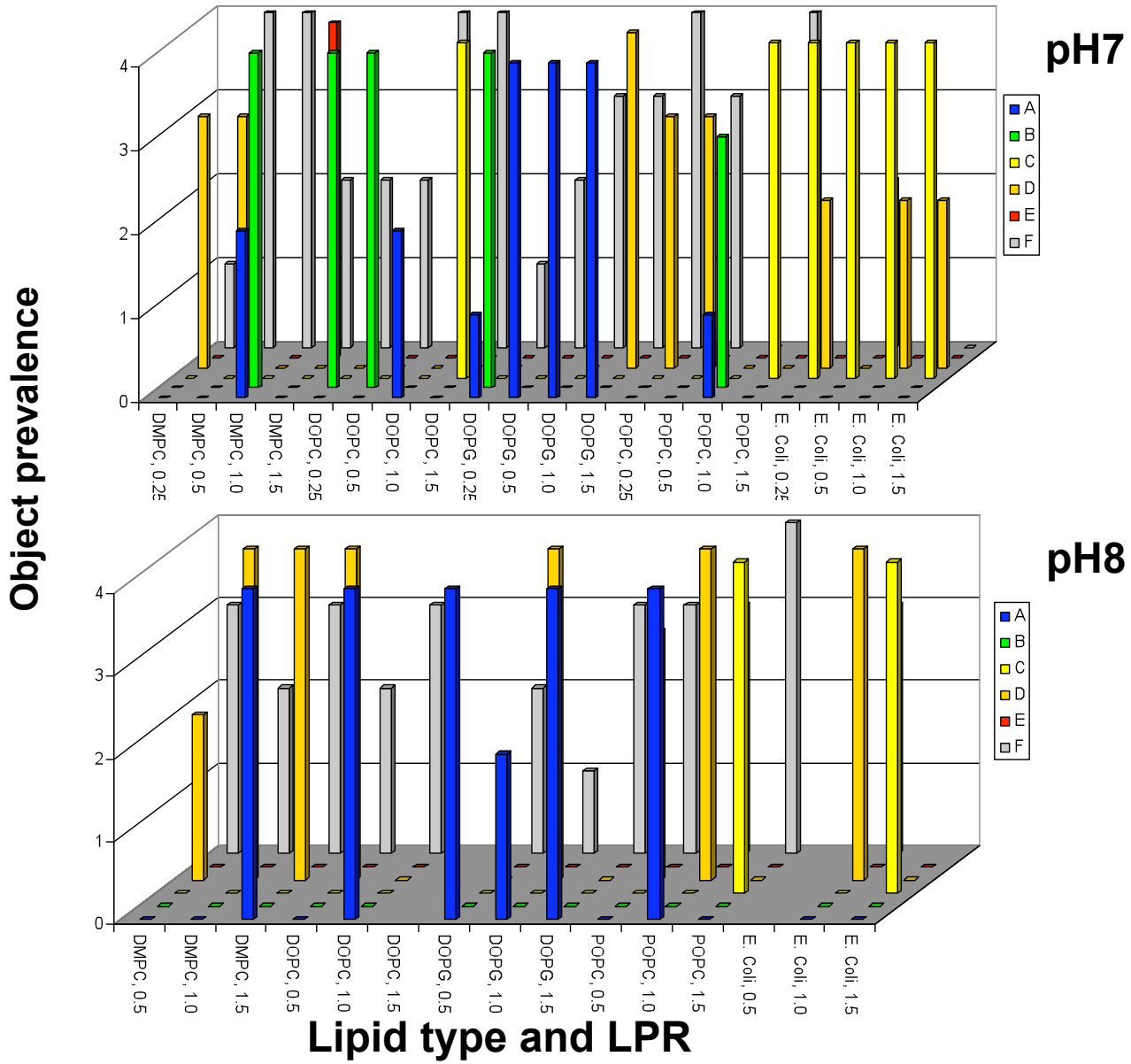

Integration with Sesame LIMS

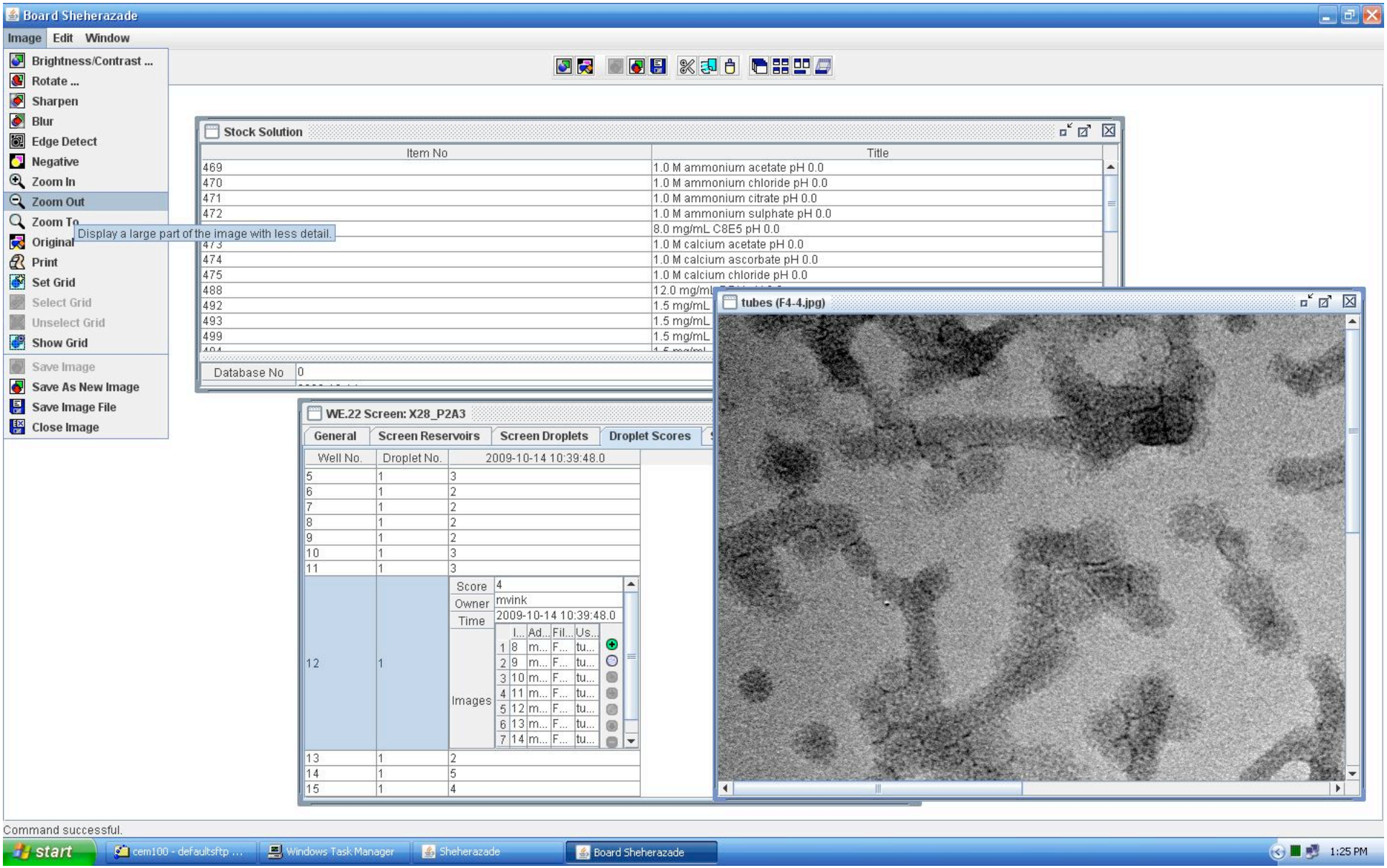

2D crystal morphologies

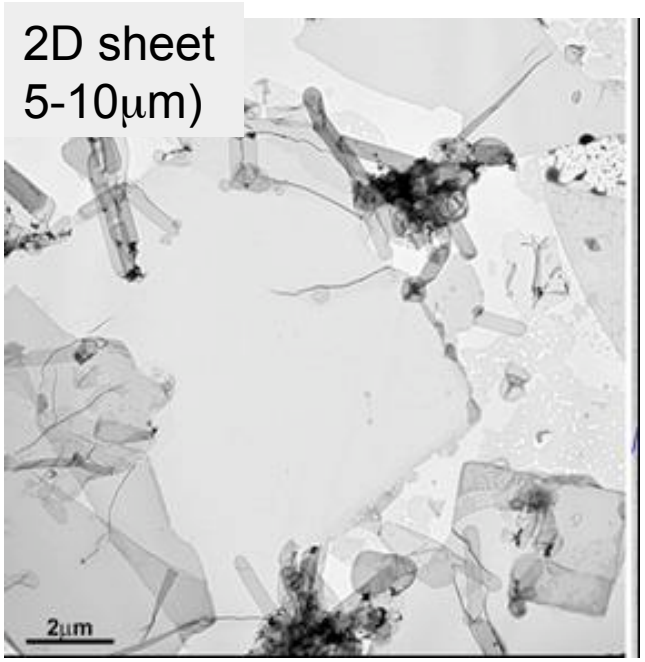

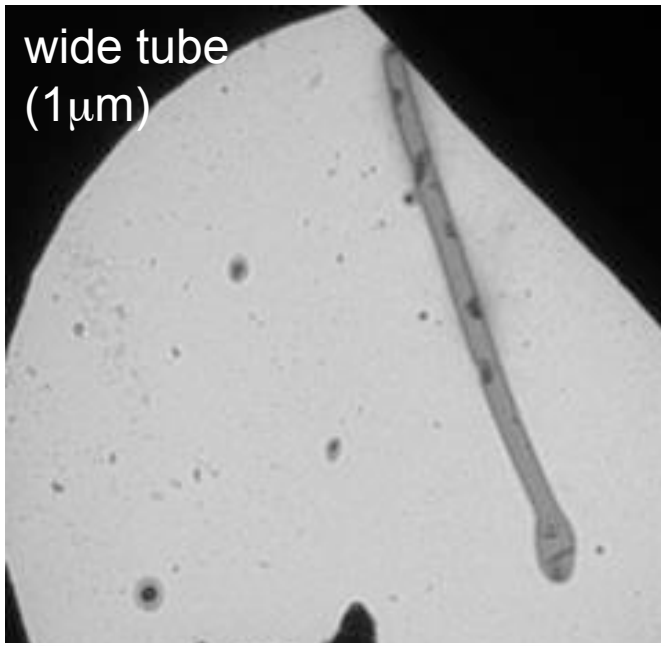

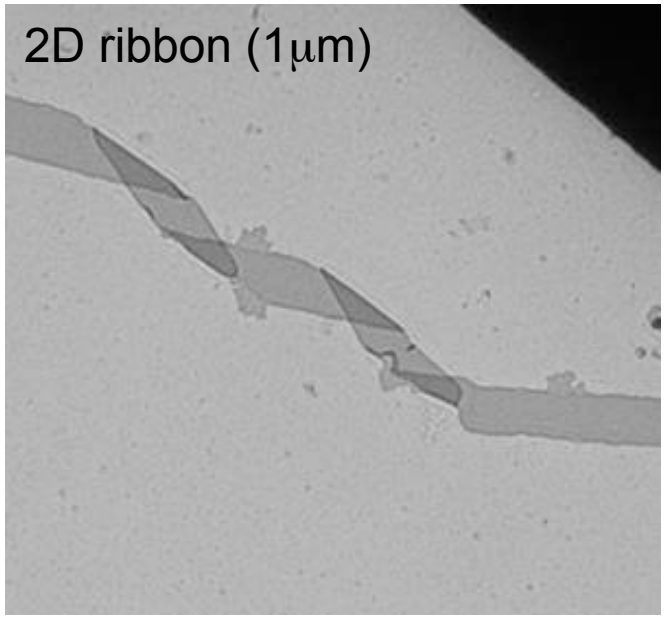

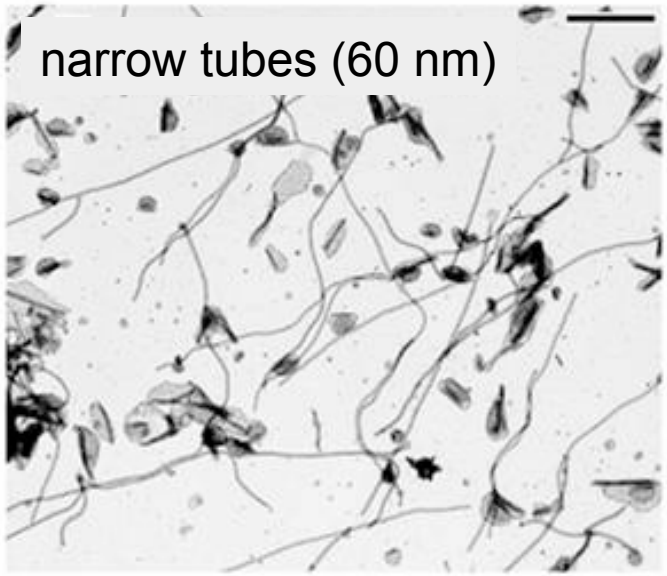

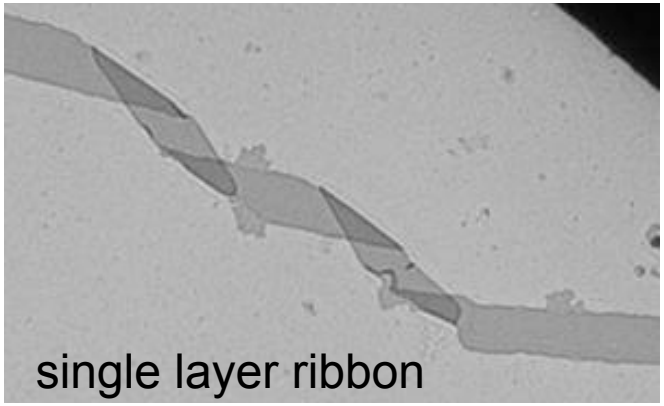

single layer ribbon

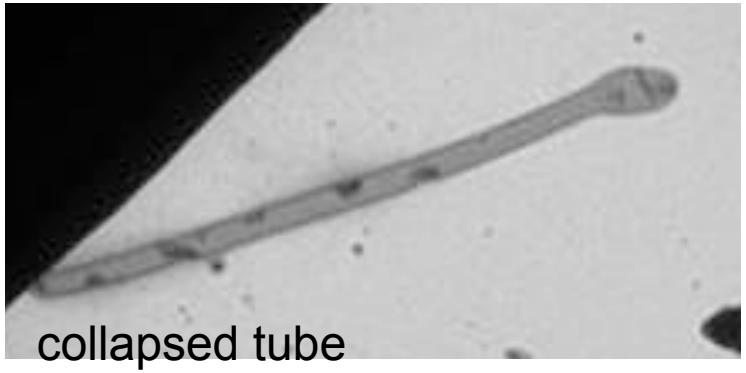

collapsed tube

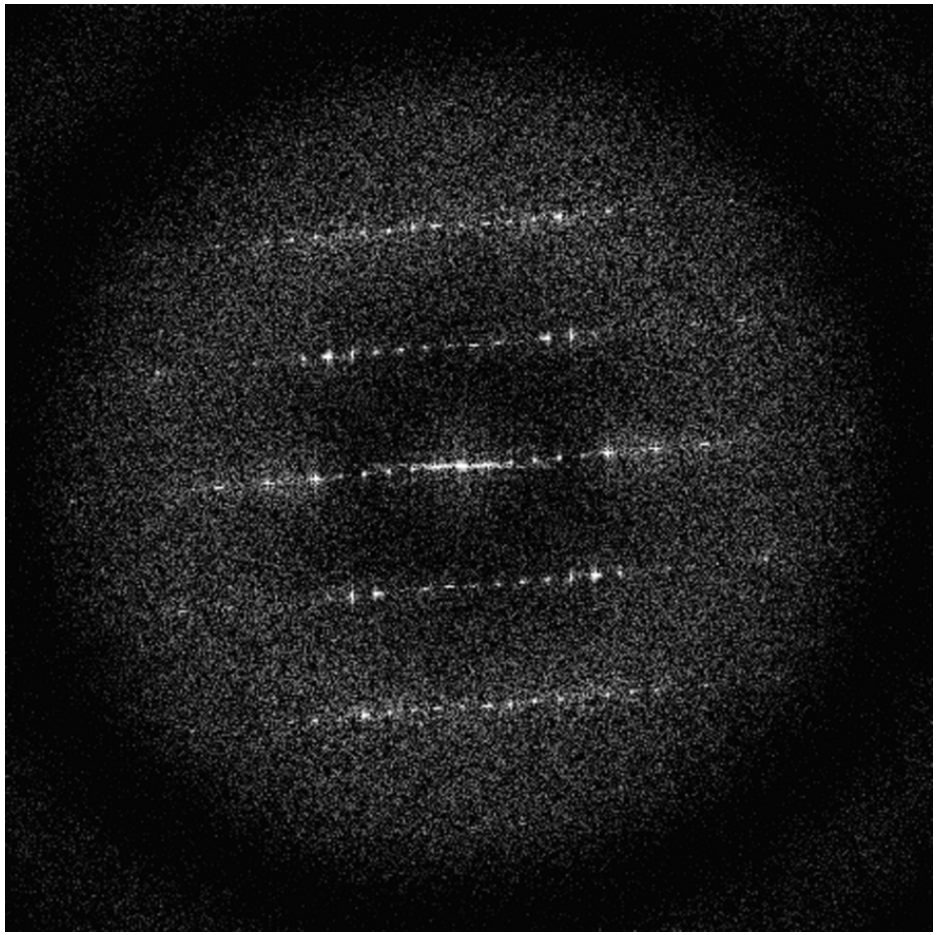

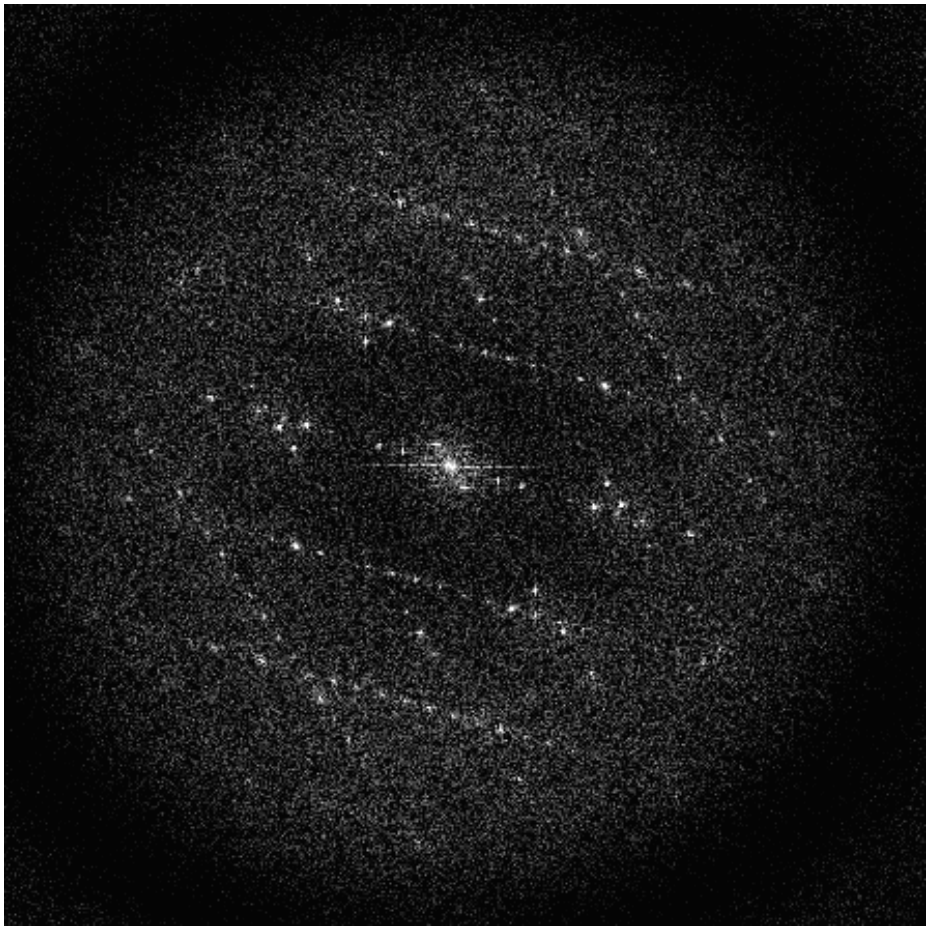

cylindrical tube with helical symmetry

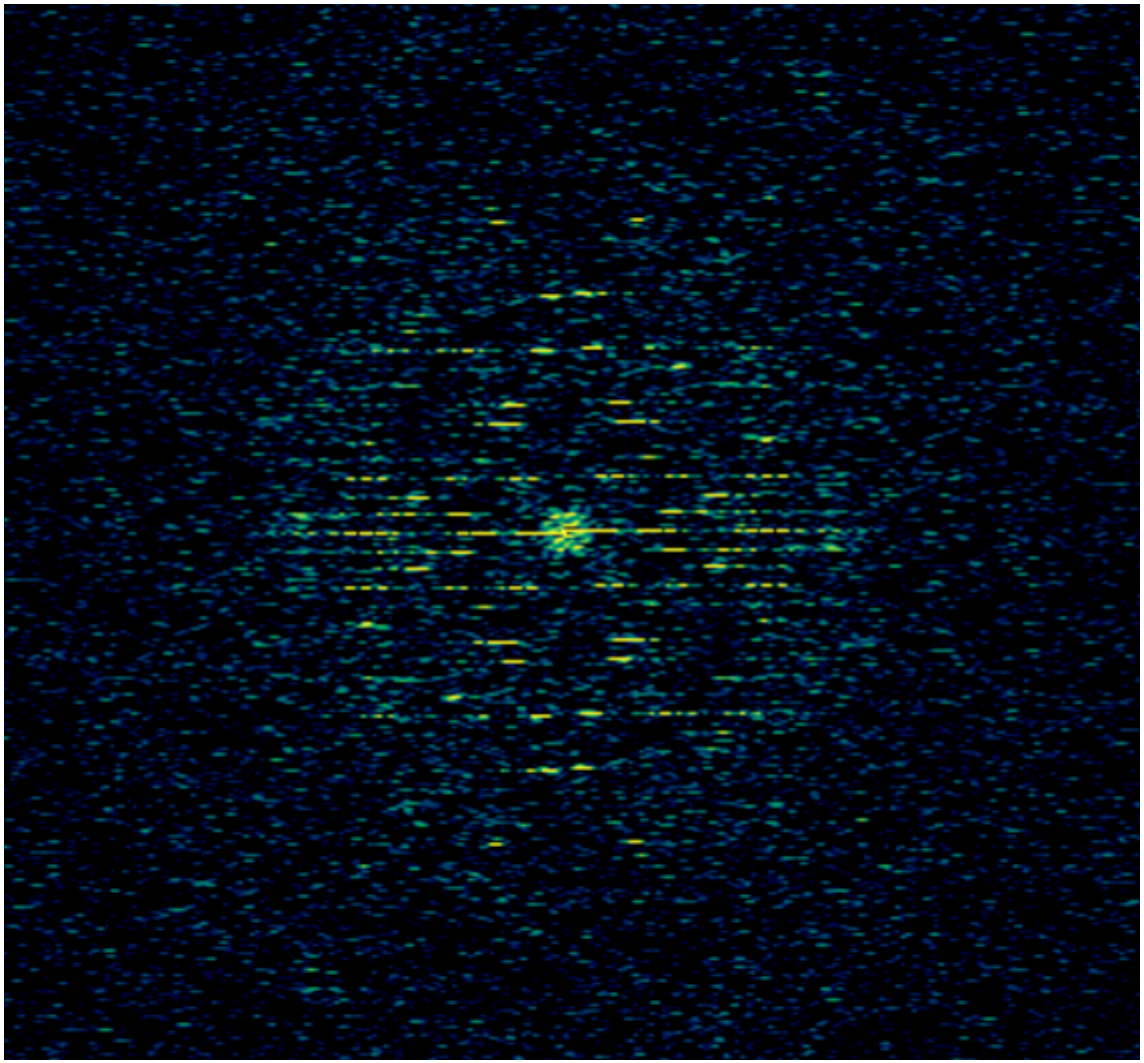

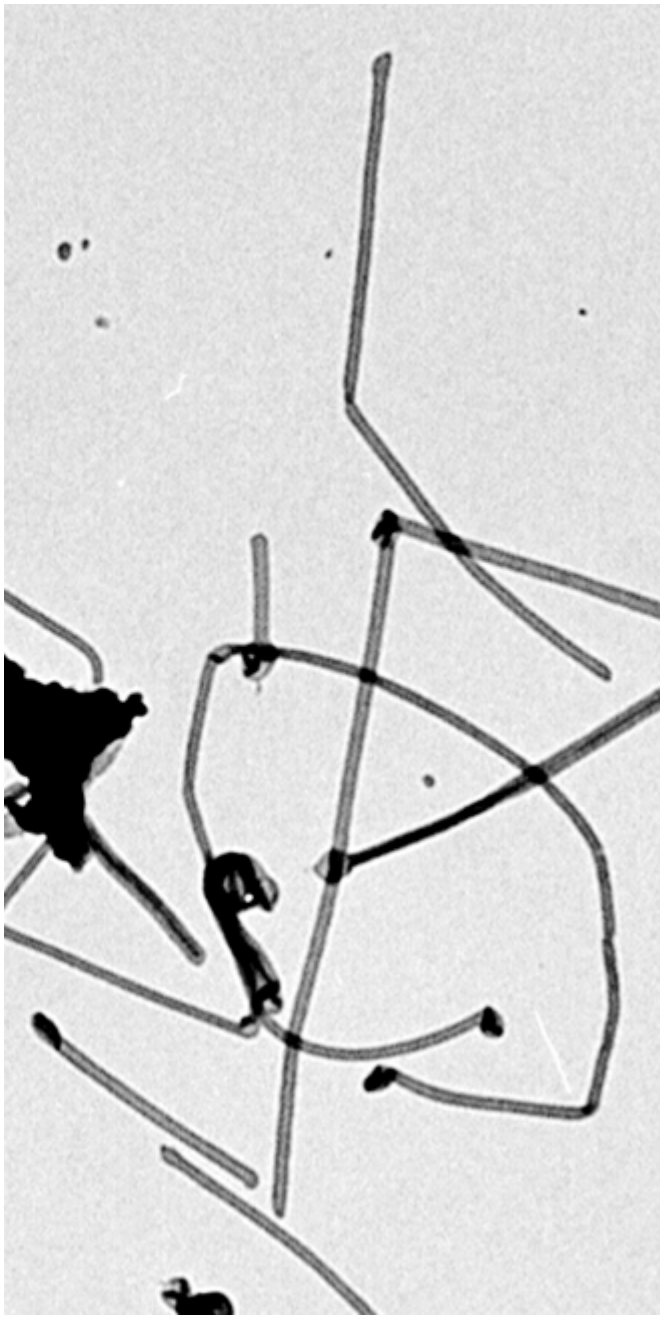

2D crystallography

- Fourier Transform composed of 2D lattice lines

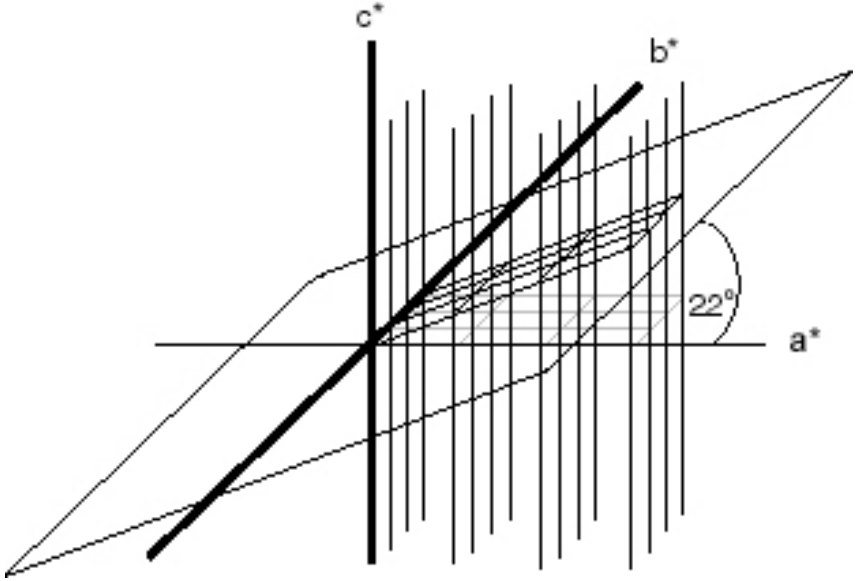

- Individual Projections sample lattice lines

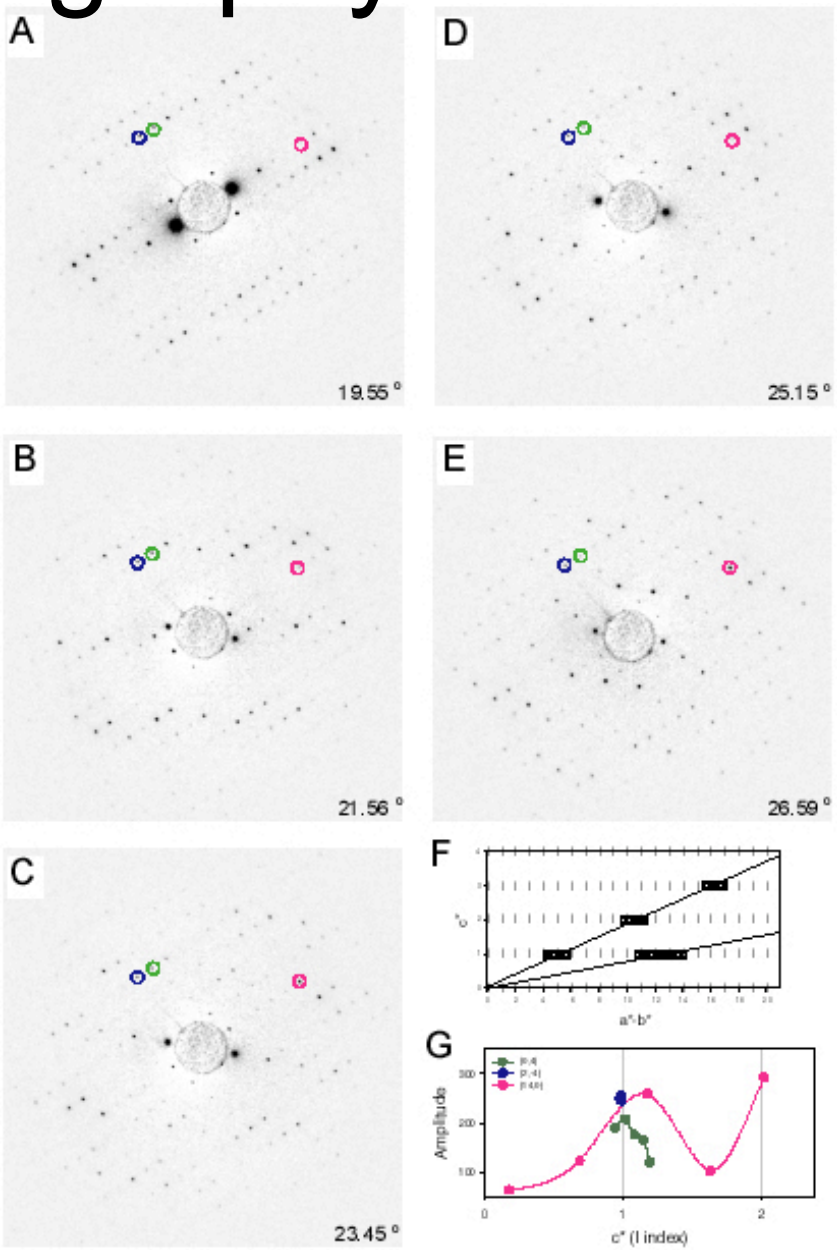

Fitting of lattice lines

- Electron Diffraction: amplitudes
- Images: phases

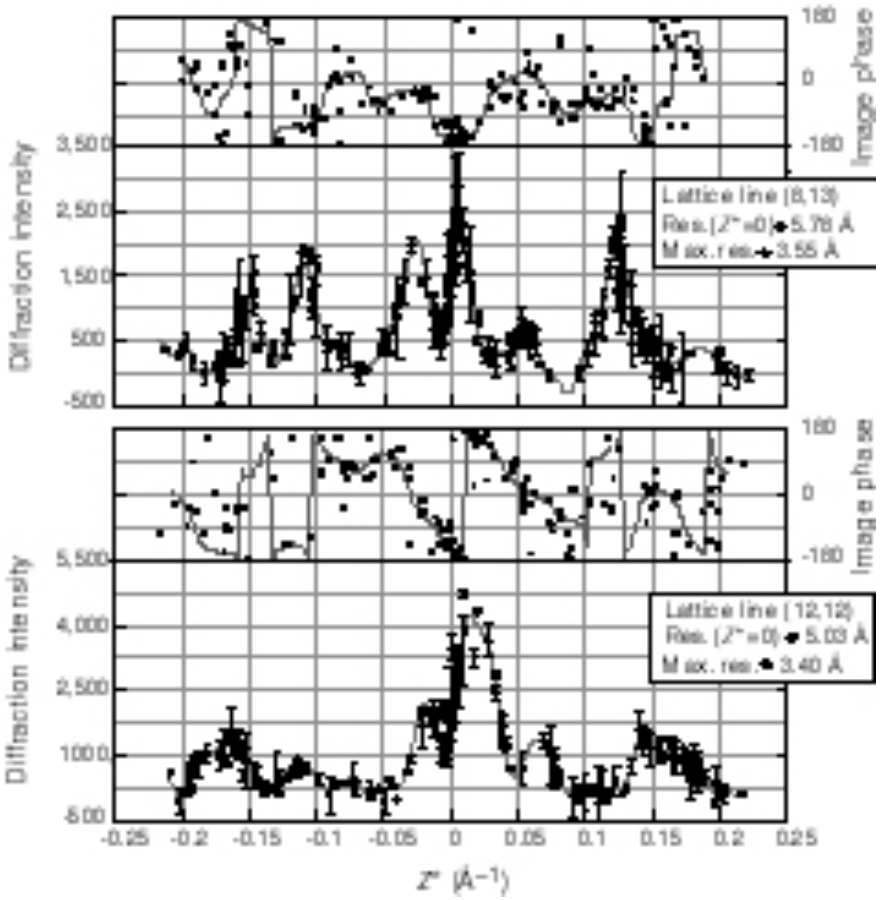

unbending a disordered 2D lattice

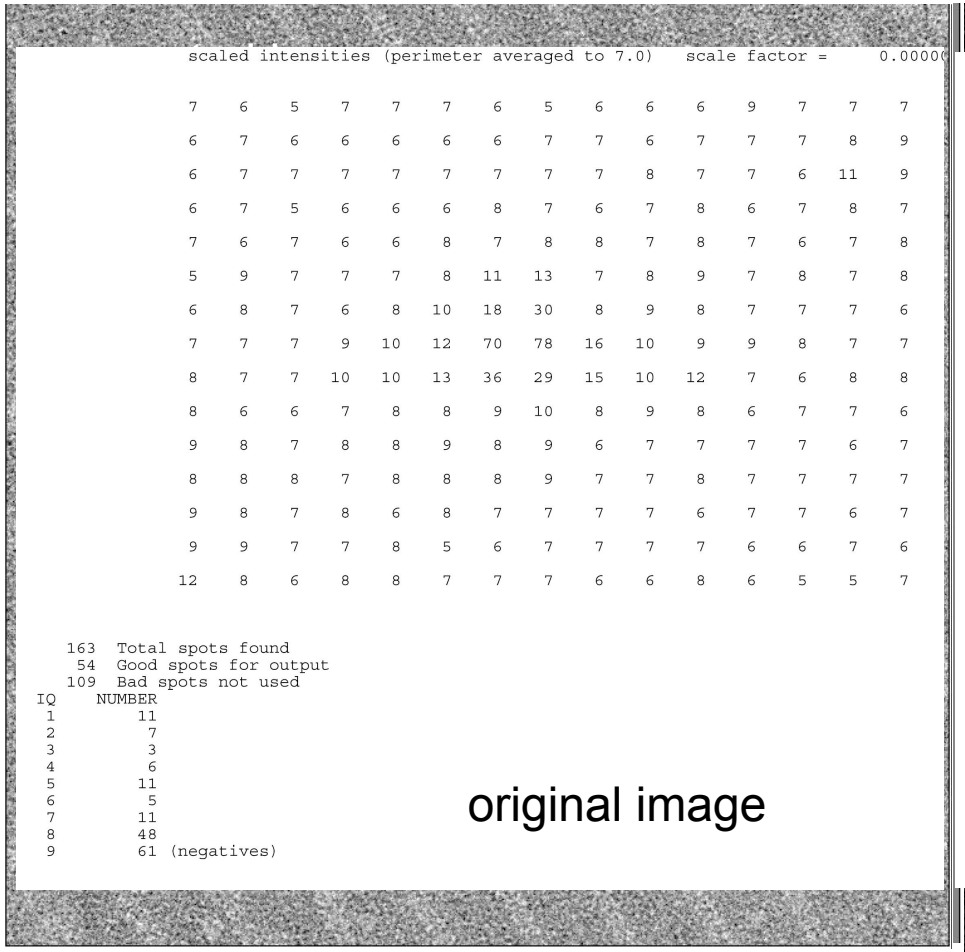

scaled intensities (perimeter averaged to 7.0) scale factor = 0.0000

7	6	5	7	7	7	6	5	6	6	6	9	7	7	7
6	7	6	6	6	6	6	7	7	6	7	7	7	8	9
6	7	7	7	7	7	7	7	7	8	7	7	6	11	9
6	7	5	6	6	6	8	7	6	7	8	6	7	8	7
7	6	7	6	6	8	7	8	8	7	8	7	6	7	8
5	9	7	7	7	8	11	13	7	8	9	7	8	7	8
6	8	7	6	8	10	18	30	8	9	8	7	7	7	6
7	7	7	9	10	12	70	78	16	10	9	9	8	7	7
8	7	7	10	10	13	36	29	15	10	12	7	6	8	8
8	6	6	7	8	8	9	10	8	9	8	6	7	7	6
9	8	7	8	8	9	8	9	6	7	7	7	7	6	7
8	8	8	7	8	8	8	9	7	7	8	7	7	7	7
9	8	7	8	6	8	7	7	7	7	6	7	7	6	7
9	9	7	7	8	5	6	7	7	7	7	6	6	7	6
12	8	6	8	8	7	7	7	6	6	8	6	5	5	7

163 Total spots found
54 Good spots for output
109 Bad spots not used

IQ	NUMBER
1	11
2	7
3	3
4	6
5	11
6	5
7	11
8	48
9	61 (negatives)

original image

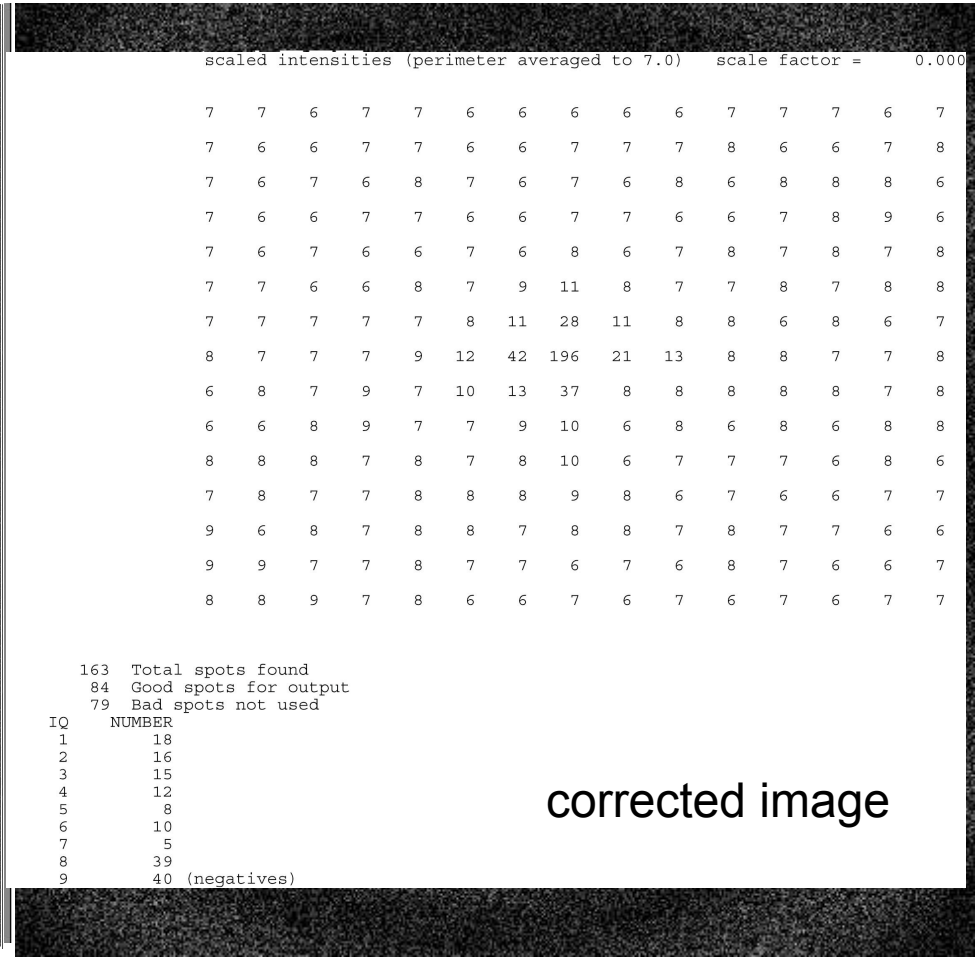

scaled intensities (perimeter averaged to 7.0) scale factor = 0.000

7	7	6	7	7	6	6	6	6	6	7	7	7	6	7
7	6	6	7	7	6	6	7	7	7	8	6	6	7	8
7	6	7	6	8	7	6	7	6	8	6	8	8	8	6
7	6	6	7	7	6	6	7	7	6	6	7	8	9	6
7	6	7	6	6	7	6	8	6	7	8	7	8	7	8
7	7	6	6	8	7	9	11	8	7	7	8	7	8	8
7	7	7	7	7	8	11	28	11	8	8	6	8	6	7
8	7	7	7	9	12	42	196	21	13	8	8	7	7	8
6	8	7	9	7	10	13	37	8	8	8	8	8	7	8
6	6	8	9	7	7	9	10	6	8	6	8	6	8	8
8	8	8	7	8	7	8	10	6	7	7	7	6	8	6
7	8	7	7	8	8	8	9	8	6	7	6	6	7	7
9	6	8	7	8	8	7	8	8	7	8	7	7	6	6
9	9	7	7	8	7	7	6	7	6	8	7	6	6	7
8	8	9	7	8	6	6	7	6	7	6	7	6	7	7

163 Total spots found
84 Good spots for output
79 Bad spots not used

IQ	NUMBER
1	18
2	16
3	15
4	12
5	8
6	10
7	5
8	39
9	40 (negatives)

corrected image

missing cone

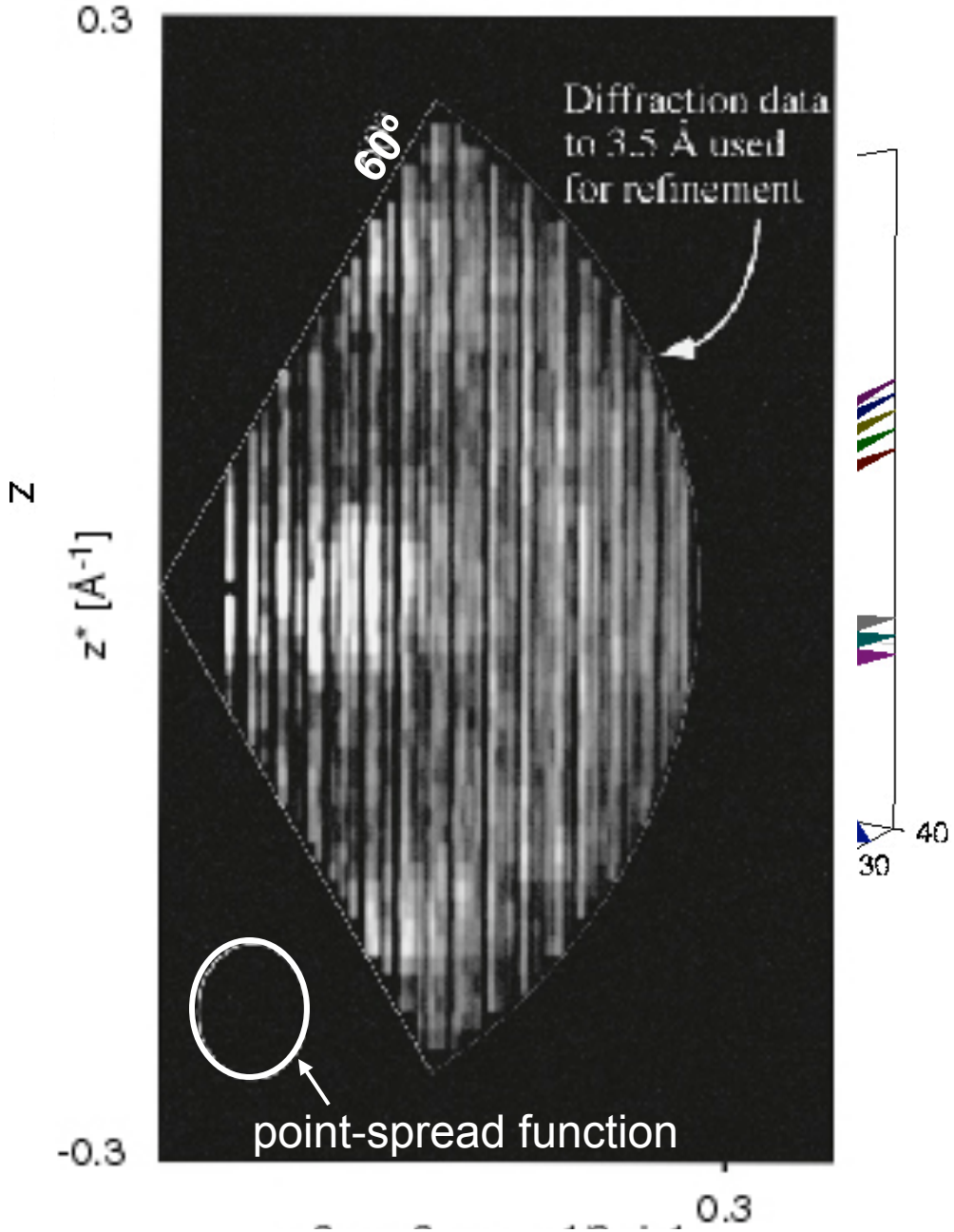

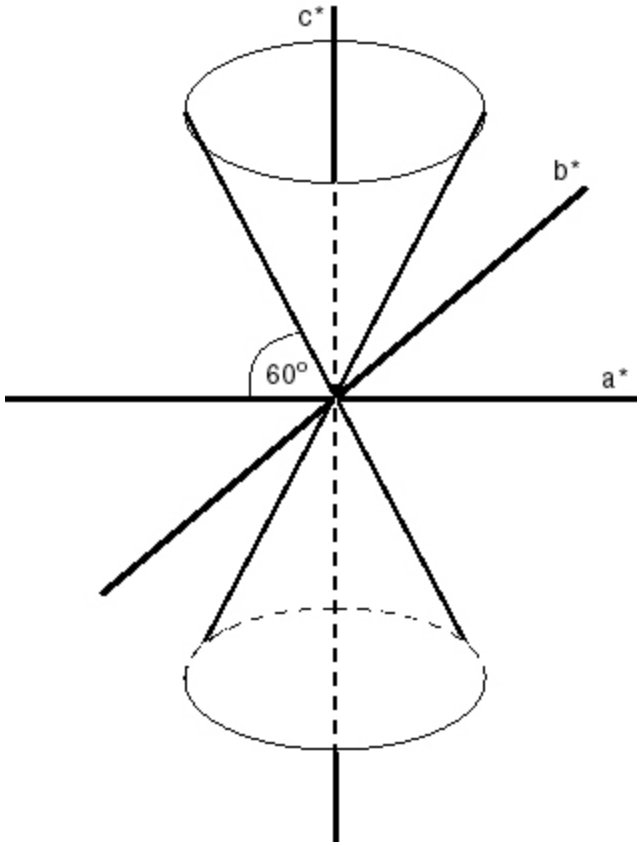

missing cone leads to loss of z resolution

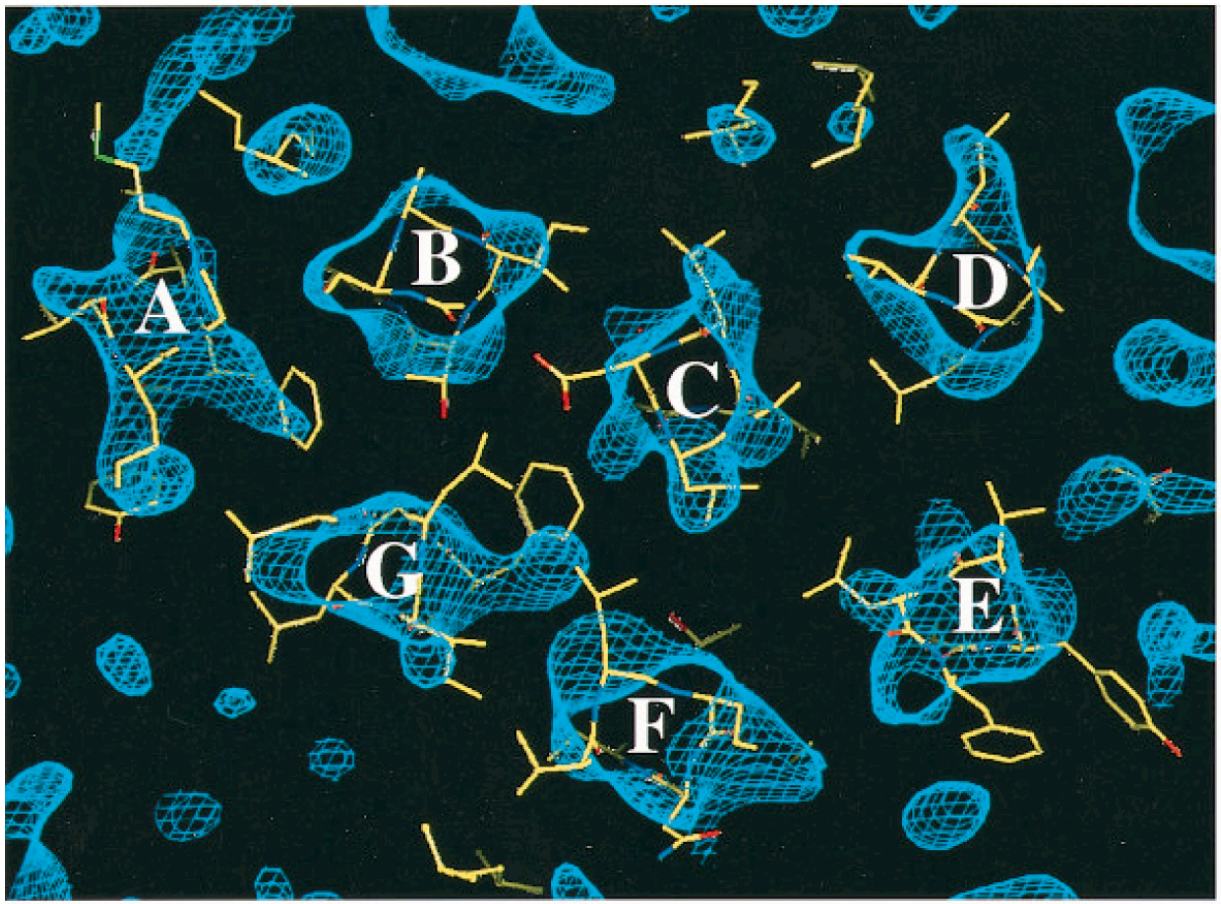

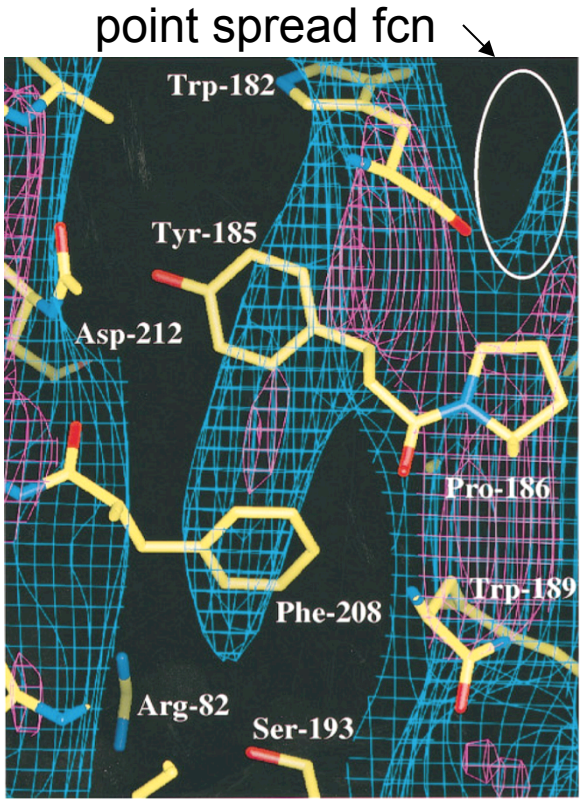

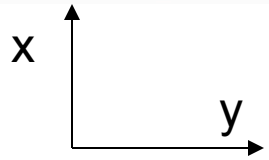

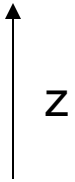


2dx_image File Edit Options
/Users/henning/Desktop/Proteins/ILIO2/ILIO45/ILIO0000443500/
2dx_image
Version 1.0.1 (July 20, 2006)
Standard Scripts
Initialization
Calculate FFT
Get Defocus & Tilt
Get Lattice & Tilt
Get Spotlist
Unbend I
Unbend II
Correct CTF
Generate Map
Specific Scripts
Mask Crystal from Polygon
Evaluate Lattice
Determine Spacegroup
Generate SymMap
Refine Parameters Unbend I
Refine Parameters Unbend II
Refine Spotlist
Refine Tilt from SpotSplitting
Image Inventory
Cleanup
Image Header
ILIO0000443500.mrc
NX, NY, NZ: 4000 4000 1
Mode: 0
Origin x,y,z: 0 0 0
Sample x,y,z: 4000 4000 1
CellA: 4000 4000 1
CellB: 90 90 90
Basis Vectors: 1 2 3
Min, Max, Mean: 0 2.6e+02 98
Space Group: 0
Symmetry Bytes: 0
Phase Origin: 0 0 0
RMS: 0
Labels: 1
Processing Data -- Standard
Manual
Algorithm Non-tilted
Raw Image
CTF world
FFT
masktran
20px
mask= 1px
Masked FFT
Masked FFT
Reference
Unbent Image
ccunbend
Profile
quadserch
CC-Map
FFT of Reference
Repeat in Loop
Perfect FFT
maketrans
(Apply Defocus)
Image File Data
Image Number: 0000443500
Image Name: mILIO0000443500
Non-Masked Image Name: ILIO0000443500
Image Side Length: 4000
Magnification: 70000
Digitizer Step Size: 7
Tilt Geometry Data
TLTAXIS: X-axis -> Tilt axis (on image): -18.66913
TLTANG: Tiltangle for carbon film: 45.75145
TLTAXA: Tilt axis -> A* vector (on image): 42.77613
TAXA: Tilt axis -> A* vector (on sample): 32.84644
TANGL: Tiltangle for crystal [=TLTANG*AisAbove*SignTLTAXA*Hand]: 45.75145
Crystal Data
Real Unit Cell Length: 91.7 89.7
Real Cell Angle: 114.5
Reciprocal Lattice: 51.493 23.041 15.941 70.027
Results
Images
mILIO0000443500.mrc
ILIO0000443500.mrc
Status
QVal 146.7 Th.Mag 68081.6
IQ-1 QVal1 173.0
11 16 19 32 32 54 39 213 317
IQ-2 QVal2 146.7
11 18 12 24 15 24 27 140 215
Defoc. Latt. SpSplit Merge
TLTAXIS -17.5 -18.6 -18.6 -
TLTANG 40.2 45.7 45.7 -
TLTAXA 35.3 42.7 42.7 -
TAXA 28.4 32.8 32.8 -
TANGL 40.2 45.7 45.7 -

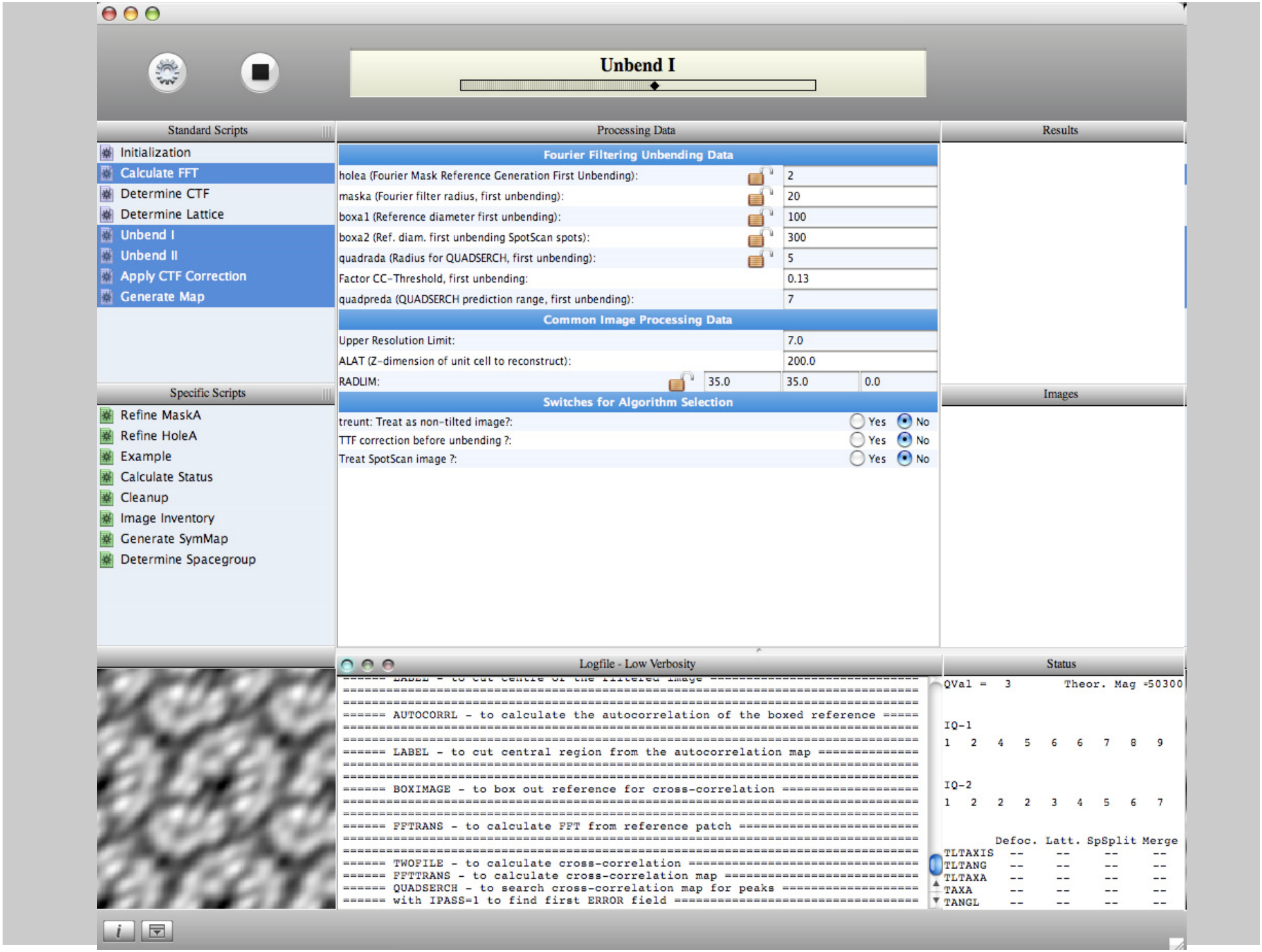
Unbend I
Standard Scripts
Initialization
Calculate FFT
Determine CTF
Determine Lattice
Unbend I
Unbend II
Apply CTF Correction
Generate Map
Specific Scripts
Refine MaskA
Refine HoleA
Example
Calculate Status
Cleanup
Image Inventory
Generate SymMap
Determine Spacegroup
Processing Data
Fourier Filtering Unbending Data
holea (Fourier Mask Reference Generation First Unbending): 2
maska (Fourier filter radius, first unbending): 20
boxa1 (Reference diameter first unbending): 100
boxa2 (Ref. diam. first unbending SpotScan spots): 300
quadrada (Radius for QUADSERCH, first unbending): 5
Factor CC-Threshold, first unbending: 0.13
quadpreda (QUADSERCH prediction range, first unbending): 7
Common Image Processing Data
Upper Resolution Limit: 7.0
ALAT (Z-dimension of unit cell to reconstruct): 200.0
RADLIM: 35.0 35.0 0.0
Switches for Algorithm Selection
treunt: Treat as non-tilted image?: Yes No
TTF correction before unbending ?: Yes No
Treat SpotScan image ?: Yes No
Results
Images
Logfile - Low Verbosity
====== AUTOCORRL - to calculate the autocorrelation of the boxed reference =====
====== LABEL - to cut central region from the autocorrelation map ==============
====== BOXIMAGE - to box out reference for cross-correlation ====================
====== FFTRANS - to calculate FFT from reference patch ==========================
====== TWOFILE - to calculate cross-correlation ==================================
====== FFTTRANS - to calculate cross-correlation map ============================
====== QUADSERCH - to search cross-correlation map for peaks ====================
====== with IPASS=1 to find first ERROR field ===================================
Status
QVal = 3 Theor. Mag =50300
IQ-1
1 2 4 5 6 6 7 8 9
IQ-2
1 2 2 2 3 4 5 6 7
Defoc. Latt. SpSplit Merge
TLTAXIS -- -- -- --
TLTANG -- -- -- --
TLTAXA -- -- -- --
TAXA -- -- -- --
TANGL -- -- -- --

Image Processing Library & Toolbox (IPLT)

(Philippsen, Schenk, Engel)

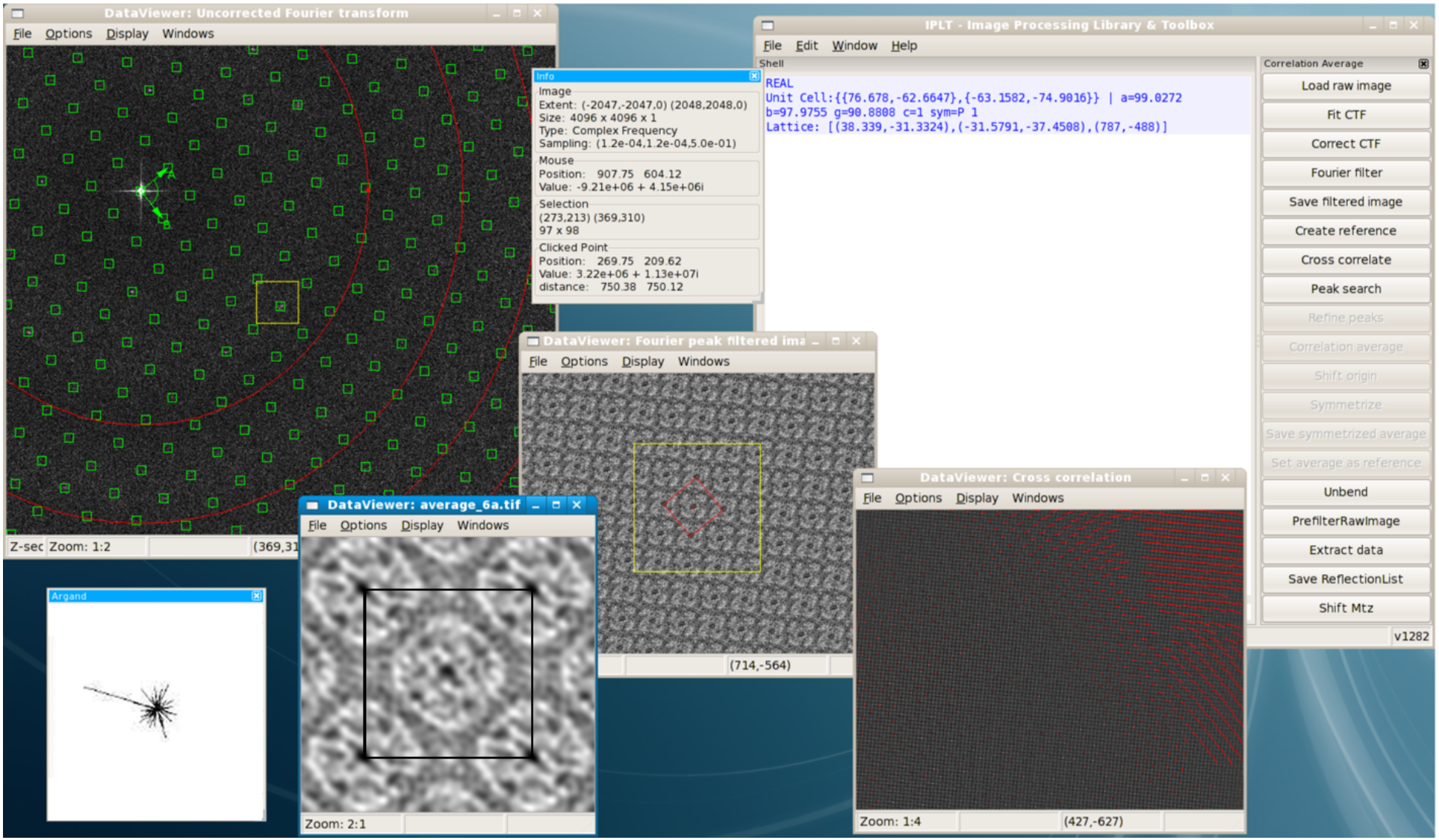

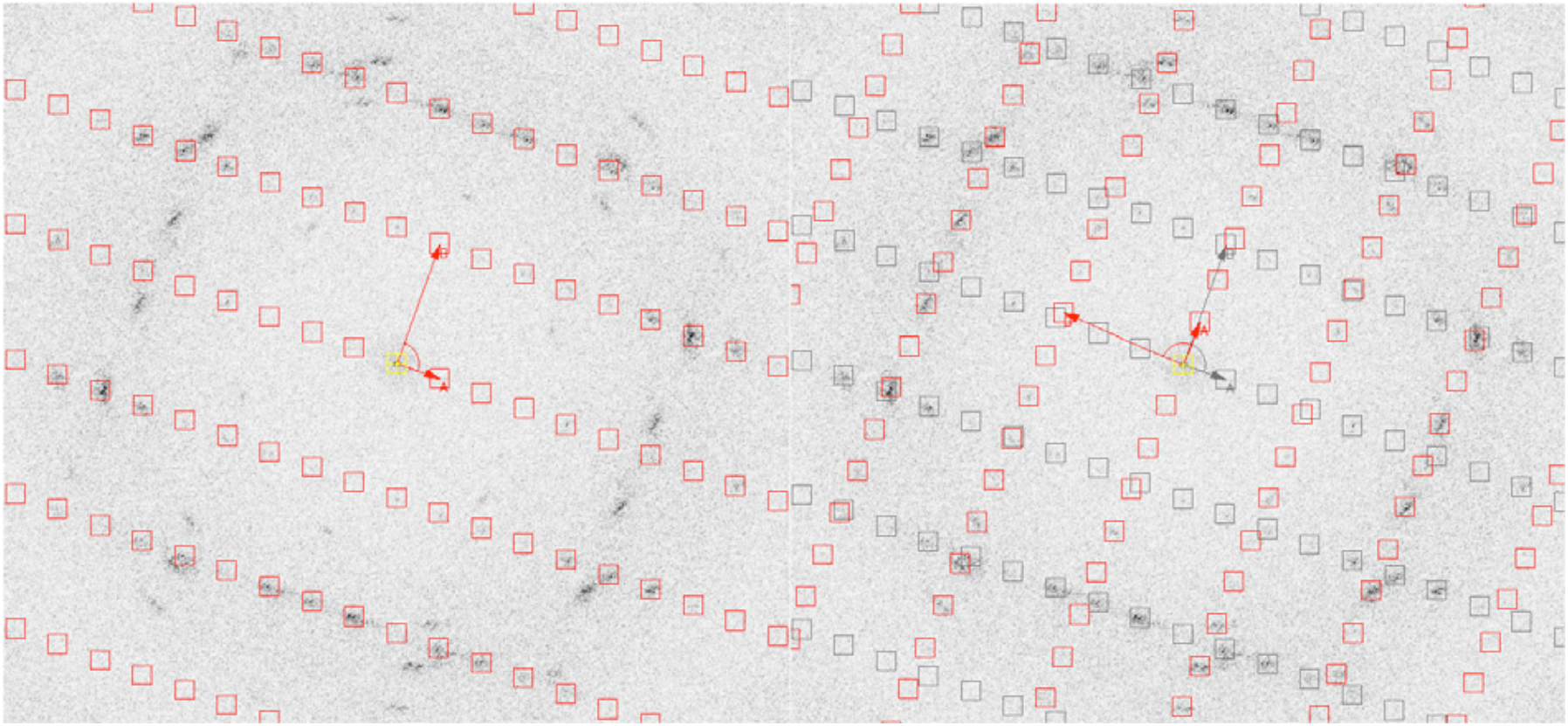

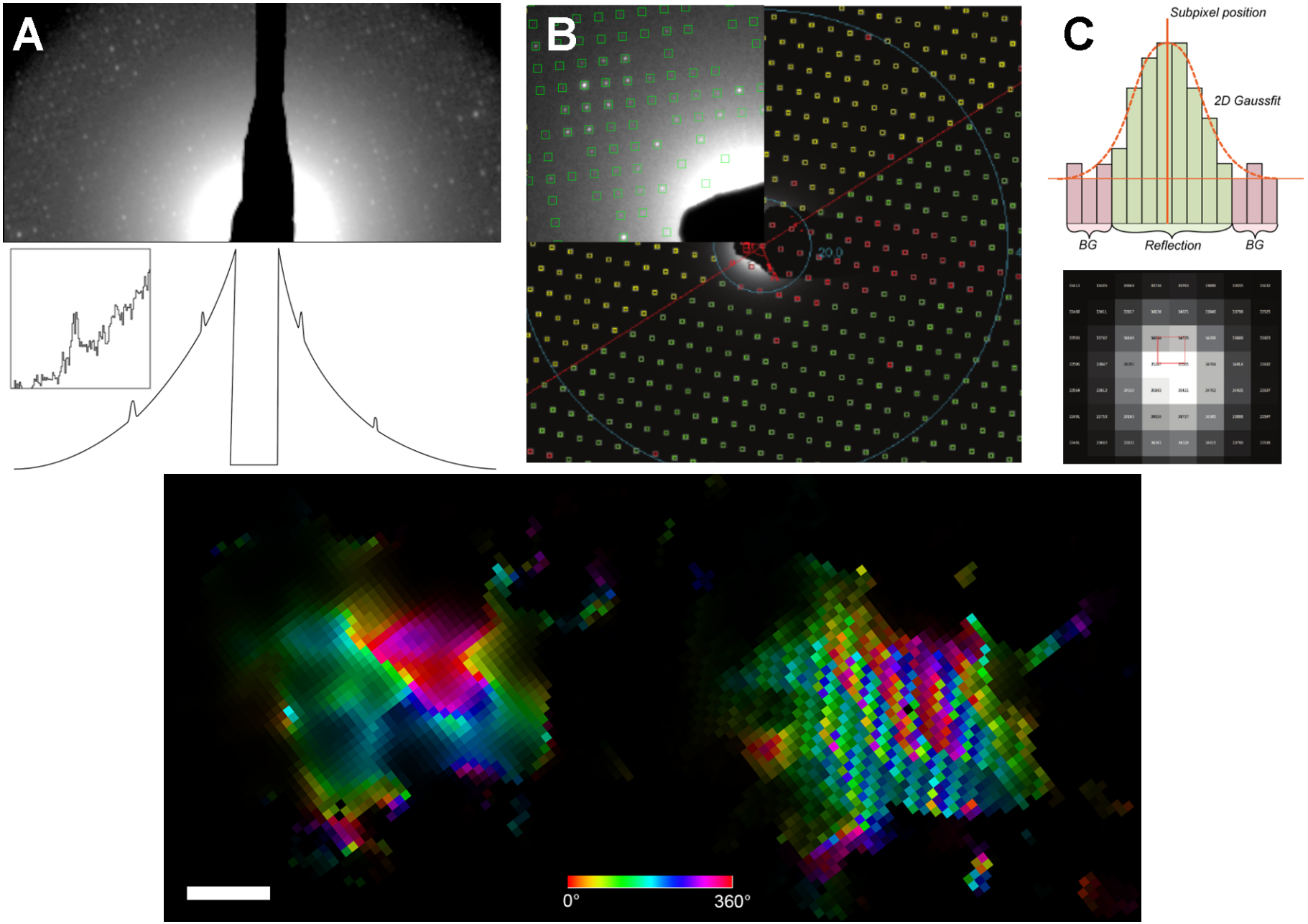
A
B
C
Subpixel position
2D Gaussfit
BG
Reflection
BG
0°
360°

IPLT unbending simulations

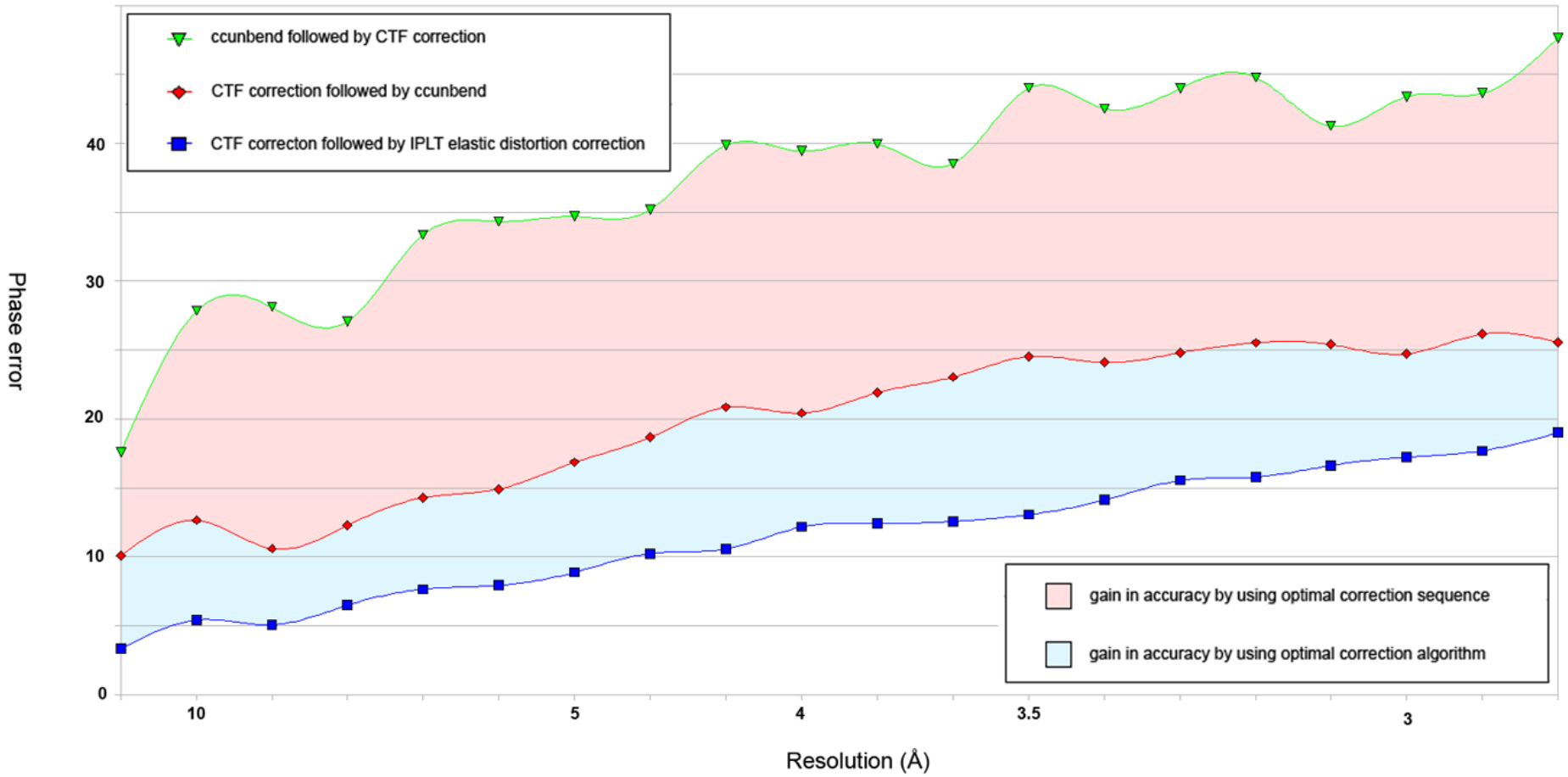

Acknowledgements

Changki Kim
Minghui Hui
Martin Vink
Iban Ubarretxena

James Love
Filippo Mancia
Ming Zhou
Wayne Hendrickson

Bill Rice
KD Derr
Ruben Diaz

NIH
R01 GM081817

JKD instruments
John Koss
Kevin D'amico

Bridget Carragher
Clint Potter
Jim Pulokos
Anchi Cheng

A HT screening for 2DX: An exampl